



The Slovak Biophysical Society

Vth. Slovak Biophysical Symposium

Program and Abstracts

Comenius University in Bratislava
Faculty of Mathematics, Physics and Informatics
Bratislava
19. - 21. 3. 2012

The Slovak Biophysical Symposium is already a well-established biannual meeting of biophysicists. The V. Slovak Biophysical Symposium held on March 19-21, 2012, has been organized by The Slovak Biophysical Society (SKBS). SKBS has established in 2001. The members of SKBS include not only teachers and researchers working in the field of biophysics but also those working in other interdisciplinary areas.

The Vth. Slovak Biophysical Symposium was focused on following topics

- membrane systems and transport processes
- photobiophysics, modern microscopy and spectroscopy techniques
- protein structure and stability, interactions of ligands with biomacromolecules
- biosensors and nanobiotechnology
- applications of biophysics in medicine
- molecular modeling
- education in biophysics

Scientific Committee

Tibor Hianik (FMFI UK Bratislava)
Marta Gaburjaková (UMFG SAV, Bratislava)
Dušan Chorvát (ILC Bratislava)
Ján Jakuš (JLF UK Martin)
Pavol Miškovský (PF UPJŠ Košice)
Ivan Zahradník (UMFG SAV, Bratislava)

Organizing committee

Tibor Hianik - chairman
Gabriela Castillo
Zuzana Garaiová
Alexandra Poturnayová
Peter Rybár
Maja Šnejdárková

Program

Monday, March 19, 2012

- 12.30-14.30 **Registration** (Ground Floor F1)
12.30-14.30 **Establishment of posters** (Ground Floor F1)
14.45-15.00 **Opening ceremony** (Lecture Room C)

15:00-15:30

SKBS Young Researcher Prize Lecture

M. Šimera, M. Veterník, I. Poliaček, J. Jakuš, Study of the antitussive effect of codeine in the brainstem in the anaesthetized animals

1. Biophysics of Brain, Tissues and Cells

Chairs: **J. Jakuš, I. Poliaček**

15.30-16.15

Tutorial Lecture

T1 **M. Kopáni**, J. Dekan, M. Miglierini, L. Dihan, R. Boca, M. Caplovicova, V. Sisovsky, J. Jakubovsky, Iron oxides particles in human brain

16.15-17.15 **Coffee break and posters**

17.15-18.45

- O1** N. Višňovcová, V. Jakušová, **N. Višňovcová Jr.**, J. Jakuš, Effects of high energy radiation on the organ systems in human medicine
O2 **I. Waczuliková**, O. Uličná, Z. Tomášková, M. Grman, O. Vančová, K. Ondriáš, Voltammetric measurements of mitochondrial (dys)function in studying the effects of external stimuli
O3 **K. Ondriáš**, A. Mišák, M. Grman, N. Pronayová, T. Liptaj, On the H₂S-NO interaction and the effects of thiols
O4 **M. Grman**, A. Mišák, K. Ondriáš, Effect of pH, thiols and oxygen on the H₂S/HS⁻ induced NO release from S-nitrosoglutathione

19.15 **Dinner**

Tuesday, March 20, 2012

2. Molecular Modeling and Ionic Channels

Chairs: **I. Zahradník, A. Zahradníková**

09.30-10.15

Tutorial Lecture

T2 **V. Frečer**, P. Seneci, S. Miertuš Computer-assisted combinatorial design of inhibitors of thymidine monophosphate kinase of *Mycobacterium tuberculosis*

10.15-11.00

O5 M. Karmazinova, S. Beyl, N. Klugbauer, S Hering, **L Lacinova**, Cysteines in the

- extracellular loop in domain I of the $Ca_v3.1$ channel are essential for channel opening
- O6** M. Gaburjaková, J. Gaburjaková, Gating behavior of coupled cardiac ryanodine receptors is not altered by luminal calcium

11.00-11.30 **Coffee break and posters**

11.30-12.30

- O7** A. Mišák, M. Grman, E. Máleková, Z. Tomášková, K. Ondriaš, pH-modulation of single-channel properties of anion channels derived from inner mitochondrial membranes of the rat heart
- O8** R. Janiček, M. Hořka, A. Zahradníková, Jr., A. Zahradníková, I. Zahradník, SpikeAnalyzer – the MATLAB-based analysis software for calcium spikes
- O9** M. Hořka, I. Zahradník, Software suite for analysis of fluctuations in electrical properties of cells

13.00-14.30 **Lunch**

3. Biophysics of DNA and Proteins

Chair: A. Chorvátová, K. Ondriaš

15.00-15.45

Tutorial Lecture

- T3** V. Víglaský, General insight to G-quadruplex structure: biophysical and biological aspects

15.45-16.30

- O10** Z. Gažová, K. Šipošová, Antošová, D. Fedunová, J. Bágel'ová, J. Imrich, Inhibitors of protein amyloid aggregation
- O11** D. Jancura, V. Berka, J. Staničová, M. Fabian, Functional equivalence of as „isolated“ and “high-energy” metastable states of the oxidized mitochondrial cytochrome c oxidase

16.30-17.00 **Coffee break and posters**

17.00-17.40

- O12** P. Šebest, H. Pivoňková, M. Fojta, The stability of the p53 protein complexes with DNA substrates against salt-induced dissociation
- O13** H. Pivoňková, K. Němcová, P. Šebest, M. Fojta, Electrochemical immunoprecipitation assays for DNA-protein interactions

17.45-18.45 **General Assembly of the Slovak Biophysical Society**

19.30 **Symposium Dinner**

Wednesday, March 21, 2012

4. New Spectroscopic Techniques

Chairs: D. Chorvát, P. Miškovský.

09.30-10.15

Tutorial Lecture

T4 V. Baumruk, Solution structure and dynamics of biomolecules from Raman optical activity

10.15-11.35

O14 A. Strejčková, G. Bánó, J. Staničová, K. Štroffeková, G. Fabriciová, P. Miškovský, Hypericin fluorescence in bilayer lipid membranes

O15 L. Dzurová, V. Huntošová, D. Petrovajová, P. Miškovský, Competition of anti-apoptotic protein kinase C α and pro-apoptotic protein kinase C δ in hypericin induced photodynamic action in U-87 MG

O16 Z. Jurašková, C. Domingo, J. V. García-Ramos, S. Sánchez-Cortés, *In situ* SERS detection of natural organic dyes and pigments in Cultural Heritage objects

O17 J. Horilová, M. Bučko, A. Illéssová, D. Chorvát, A. Chorvátová, Time-resolved measurements of endogenous NAD(P)H fluorescence in living systems

11.35-12.10 **Coffee break**

5. Education in Biophysics

Chairs: **T. Hianik**, **P. Miškovský**

12.10-13.30

O18 D. Chorvát, LASERLAB-EUROPE working modes and opportunities

O19 A. Chorvátová, Inauguration of SPIE Student Chapter in Slovakia

O20 J. Jakuš, PhD study in medical biophysics in Jesenius Medical Faculty of Comenius University in Martin

O21 T. Hianik, PhD study in biophysics in FMFI UK

O22 P. Miškovský, PhD study in biophysics in Faculty of Natural Sciences of Safarik University

General discussion

13.30 Closing ceremony

14.00 Lunch

ABSTRACTS

SKBS YOUNG RESEARCHER PRIZE LECTURE

M. Šimera, M. Veterník, I. Poliaček, and J. Jakuš, Study of the antitussive effect of codeine in the brainstem in the anaesthetized animals

TUTORIAL LECTURES

- T1** **M. Kopáni**, J. Dekan, M. Miglierini, L. Dlhan, R. Boca, M. Caplovicova, V. Sisovsky, J. Jakubovsky, Iron oxides particles in human brain
- T2** **V. Frečer**, P. Seneci, S. Miertuš, Computer-assisted combinatorial design of inhibitors of thymidine monophosphate kinase of *Mycobacterium tuberculosis*
- T3** **V. Víglaský**, General insight to G-quadruplex structure: biophysical and biological aspects
- T4** **V. Baumruk**, Solution structure and dynamics of biomolecules from Raman optical activity

SHORT ORAL PRESENTATIONS

- O1** N. Višňovcová, V. Jakušová, **N. Višňovcová Jr.**, J. Jakuš, Effects of high energy radiation on the organ systems in human medicine
- O2** **I. Waculiková**, O. Uličná, Z. Tomášková, M. Grman, O. Vančová, K. Ondriaš, Voltammetric measurements of mitochondrial (dys)function in studying the effects of external stimuli
- O3** **K. Ondriaš**, A. Mišák, M. Grman, N. Pronayová, T. Liptaj, On the H₂S-NO interaction and the effects of thiols
- O4** **M. Grman**, A. Mišák, K. Ondriaš, Effect of pH, thiols and oxygen on the H₂S/HS⁻ induced NO release from S-nitrosoglutathione
- O5** M. Karmazinova, S. Beyl, N. Klugbauer, S Hering, **L. Lacinova**, Cysteines in the extracellular loop in domain I of the Ca_v3.1 channel are essential for channel opening
- O6** **M. Gaburjaková**, J. Gaburjaková, Gating behavior of coupled cardiac ryanodine receptors is not altered by luminal calcium
- O7** **A. Mišák**, M. Grman, E. Máleková, Z. Tomášková, K. Ondriaš, pH-modulation of single-channel properties of anion channels derived from inner mitochondrial membranes of the rat heart
- O8** **R. Janíček**, M. Hořka, A. Zahradníková, Jr., A. Zahradníková, I. Zahradník, SpikeAnalyzer – the MATLAB-based analysis software for calcium spikes
- O9** **M. Hořka**, I. Zahradník, Software suite for analysis of fluctuations in electrical properties of cells
- O10** **Z. Gažová**, K. Šipošová, Antošová, D. Fedunová, J. Bágel'ová, J. Imrich, Inhibitors of protein amyloid aggregation
- O11** **D. Jancura**, V. Berka, J. Staničová, M. Fabian, Functional equivalence of as „isolated“ and “high-energy” metastable states of the oxidized mitochondrial cytochrome c oxidase
- O12** **P. Šebest**, H. Pivoňková, M. Fojta, The stability of the p53 protein complexes with DNA substrates against salt-induced dissociation
- O13** **H. Pivoňková**, K. Němcová, P. Šebest, M. Fojta, Electrochemical

- immunoprecipitation assays for DNA-protein interactions
- O14** **A. Strejčková**, G. Bánó, J. Staničová, K. Štroffeková, G. Fabriciová, P. Miškovský, Hypericin fluorescence in bilayer lipid membranes
- O15** **L. Dzurová**, V. Huntošová, D. Petrovajová, P. Miškovský, Competition of anti-apoptotic protein kinase C α and pro-apoptotic protein kinase C δ in hypericin induced photodynamic action in U-87 MG
- O16** **Z. Jurašková**, C. Domingo, J. V. García-Ramos, S. Sánchez-Cortés, *In situ* SERS detection of natural organic dyes and pigments in Cultural Heritage objects
- O17** **J. Horilová**, M. Bučko, A. Illésová, D. Chorvát, A. Chorvátová, Time-resolved measurements of endogenous NAD(P)H fluorescence in living systems
- O18** **D. Chorvát**, LASERLAB-EUROPE working modes and opportunities
- O19** **A. Chorvátová**, Inauguration of SPIE Student Chapter in Slovakia
- O20** **J. Jakuš**, PhD study in medical biophysics in Jesenius Medical Faculty of Comenius University in Martin
- O21** **T. Hianik**, PhD study in biophysics in FMFI UK

POSTERS

- P1:** L. Balogová, M. Maslaňáková, P. Miškovský, K. Štroffeková, Proapoptotic proteins distribution in U-87 MG glioma cells before and after photodynamic action
- P2:** L. Dzurová, D. Petrovajová, K. Štroffeková, Z. Naďová, P. Miškovský, Activity of PKC isoforms in U-87MG glioma cells before and after PDT treatment- Western blot study
- P3:** I. Čavarga, B. Bilčík, P. Výboh, P. Miškovský, Ľ. Košťál, P. Kasák, B. Čunderlíková, P. Mlkvý, A. Mateášik, D. Chorvát, A. Chorvátová, The use chorioallantoic membrane of quail embryo as an *in vivo* model for the study of photodynamically active drugs
- P4:** M. Zvarík, L. Šikurová, Ľ. Hunáková, D. Martinický, Changes in synchronous fluorescence spectra of human urine induced by ovarian tumors
- P5:** M. Uherek, L. Šikurová, O. Uličná, A study of fish oil influence on aorta fluorescence of healthy and diabetic rats
- P6:** M. Morvová, L. Šikurová, Measurement of fluorescence anisotropy as a parameter of membrane fluidity in patients with chronic kidney disease
- P7:** D. Fedunová, P. Huba, J. Bágeľová, M. Antalík, Thioflavin as probe for different biophysical processes
- P8:** K. Šipošová, M. Kubovčíková, Z. Bednáriková, A. Antošová, M. Koneracká, V. Závašová, P. Kopčanský, Z. Daxnerová, Z. Gažová, Magnetic fluid targets insulin-related amyloidosis
- P9:** J. Sukeľová, Z. Nichtová, M. Novotová, I. Zahradník, Implementation of the method of correlative light/electron microscopy on the same cell
- P10:** H. Vrbovská, A. Olas, M. Babincová, Interaction of magnetic nanostructures with antioxidants: Risks, benefits, and possible therapeutic applications
- P11:** J. Gallová, C. Ďurčovičová, P. Balgavý, Partial molecular volumes of DMPC and cholesterol in mixed bilayers
- P12:** Z. Garaiová, D. Wrobel, I. Waczulíková, M. Ionov, M. Bryszewska, T. Hianik, Fluorescence anisotropy measurements of lipid vesicles incorporated calixarenes
- P13:** A. Poturnayová, M. Šnejdárková, I. Neudlinger, A. Ebner, T. Hianik, AFM imaging of lipid layers containing calixarenes after addition of cytochrome c
- P14:** M. Šnejdárková, A. Poturnayová, I. Neundlinger, A. Ebner, T. Hianik, DNA-aptamers: sensitive tool for thrombin detection by quartz crystal microbalance
- P15:** G. Castillo, A. Miodek, H. Dorizon, H. Korri-Youssoufi, T. Hianik, Functionalization of multiwalled carbon nanotubes with dendrimers for aptamer-based biosensor sensitive to human cellular prions
- P16:** L. Navratilova, M. Adamik, M. Brazdova, H. Pivonkova, M. Fojta, Binding of p53 (wt/mut), p63 and p73 to different DNA substrates
- P17:** M. Veterník, M. Šimera, J. Jakuš, I. Poliaček, Effect of moving average window width on integration of EMG signal
- P18** D. Račko, Effect of confinement on molecular mobility and free volume as seen by computer simulations and positron annihilation lifetime spectroscopy
- P19** C. Uličná, J. Uličný, Quantitative proteomics and integration of systems biology models - our first experience

SKBS YOUNG RESEARCHER PRIZE LECTURE

Study of the antitussive effect of codeine in the brainstem in the anesthetized animals.

M. Šimera, M. Veterník, I. Poliaček, J. Jakuš

Department of Medical Biophysics, Jessenius Faculty of Medicine, Comenius University, Malá Hora 4, 036 01 Martin, Slovakia, e-mail: simera@jfmed.uniba.sk

Neural circuits controlling breathing and respiratory reflexes such as cough are organized within a network of respiratory-related neurones in the brainstem. This central nervous mechanism known as the respiratory central pattern generator (CPG) extends from the pons to the lower medulla [1]. The brainstem respiratory network has rhythmogenic capability probably at multiple hierarchical levels, which together with complexity and adaptability enables large system flexibility depending on physiological and metabolic conditions [1]. The basic elements of the CPG are brainstem respiratory neurones with dynamic interactions between pre-Bötzinger complex (pre-BötC) containing pacemaker inspiratory neurones, the rostral ventral respiratory group (rVRG) with mainly inspiratory neurones and the retrotrapezoid/parafacial respiratory group (RTN/pFRG) which control the active expiration and play an important role in central chemosensitivity [2,3,4]. Population of the pre-BötC inspiratory neurones provide an inhibition within the respiratory network, and the population of the BötC thus generates expiratory inhibition [1]. Mentioned brainstem regions are connected with the nuclei of the solitary tract (NTS), which are innervated by visceral inputs from peripheral receptors located within the gastrointestinal, gustatory, cardiovascular and pulmonary/respiratory systems, and reflexly affect an autonomic motor outputs, controlling also breathing and airway resistance [5,6].

Central antitussives such as codeine modulate cough-related neuronal network at the level of brainstem (mentioned before), where the basic neural circuitry responsible for generation of cough is located [7]. Codeine binds mainly to μ -, but also to δ - and κ -opioid receptors with different affinities [5, 8, 9]. E.g. μ -opioid receptors are located in the ambiguous nucleus, NTS, the dorsal vagal nerve nucleus, the medial parabrachial nucleus, and the raphe nuclei. Similar or less density of the κ -opioid receptors is placed in these region, too. δ -opioid receptors are generally less expressed in the brainstem, being sparsely found in NTS. Contrary the pneumotaxic center, including the nucleus parabrachialis, contains a very high density of δ -binding sites [10].

There are several reports [5,11,12] indicating that opioids inhibit synaptic transmission by decreasing a transmitter release from presynaptic terminals, also activate K^+ channels in the presynaptic terminals and inhibit N- and P/Q-type Ca^{2+} channels. Since μ -opioid receptors are predominantly expressed within NTS region [5,13], it seems the cough reflex induced by mechanical stimulation of the "the cough receptors" can be attenuated by codeine at NTS level *via* an inhibition of glutamatergic transmission. Gaba-ergic, serotonergic systems and activity of NMDA receptors also play an important role in the mechanism of action of antitussive drugs [10,14]. Central action of codeine and another central antitussives is deduced from their much higher efficiency when they are administered centrally (either *via* the vertebral or carotid arteries or intracerebroventricularly – i.c.v.), compared to their intravenous (i.v.) route of application [15].

Our previous results [16] in anesthetized rabbits confirmed the central antitussive effect of codeine with the effective cumulative dose necessary for 50% reduction of cough number in doses of 3.9 mg/kg and 0.11 mg/kg following (i.v.) and (i.c.v.) administrations, respectively. It represents about 35-fold higher efficacy of i.c.v. in comparison with i.v. application. We did not detect significant changes in analyzed temporary parameters of the cough, however, the tendency to prolong the quiescent periods of the cough expiratory phase

and the total cough cycle durations were proved. No significant changes in single expiratory responses as well as no alteration in parameters of the sneeze reflex were established. Very low sensitivity of sneeze and possibly the expiration reflex to codeine were proved, too. Pretreatment by Naloxone (an μ -opioid receptor competitive antagonist) regularly abolished the antitussive effect of the codeine in rabbits (Fig. 1). Our findings confirmed the involvement of μ -opioid mechanism mediating the central antitussive effect of codeine in this animal species.

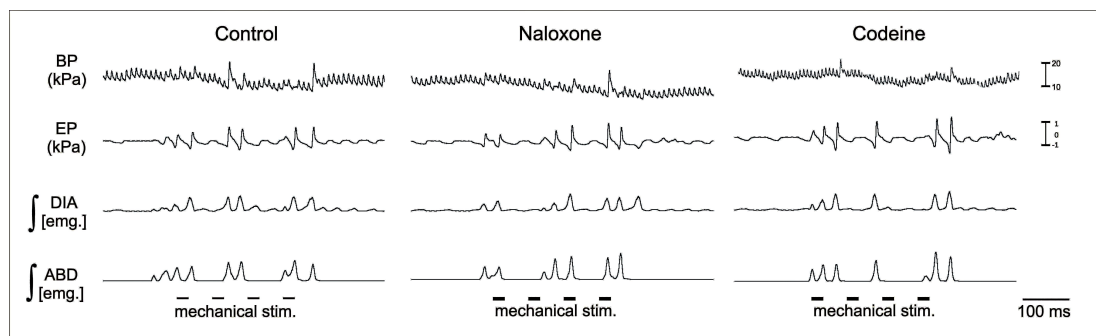


Fig. 1. Pretreatment by naloxone (4 mg/kg i.v.) abolished the antitussive effect of the codeine in rabbits. (7 mg/kg i.v. dose > ED50%). BP – blood pressure, EP – esophageal pressure, ∫DIA, ∫ABD emg. – integrated electromyographic activity of the diafragma and the abdominal muscles.

Acknowledgement

This work was supported by the Slovak Grant Agency VEGA, project No. 1/0038/09 (prof. Jakuš). The project is co-financed from EU sources – ERDF – European Regional Developmental Fund.

References

- [1] J.C. Smith, A.P. Abdala, I.A. Rybak, J.F. Paton. *Phil. Trans R Soc. Lond. B Biol. Sci.* 364 (2009) 2577-2587.
- [2] N.M. Mellen, M.T. Brisson, *Current Opinion in Neurobiology* 22 (2012) 1–10
- [3] J. Jakuš, *Neurónové mechanizmy dýchania a respiračných reflexov*. UK Bratislava, 1999.
- [4] A.L. Bianchi, L. Grélot, S. Iscoe, J.E. Remmers, *J. Physiol.* 407 (1988) 293-310.
- [5] Y. Ohi, F. Kato, A. Haji, *Neuroscience* 146 (2007) 1425–1433.
- [6] F.R. Paton, *Experimental Physiology* 84 (1999) 815 -833.
- [7] D.C. Bolser, J.A. Hey, R.W. Chapman, *Appl. Physiol.* 86 (1999) 1017-1024.
- [8] H. Schmidt, S. Vormfelde, K. Klinder, U. Gundert-Remy, C.H. Gleiter, G. Skopp, R. Aderjan, U. Fuhr, *Pharm. Toxicol.* 91 (2002) 57–63.
- [9] C. Mignat, U. Wille, A. Ziegler, *Life Sci.* 56 (1995) 793–799.
- [10] K. Takahama, T. Shirasaki, *Cough.* 3 (2007) 8.
- [11] K.Z. Shen, S.W. Johnson, *J. Physiol.* 541 (2002) 219–230.
- [12] T. Endoh, *Br. J. Pharmacol.* 147 (2006) 391–401.
- [13] S.A. Aicher, A. Goldberg, S. Sharma, V.M. Pickel, *J. Comp. Neurol.* 422 (2000) 181–190.
- [14] G. Nosalova, *Bratisl Lek Listy.* 99 (1998) 531-535 (in Slovak).
- [15] D.C. Bolser, F.C. Degennaro, S. O'Reilly, J.A. Hey, R.W. Chapman, *Eur. J. Pharmacol.* 277 (1995) 159-164.
- [16] M. Simera, I. Poliacek, J. Jakus, *Eur. J. Med. Res.* 15 Suppl 2 (2010) 184-188.

T1

Iron oxides particles in human brain

M. Kopani¹, J. Dekan², M. Migliorini^{2,3}, L. Dlhán⁴, R. Boca⁴, M. Caplovicová⁵,
V. Sisovsky¹, J. Jakubovsky¹

¹Department of Pathology, Faculty of Medicine, Comenius University, Sasinkova 4, 811 08 Bratislava, Slovakia, e-mail: martin.kopani@fmed.uniba.sk

²Institute of Nuclear and Physical Engineering, Faculty of Electrical Engineering and Information Technology, Slovak University of Technology, Bratislava, Slovakia,

³Regional Centre of Advanced Technologies and Materials, Palacky University, Olomouc, Czech Republic

⁴Department of Inorganic Chemistry, Faculty of Chemical and Food Technology, Slovak University of Technology, Bratislava, Slovakia,

⁵Department of Geology of Mineral Deposits, Faculty of Natural Sciences, Comenius University, Bratislava, Slovakia,

Introduction

Iron is the most important metal with high concentration in some regions of the brain. The basal ganglia have the highest iron concentrations in the brain, particularly the globus pallidus and substantia nigra. Iron catalyzes reactions forming reactive oxygen species and is one of the major factors associated with neurodegenerative disease [1]. But its activity depends greatly on its ligand-based environment.

Results**Histochemical analysis**

Sites of Fe(III) and Fe(II) accumulation in the samples of human *basal ganglia* showed round, lamellar hematoxylin and eosine positive structures with the size of 15-40 μm . Iron positive sites revealed PAS (neutral) and Alcian blue (acidic glycoconjugates) positive round structures with diameter from 5-25 μm . Histochemical analysis revealed both sulphated and carboxylated glycoconjugates. Ag-NOR staining revealed sporadically argyrophilic positive black round deposits in the form of iron phosphate (ferritin). The size of these deposits was 5-20 μm . Scanning electron microscope with EDX microanalysis showed the occurrence of regular globular iron positive deposits of the size from 5-10 μm .

Mössbauer spectrometry

⁵⁷Fe Mössbauer spectra were taken from suitably prepared samples at room temperature using a standard constant acceleration spectrometer with ⁵⁷Co/Rh source. Transmission geometry was used. The spectra were first recorded in high velocity range (± 10.5 mm/s) to check for possible occurrence of magnetically active iron compounds. They were not identified which means that the size of probable Fe-containing structures should be lower than several nanometres. Consequently, Mössbauer spectra were acquired at lower velocity range (± 3 mm/s) to allow more precise identification of iron structural positions. All investigated samples exhibit quadrupole doublets.

A typical example of a room temperature Mössbauer spectrum (male, 26 years) is shown in Fig. 1. Decomposition of the spectra into their components has demonstrated a presence of two different doublets, i.e. structural positions of the resonant atoms. They mainly belong to Fe(II) high spin states but in some samples also Fe(III), and Fe³⁺ tetrahedral structural positions as well as ferrihydrite were revealed. According to the spectral parameters (isomer shift and quadrupole splitting), Fe(II) atoms are localised in five distinct positions.

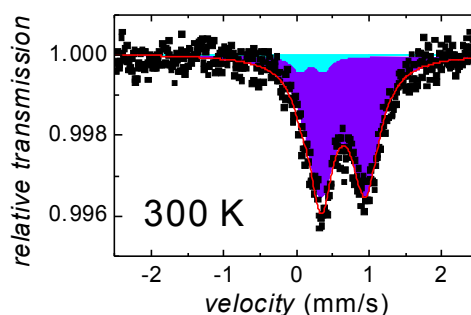


Fig. 1. ^{57}Fe Mössbauer spectrum of male basal ganglia, 26 years old taken at 300 K.

SQUID magnetometry

The samples of *basal ganglia* showed a dominating diamagnetism and/or paramagnetism superimposed by a ferromagnetic impurity (probably magnetite). The hysteresis loop has a complex shape that alters with temperature (Fig. 2).

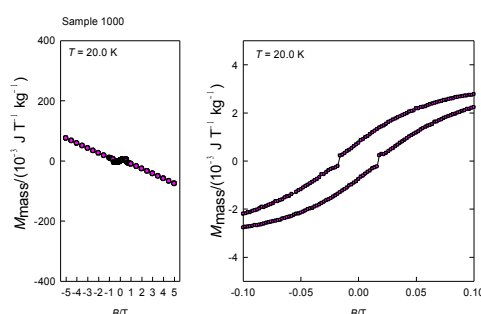


Fig. 2 Hysteresis curves of female basal ganglia, 83 years old taken at 300 K at 20 K.

Discussion

Eosinophilic and argyrophilic spheroid-like structures and iron pigment in monkeys globus pallidus were found by many authors regardless of the presence of diseases or conditions and are associated with iron mediated oxidative stress [2]. Our histochemical findings indicate the presence of iron accumulation in the physiological form (ferritin). Mössbauer spectra and SQUID measurements show the presence of various forms of iron compounds.

Glycoconjugates are complex macromolecules containing oligosaccharides side chains covalently linked to a protein backbone. Polysaccharides interact with Fe(III) cations to form water soluble complexes or serve as template assembly of nanocrystals. Presence of glycoconjugates in the samples is result of elimination and inactivation of iron as inductor of reactive oxygen species and can be useful neuroprotective agent in CNS degradation.

Acknowledgement

This work was supported by the Slovak Grant Agency VEGA, projects 1/0220/12, 1/1265/10, by the Slovak Research and Development Agency under the contract No. APVV-0111-10, project CZ.1.05/2.1.00/03.0058.

References

- [1] D.G. Jo, J.Y. Lee, Y.M. Hong, S. Song, I. Mook-Jung, J.Y. Koh, Y.K. Jung J Neurochem 88 (2004) 604–611
- [2] K. Kaneko, K. Yoshida, K. Arima, S. Ohara, H. Miyajima, T. Kato, M. Ohta, S. Ikeda, J Neuropathol Exp Neurol 61 (2002) 1069–1077

T2

Computer-assisted combinatorial design of inhibitors of thymidine monophosphate kinase of *Mycobacterium tuberculosis*

V. Frečer^{1,2}, P. Seneci³, S. Miertuš⁴

¹ Department of Physical Chemistry of Drugs, Faculty of Pharmacy, Comenius University, Odbojárov 10, 832 32 Bratislava, Slovakia, e-mail: frecer@fpharm.uniba.sk

² Cancer Research Institute, Slovak Academy of Sciences, Vlárská 7, 833 91 Bratislava, Slovakia

³ Department of Organic and Industrial Chemistry, University of Milan, 20133 Milan, Italy

⁴ International Centre for Applied Research and Sustainable Technology, 841 04 Bratislava, Slovakia

It is estimated that about one-third of the world's population is currently infected with *Mycobacterium tuberculosis* (MTB), the causative agent of tuberculosis (TB). TB is an airborne disease leading annually to more than 9 million infections and claiming almost 2 million of lives each year [1]. Currently active TB is treated with first-line drugs introduced to clinical practice more than 4 decades ago and requires treatment with duration of at least six months. According to WHO, up to 80% of the treated TB cases develop drug-resistance [2]. Extended treatment for up to two years is needed for cases infected with multidrug-resistant (MDR) and extensively drug-resistant (XDR) strains, using expensive injectable second-line drugs with much more severe side effects [3]. Consequently, TB has re-emerged as a serious public health threat worldwide.

The global emergency posed by the M/XDR TB has stimulated the search for new targets and discovery of innovative more effective antibiotic drugs. Determination of the complete genome sequence of MTB strain H37Rv allowed identification of new potential anti-mycobacterial drug targets [4]. *M. tuberculosis* thymidine monophosphate kinase (TMPK_{mt}) has emerged as an attractive target [5]. It catalyses the phosphorylation of deoxythymidine monophosphate (dTMP) to deoxythymidine diphosphate utilizing adenosine triphosphate as the phosphoryl donor. This step lies at the junction of the de novo and salvage pathways of deoxythymidine triphosphate (dTTP) metabolism and is the last specific enzyme for its synthesis [6]. TMPK_{mt} was shown to be essential in providing the bacteria with dTTP and for DNA synthesis [5]. Low sequence identity (22%) of TMPK_{mt} with its human isozyme and identification of 3'-azido-2'-deoxythymidine monophosphate (AZTMP, inhibition constant $K_i = 10 \mu\text{M}$, Figure 1) as a selective competitive inhibitor made TMPK_{mt} an attractive target for blocking the mycobacterial DNA synthesis [5-7].

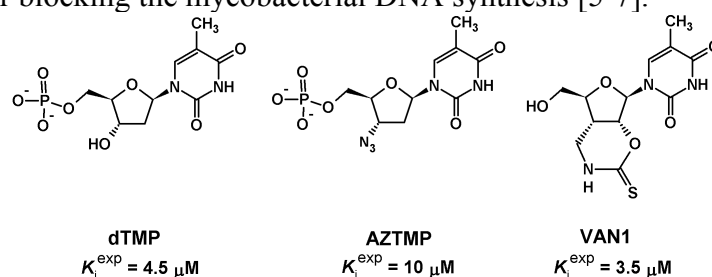


Figure 1. Chemical structures of the substrate and of competitive inhibitors of TMPK_{mt} [5,8,9].

The three-dimensional structure of TMPK_{mt} bound to dTMP was solved, thus allowing to perform structure-based drug design studies [7,10]. The active site of TMPK_{mt} complexed with dTMP displays a fully closed conformation and contains an Mg^{2+} ion that is responsible for positioning the phosphate oxygens of dTMP. Closer examination of the catalytic site revealed that the main interactions between dTMP and the enzyme include a stacking interaction between the pyrimidine ring of thymine and Phe70, as well as a number of hydrogen bonds.

In this work we have carried out computer-assisted combinatorial design of bicyclic thymidine analogs as inhibitors of the TMPK_{mt} [11]. We have explored the chemical space around the 2', 3'-bicyclic thymidine nucleus by designing and *in silico* screening of a virtual

focused library selected via structure-based methods to identify more potent analogs endowed with favorable ADME-related properties. In all the library members we have exchanged the ribose ring of the template with a cyclopentane moiety that is less prone to enzymatic degradation. In addition, we have replaced the six-membered 2', 3'-ring by a number of five-membered and six-membered heterocyclic rings containing alternative proton donor and acceptor groups, to exploit the interaction with the carboxylate groups of Asp9 and Asp163 as well as with several cationic residues present in the vicinity of the TMPK_{mt} binding site. The three-dimensional structure of the TMPK_{mt} complexed with 5-hydroxymethyl-dUMP, an analog of dTMP, was employed to develop a QSAR model, to parameterize a scoring function specific for the TMPK_{mt} target and to select analogues which display the highest predicted binding to the target. As a result, we identified a small highly focused combinatorial subset of bicyclic thymidine analogues as virtual hits that are predicted to inhibit the mycobacterial TMPK in the submicromolar concentration range and to display favorable ADME-related properties (Figure 2).

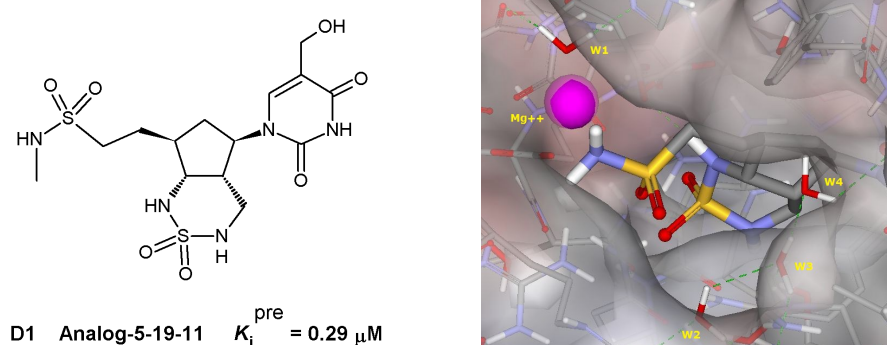


Figure 2. Chemical structure of the best designed analog D1 (left). D1 docked to the active site of the TMPK_{mt} receptor (right).

Acknowledgement

This work was partially supported by the Slovak Grant Agency VEGA, project No. 2/0153/11.

References

- [1] A. M. Ginsberg, M. Spigelman, *Nat. Med.* 13 (2007) 290-294.
- [2] WHO Global Task Force: Outlines Measures to Combat XDR-TB Worldwide (2006) WHO press release, World Health Organization, Geneva, <http://www.who.int/mediacentre/news/notes/2006/np29/en/>
- [3] C. D. Mitnick, B. McGee, C. A. Peloquin, *Expert Opin. Pharmacother.* 10 (2009) 381-401.
- [4] S. T. Cole, R. Brosch, J. Parkhill, T. Garnier, C. Churcher, D. Harris, S. V. Gordon, K. Eiglmeier, S. Gas, C. Barry III, C. F. Tekaia, K. Badcock, D. Basham, D. Brown, D. T. Chillingworth, R. Connor, R. Davies, K. Devlin, T. Feltwell, S. Gentles, N. Hamlin, S. Holroyd, T. Hornsby, K. Jagels, B. G. Barrell, *Nature* 393 (1998) 537-544.
- [5] H. Munier-Lehmann, A. Chafotte, S. Pochet, G. Labesse, *Protein Sci.* 10 (2001) 1195-1205.
- [6] E. Anderson, in *The Enzymes*, vol. 8, P. D. Boyer PD (Ed.), Academic Press, New York, 1973.
- [7] I. Li de la Sierra, H. Munier-Lehmann, A. M. Gilles, O. Barzu, M. Delarue, *J. Mol. Biol.* 311 (2001) 87-100.
- [8] V. Vanheusden, H. Munier-Lehmann, S. Pochet, P. Herdewijna, S. Van Calenbergh, *Bioorg. Med. Chem. Lett.* 12 (2002) 2695-2698.
- [9] V. Vanheusden, H. Munier-Lehmann, M. Froeyen, R. Busson, J. Rozenski, P. Herdewijn, S. Van Calenbergh, *J. Med. Chem.* 47 (2004) 6187-6194.
- [10] I. Li de la Sierra, H. Munier-Lehmann, A. M. Gilles, O. Barzu, M. Delarue, *Acta Crystallogr. Sect. D Biol. Crystallogr.* 56 (2000) 226-228.
- [11] V. Frecer, P. Seneci, S. Miertus, *J. Comput. Aided Mol. Des.* 25 (2011) 31-49.

T3

General insight to G-quadruplex structure: biophysical and biological aspectsV. Víglašký

Department of Biochemistry, Institute of Chemistry, Faculty of Science, P. J. šafarik University, Moyzesova 11, 040 01 Košice, Slovakia, e-mail: viktor.viglasky@upjs.sk

G-rich DNA sequences can fold into secondary structures so-called G-quadruplexes. These structural motifs are four-stranded and they are stabilized by the stacking of guanine G-quartets and extensive Hoogsteen hydrogen bonding. At the beginning G-quadruplexes were simply a structural curiosity, but recently it has become clear that they play important physiological roles. This interest has been reflected in the rate of publications with an exponential growth in the number of articles mentioning the term G-quadruplex over the past decade. These unusual DNA motifs are believed to be involved in a variety of biological functions; it is suggested that they may also be important causal factors in cell aging and human diseases such as cancer [1,2].

Considerable circumstantial evidence suggests that these structures can exist *in vivo* in specific regions of the genome including the telomeric ends of chromosomes, many oncogene regulatory regions and RNA transcripts. There is also evidence that telomeres serve as a type of biological clock, as the telomere structures appear to become shorter with each successive cell cycle. In immortalized cells and in cancer cells, however, telomerase is activated to maintain the length of the telomere [3]. Higher-order DNA and RNA G-quadruplexes are attractive anticancer drug targets. A highly G-rich regions are frequently located upstream of many oncogenic promoters and it is believed that it is G-quadruplex formation, and not the sequence itself, that plays an important role in the transcriptional regulation. The quadruplex-forming sequence shows a high level of sequence conservation across mammals (human, mouse, rat, and chimpanzee) and viruses [4]. Many recent studies have demonstrated that small molecules can facilitate the formation of, and stabilize, G-quadruplexes. [5] Therefore, these structures have become an attractive target for the anticancer drugs, because it effectively inhibits telomerase activity.

G-quadruplexes show extreme structural variability and we now have only poor information about their formation. For example telomeric DNA can spontaneously assemble into a number of different G-quadruplex conformations, as can be monitored by NMR, X-ray crystallography, atomic absorption spectroscopy, FRET and CD spectral analysis. We analyzed different telomeric, viral and oncogenic G-quadruplex forming sequences in the presence of Na⁺, K⁺ and PEG 200 by using UV absorption spectroscopy, circular dichroism and electrophoretic methods. The presence of multiple G-quadruplex conformations in solution was observed, making structural elucidation difficult. Temperature gradient gel electrophoresis (TGGE) was used for the elucidation of structural variability and thermal stability of quadruplex conformers. TGGE allows us to separate and evaluate the most abundant conformers and to obtain relevant thermodynamic parameters [6]. Our work describes the structural diversity and folding of quadruplexes, and it examines fundamental aspects of topology and the emerging relationships with sequence.

Acknowledgement. This work was supported by the Slovak Grant Agency VEGA, project No. 1/0504/12

References

- [1] N. Grandin, M. Charbonneau, *Biochimie* 90 (2008) 41–59.
- [2] M. J. McEachern, A. Krauskopf, E. H. Blackburn, *Annu. Rev. Genet.* 34 (2000) 331–358.
- [3] J. A. Londono-Vallejo, J. A., *Biochimie* 90 (2008) 73–82.
- [4] H. Fernando, A. P. Reszka, J. Huppert, S. Ladame, S. Rankin, A. R. Venkitaraman, S. Neidle, S. Balasubramanian, *Biochemistry* 45 (2006) 7854–7860.
- [5] S. M. Haider, S. Neidle, G. N. Parkinson, *Biochimie* 93 (2011) 1239–1251.
- [6] V. Víglašký, L. Bauer, K. Tluczková, *Biochemistry* 49 (2010) 2110–2120.

T4

Solution structure and dynamics of biomolecules from Raman optical activityV. Baumruk

Institute of Physics, Faculty of Mathematics and Physics, Charles University in Prague, Ke Karlovu 5, 121 16 Prague 2, Czech Republic, e-mail: baumruk@karlov.mff.cuni.cz

Raman optical activity (ROA) is a chirality related variant of vibrational spectroscopy which measures small intensity difference of Raman scattering from chiral molecules in right and left circularly polarized incident light or, alternatively, a small circular component in the scattered light [1]. ROA is closely related to its companion effect, the vibrational circular dichroism (VCD), and these two techniques together form a wider branch of vibrational spectroscopy known as vibrational optical activity (VOA) [2]. The VOA spectrum of a chiral molecule contains up to $3N-6$ fundamental bands (N being the number of atoms), each associated with a specific normal mode of vibration. These contain information on conformation and absolute configuration of the particular part of the structure embraced by the normal mode in question. Unlike electronic optical activity, VOA probes the stereochemistry of molecular framework locally. The enormous increase of stereochemical information content in the VOA spectrum thus represents its primary advantage when compared to conventional electronic CD.

The attempts to extract structural information embedded in ROA spectra of biological systems range from totally empirical correlations to fully theoretical predictions. For proteins, principal component analysis (PCA) approach (based on pattern recognition) has been developed to identify protein folds from ROA spectral band shapes [3]. At the same time, at least for short peptides, full *ab initio* quantum mechanical ROA simulations are possible and computational protocols now provide sufficiently impressive results to suggest that ROA measurements together with theoretical simulations will become the method of choice for determination of aqueous solution structure, at least for small biomolecules [4]. Simulation of ROA spectra is a complex process that involves several steps. Initially, a starting geometry is proposed. In this step for complex systems molecular mechanics was often successfully used. Then the starting geometry is optimized on a selected level of approximation (functionals in density functional theory (DFT), basis sets, solvent models, etc.). Harmonic approximation was used for frequency calculations. High precision of the computed force field (Hessian) is required for correct reproduction of the fine mode splitting that determines the ROA intensities. This could not be achieved without the use of realistic solvent model. It has been shown that simulation techniques considering system dynamics and averaging over molecular conformations and solvent configurations are able to provide Raman and ROA spectra of flexible and polar molecules in a good agreement with experiment in terms of correct band intensities, line widths and in case of ROA also signs [5].

Recently, we concentrated our efforts to study flexibility and dynamics of the three rotating side groups in alanine zwitterion, as such motion seems to be crucial for correct interpretation of Raman and ROA spectra [5]. Detailed analysis of Raman and ROA spectra of L-alanine zwitterion revealed that bandshapes are to a large extent determined by the rotation of NH_3^+ , CO_2^- and CH_3 groups. The bands exhibit different sensitivity to the motion of the rotating group; typically for more susceptible bands the Raman signal becomes broader and the ROA intensity decreases or even cancels. When these dynamical factors are taken into account in Boltzmann averaging of individual conformer contributions, simulated spectra agree better with experiment. Besides, spectra of zwitterionic dipeptides (Gly-Pro, Pro-Gly, Ala-Pro, Pro-Ala) suggest that the potential of this method to monitor molecular flexibility is retained even for larger systems.

Analysis of Raman and ROA spectra of poly-L-proline based on comparison of *ab*

initio simulations of spectral band positions and intensities confirmed presence of two conformers of the five-membered ring, which are approximately equally populated in the polypeptide [6]. Additionally, Raman and ROA spectral patterns indicated that the peptide adopts polyproline II helical conformation (PPII) both in aqueous and TFE solutions. The helix, however, is perturbed by fluctuations, which affects the vibrational coupling among amino acid residues and broadens the ROA bands. Contributions of the side and main peptide chains to the poly-L-proline ROA intensity have comparable magnitudes. Thus the understanding of the origins of both signals is important for determination of the peptide structure by ROA. To understand in detail the dependence of the secondary structure on the length and the interplay between the side chain and main chain conformation, zwitterionic (Pro)_N models (with $N = 2, 3, 4, 6, 9, 12$) were studied by combination of Raman and ROA spectroscopy with the density functional theory. Potential surfaces were systematically explored for the shorter oligoprolines, and Boltzmann conformational ratios were obtained both for the main chain and the proline ring puckering. The predictions were verified by comparison of the experimental and simulated ROA spectra [7].

Disulfide group is the only chromophore in proteins and peptides, which by itself exhibits inherent chirality and therefore should give rise to substantial chiroptical manifestation in electronic spectra. In practice, it is unfortunately not the case and especially the low energy CD bands of the disulfide group with the maximum at about 260 nm are low in intensity and rather broad. If we consider, in addition, the possible overlap with CD bands of aromatic chromophores of phenylalanine, tyrosine and tryptophan residues, it is not surprising that structure oriented application of electronic CD spectroscopy to a disulfide chromophore is quite difficult. Recently we scrutinized chiral disulfides by ROA. Raman spectroscopy is for this purpose rather promising already in its non chiral variant, but one should underline that the obtained information is not complete. In that way no information about ‘absolute conformation’ of the disulfide bridge can be acquired. We have identified features in ROA spectra which are associated with the S-S ($\sim 500 \text{ cm}^{-1}$) and C-S ($\sim 700 \text{ cm}^{-1}$) stretching vibrations. These allow us to infer the sense of disulfide twist in particular compounds when signs of ROA features are compared to ROA calculations on simple model disulfides [8] and verified by a comparison with spectra of disulfide-bridged cyclodextrins [9]. ROA signals in the S-S and C-S stretching vibration regions are observable also with neurohypophyseal hormones and their sign can be used to deduce the sense of disulfide twist.

Acknowledgement

This work was supported by the Czech Science Foundation (projects No. GA203/95/0105, GA203/01/0031, GA202/07/0732, GA203/07/1335, GAP205/10/1276 and GAP208/11/0105).

References

- [1] L. D. Barron, *Molecular Light Scattering and Optical Activity*. Cambridge University Press, Cambridge, 2004.
- [2] L. A. Nafie, *Vibrational Optical Activity. Principles and Applications*. J. Wiley & Sons, Chichester 1996.
- [3] E. W. Blanch, D. J. Robinson, L. Hecht, L. D. Barron, *J. Gen. Virol.* 83 (2002) 241-246.
- [4] J. Kapitán, V. Baumruk, V. Kopecký Jr., P. Bouř, *J. Phys. Chem. A* 110 (2006) 4689-4696.
- [5] J. Hudecová, J. Kapitán, V. Baumruk, R. P. Hammer, T. A. Keiderling, P. Bouř, *J. Phys. Chem. A* 114 (2010) 7642-7651.
- [6] J. Kapitán, V. Baumruk, P. Bouř, *J. Am. Chem. Soc.* 128 (2006) 2438-2443.
- [7] V. Profant, V. Baumruk, X. Li, M. Safařík, P. Bouř, *J. Chem. Phys. B* 115 (2011) 15079-15089.
- [8] L. Bednářová, P. Bouř, P. Maloň, *Chirality* 22 (2010) 514-526.
- [9] P. Maloň, L. Bednářová, M. Straka, L. Krejčí, L. Kumprecht, T. Kraus, M. Kubáňová, V. Baumruk, *Chirality* 22 (2010), E47-E55.

O1**Effects of high energy radiation on the organ systems in human medicine**

N. Višňovcová¹, V. Jakušová², N. Višňovcová Jr.³, J. Jakuš¹

¹Department of Medical Biophysics, Jessenius Faculty of Medicine, Comenius University, Malá Hora 4, 036 01 Martin, Slovakia, e-mail:nvisnovcova@jfmed.uniba.sk

²Department of Public Health, Jessenius Faculty of medicine, Comenius university, Sklabinská 2, 036 01 Martin, Slovakia

³Clinic of Pediatric Surgery, Faculty of Medicine, Comenius University, Kollárova 2, 036 01 Martin, Slovakia

Introduction

Treatment with ionizing radiation is after the surgery the second oldest treatment modality of the cancer therapy. After a paliative (non radical) surgery the ionizing radiation is a kind of effective treatment also in a case of breast carcinoma what is described as the primary radiotherapy of a mammary gland in a literature. More than 90 % of female patients underwent treatment by the high energy radiation have met with undesirable sides effects visible mainly on a skin. These reactions are manifested like skin erythema characterized by a red coloured skin, swelling, burning sensation, etc. The skin is dry, squamous, scurfy and can itch. [1, 4] Another undesirable sides effects can also develop such as wet squamous and painful skin with an exudative ulcers and necrosis. [1, 2, 4]. These skin reactions can influence a progress of the radiotherapy and even can hurt a general quality of a life of irradiated patient. Thus, proper management of a skin radiation side effects requires a multidisciplinary cooperation (between oncologist, physicist, radiology asistent and nurses psychologist, etc.) as an important part of a complex therapy. [3, 5]

Material and methods

We have observed 100 female patients being suffered from early state of a mammary gland carcinoma. Entering criteria were: age under 70 years, 100 % of the Karnofsky Score had excluded tumor bilaterality, tumors in stages T1 and T2. Female patients had finished non-radical surgery, consisting from quadrantectomy and excentration of the axilla (at 1. and 2. levels). In the patients an adjunct chemotherapy was applied (in those with a high relaps risk and the positive axillar nodes) as well as the curative radiotherapy afterwards. In our patients three phototypes of the skin were classified and consulted with the dermatologist. Patients were treated in a period 2009-2011 years, both at the Radiotherapy Clinic, Oncology Centre of the University hospital in Martin and at Clinic of Radiotherapy, Faculty hospital in Žilina. Median of patient's observation was 5 weeks (we observated an acute post-radiation changes on the skin, which originated from an irradiation. The radiotherapy was applied to all patients by the megavolt irradiator – the linear irradiator LINAC, the energy of the high energy radiation (HER) X rays was 6 MeV and 18 MeV in an average dose TD 43,44 Gy \pm 1,07 Gy, and by accelerated electrons an average dose 11,6 \pm 0,33 Gy such as boots. Female patients were irradiated by the technique of 2 tangential fields on the breast area and 2 opposite fields on the catchment area of the lymph nodes.

We have observed and wanted to determine the following parameters:

1. size of an average dose of high energy radiation (HER) and the level of breast skin change
2. relationship between localization and the level of a breast skin change

Results**Dependence of an average dose size and a level of breast skin change**

We observed that each average entering dose of HER (accelerated electrons and X rays) caused a presence of change level No.1 and 2 (Fig.1, Table 1). The changes were proved by a light macroscopy method (in accordance with RTOG/EORTC criteria).

No.1 level of the skin change risen up with an average dose of 37 Gy and the level of skin No.2 had appeared with an average dose of 44 Gy.

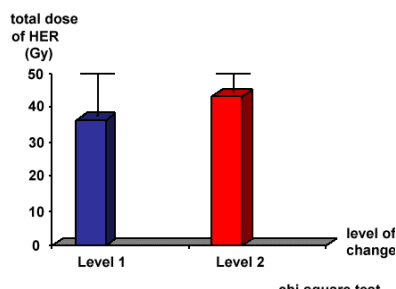


Fig. 1. Dependence of an average dose of high energy radiation (HER) and a level of skin change

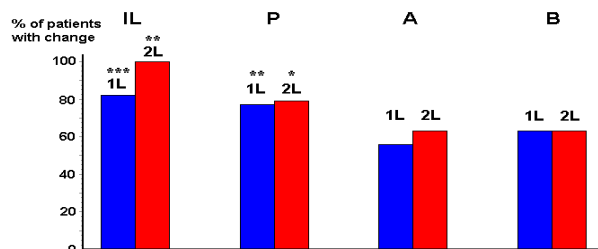


Fig. 2. Dependence of the localization on the breast skin and the change level statistics kruskal – wallis test

Table 1. Dependence of average dose size of HER (X rays and electrons) and a level of the skin change

Change level	Interval of dose (Gy)	Median (Gy)	SE	SD
level no.1	30 - 46	37	± 1,16	9,8
level no.2	42 - 46	44	± 1,07	5,3

Dependence of the localization of the breast skin and the change level

Another parameter, which we observed was a dependence of change level and a location of the change on the breast skin (Fig. 2, Table 2). We have assumed, that more frequent localization of the acute postradiation changes is placed in the intramammary breast line (because there is a connection of the breast skin with the skin on the thoracic area). Another frequent location we assumed is an area of the papilla. We have found, that area of the intramammary breast line and the papilla were significantly affected by the change levels No.1 and 2. and there is no significant dependence between the breast area and axilla and the change levels No.1 and 2.

Table 2 Dependence of the localization on the breast skin and the change level

Level of change	Intramammary Breast line	papilla	all breast	axilla
level n. 1	p = 0,001	p = 0,003	ns	ns
level n. 2	p = 0,003	ns	ns	ns

Conclusion

We approved the effectiveness of High Energy Radiation (X rays and accelerated electrons) in the radiotherapy of the breast carcinoma with a mean dose of Radiation 37 Gy and 44 Gy for Level No 1 and 2, respectively. In accordance with a high efficiency (and good economy) of HER therapy, it is important to think also on cosmetic and social effects of the therapy, as strong psychological factors for female patients.

References

- [1] D. James et al., Radiation Oncology Biology, Physic., 31 (1995) 1341-1346.
- [2] A. Trotti et al. Radiation Oncology Biology Physic, 47 (2000) 13-47.
- [3] U. Hoeller et al. Radiation Oncology Biology Physic, 55 (2003) 1013-1018.
- [4] J. McKayová, N. Hiranoová, Jak přežít chemoterapii a ožarování. 1.vyd. Praha: Triton, 2005.
- [5] Y.M. Hanna et al., Breast J., 8 (2002)149-153.

O2

Voltammetric measurements of mitochondrial (dys)function in studying the effects of external stimuli

I. Waczulíková¹, O. Uličná², Z. Tomášková³, M. Grman^{1,3}, O. Vančová², K. Ondriáš³

¹ Department of Nuclear Physics and Biophysics, Faculty of Mathematics, Physics and Informatics, Comenius University, Mlynská dolina F1, 842 48 Bratislava, Slovakia, e-mail: waczulikova@fmph.uniba.sk

² Pharmacobiochemical Laboratory of 3rd Department of Internal Medicine, Faculty of Medicine, Comenius University, Špitálska 24, 813 72 Bratislava, Slovakia.

³ Institute of Molecular Physiology and Genetics, Department of Cell Physiology and Genetics, Slovak Academy of Sciences, Vlarska 5, 833 34 Bratislava, Slovakia.

Background: Tissues, especially those with high-energy requirements, such as heart muscle, display enhanced vulnerability to any insult inducing deprivation of oxygen and/or metabolic substrates. Since mitochondrial functions are tightly integrated with cellular processes securing ionic and energetic homeostasis, in particular, efficient coupling of mitochondrial ATP production with cellular sites of ATP utilization and/or ATP sensing, any mitochondrial dysfunction, which disrupts cellular energy metabolism, may induce acute injury to the tissue or precipitate progression of degenerative disease states. Thus, assessing function of mitochondria has become of increasing significance in the biomedical science thus delivering valuable knowledge targeting both, clinical practice and basic research.

Method: A common approach to assess mitochondrial bioenergetic function is to measure mitochondrial respiration and coupling between respiration and phosphorylation (i.e. between electron transport and proton extrusion) using a Clark oxygen electrode [1]. Two parameters are usually used to quantify mitochondrial behaviour under various conditions: the 1st is the mitochondrial RCR - respiratory control ratio, defined as the respiration in state 3 (with ADP added) divided by that in state 4 (with ADP consumed). A high RCR indicates that the mitochondria have a high capacity for substrate oxidation and ATP production, which implies a tight coupling between respiration and phosphorylation and low proton leak. However, there is no absolute RCR value that is diagnostic of dysfunctional mitochondria - RCI values vary from 3 to 10, as they are dependent on the substrate and tissue, as well as on the quality of the preparation. The 2nd parameter is the ADP:O ratio (in nmol ADP·nAtO⁻¹). It indicates amount of ATP (mol) synthesized per mol of O (1/2O₂). It is determined by measuring the decrease in oxygen concentration during the rapid respiration after adding a known amount of ADP. This ratio is about 2.5 for NAD-linked substrates and about 1.5 for succinate. A derived parameter is the oxidative phosphorylation rate (OPR; in nmol ATP·mg prot⁻¹·min⁻¹) which determines the rate of ATP generation in state 3.

General experimental design for mitochondrial function assessment. Mitochondrial respiration was determined using the voltamperometric method with a Clark oxygen electrode (oxygraph Gilson 5/6 H) at 30°C. The incubation medium consisted of 12.5 mmol·l⁻¹ HEPES, 122 mmol·l⁻¹ KCl, 3 mmol·l⁻¹ KH₂PO₄, 0.5 mmol·l⁻¹ Titriplex III, and 2% dextrane. Glutamate/malate at 2.5 mmol·l⁻¹ was used as a NAD-linked substrate. To initiate state 3 respiratory activity, 500 nmol of ADP was added.

Recent results: We successfully used this method for proving presumed adverse effects of atorvastatin, which is frequently used in the treatment of hypercholesterolemia in humans, on the oxidative phosphorylation, membrane fluidity, and coenzyme Q (CoQ₉) content in rat liver mitochondria. We have found that the drug administered at either low (10 mg·kg⁻¹) or high dose (80 mg·kg⁻¹) dose-dependently decreased CoQ₉ content (by 56% and 63% in treated controls and hypercholesterolemic rats, respectively) and reduced capacity of the respiratory chain (by 9.3% and 30.2%, assigned as above) and rate of ATP synthesis (by 35% and 63%, all with p < 0.05). Our findings point to that compromised bioenergetic may play a significant role in the statin-induced hepatopathy, which contributes to the views concerning adverse

effects of statins [2].

New experimental approach: Apparently, mitochondria sense and accommodate various external stimuli, which provides an exciting opportunity to study signaling events by direct modulation of mitochondrial respiration, ATP production, ion transport, redox state, and/or free radical generation. Hydrogen sulphide (H_2S) has been shown to act as a gasotransmitter, similarly to nitric oxide (NO) with all of the positive effects of NO, but the capacity to form a toxic metabolite such as $ONOO^-$. H_2S affects many cellular processes ranging from regulation of protein expression to direct effect on the proteins [as reviewed in 3]. Malekova et al. [4] published a study on the inhibitory effect of H_2S on chloride channels derived from mitochondrial membranes. These channels are involved in the regulation and maintenance of mitochondrial membrane potential, which in turn affects the action potential on the plasma membrane in cardiomyocytes [5]. We have been looking for the effect of NaHS, a H_2S donor, on the mitochondrial respiration, which is in a tight relationship with the mitochondrial membrane potential. The preliminary results on heart mitochondria have indicated that NaHS at concentrations ranging from 25 to 400 $\mu\text{mol}\cdot\text{l}^{-1}$, added 30 s before addition of ADP, would decrease the rate of oxygen consumption in a concentration dependent manner. Since prolonged storage of the stock NaHS solution (100 $\text{mmol}\cdot\text{l}^{-1}$) decreased the effect of NaHS on mitochondria, it is likely that it was indeed H_2S what affected the respiration, as NaHS dissociates in water to HS^- ion and a volatile H_2S molecule.

Conclusion. Results of our recent (atorvastatin effects) and ongoing experiments on H_2S effects proved voltammetric method to be a valuable tool for measurement mitochondrial bioenergetic function in the selected experimental conditions and allowed for targeting the sites of action. The biological profile of H_2S strongly suggests that this gaseous signaling molecule is likely to protect a variety of organs [3]. Simultaneous measurements of respiration and membrane potential with use of specific inhibitors and/or redox-state modulators will provide useful additional information and enable deeper quantitative analyses in order to better understand the physiological and pharmacological actions of H_2S in the heart.

Acknowledgement

This work was supported by the Slovak Grant Agency VEGA, projects No. 1/0328/10, 02/0094/12, and partially by a scientific grant MZ SR 2007/29-UK-06.

References

- [1] A. Gvozdjaková (Ed.), J. Kucharská, A. Hlavatá, in *Mitochondrial Medicine*, A. Gvozdjaková (Ed.), The Netherlands, Springer, 2008.
- [2] O. Uličná, O. Vančová, I. Waczulíková, P. Božek, L. Šikurová, V. Bada, J. Kucharská, *Physiol. Res.*, in press (2012)
- [3] Z. Tomaskova, A. Bertova, K. Ondrias, *Curr. Pharm. Biotechnol.* 12 (2011) 1394-1405.
- [4] L. Malekova, O. Krizanova, K. Ondrias, *Gen. Physiol. Biophys.* 28 (2009) 190-194.
- [5] M.A. Aon, S. Cortassa, F.G. Akar, D.A. Brown, L. Zhou, B. O'Rourke, *Int J Biochem Cell Biol* 41 (2009) 1940-1948.

O3

On the H₂S-NO interaction and the effects of thiols

K. Ondrias¹, A. Mišák¹, M. Grman^{1,2}, N. Pronayová³, T. Liptaj³

¹ Institute of Molecular Physiology and Genetics, Slovak Academy of Sciences, Vlárská 5, 833 34 Bratislava, Slovakia, e-mail: karol.ondrias@savba.sk

² Department of Nuclear Physics and Biophysics, FMFI UK, Mlynská dolina F1, 842 48 Bratislava, Slovakia,

³ Faculty of Chemical and Food Technology, Slovak University of Technology, Bratislava, Slovakia

Hydrogen sulfide (H₂S) and nitrogen oxide (NO) are gaseous transmitters involved in many (patho)physiological processes [1]. The efficiency of the H₂S donor Na₂S in phosphate buffer (7.4 pH) and its mixtures with cysteine (Cys), cystine (CySS), methionine (Met), N-acetylcysteine (NAC), glutathione (GSH) and oxidized glutathione (GSSG) incubated under air (1-270 minutes) to release NO from nitrosogluthathione (GSNO) was studied. We report here that the presence of GSSG ≥ CySS > Cys (but not Met) in the incubated Na₂S solution increased the amount of the NO release and prolonged (the presence of NAC and GSH decreased and shortened) the time dependent of the NO release. The time dependent ¹H NMR studies revealed that the Cys solution was oxidized to CySS, and GSH solution was oxidized partially to GSSG, during the 60-120 minutes of the incubation what was protected by Na₂S. Na₂S partially reduced CySS or GSSG and shifted Cys and CySS ¹H NMR spectra to lower ppm. Na₂S had the most significant effect on GSSG and CySS, moderate effect on GSH and Cys, minor effect on NAC, and no effect on Met ¹H NMR spectra. The NMR results indicate that H₂S interacts with GSSG, CySS, GSH, Cys, and NAC and the interaction is structurally dependent and responsible for the modulation of NO release from GSNO. We may suggest that GSSG, CySS, GSH, Cys, and NAC serve as a short temporally stores of H₂S and H₂S-GSSG, H₂S-CySS, H₂S-GSH, H₂S-Cys and H₂S-NAC complex(es) and/or their derivatives release NO from GSNO directly and/or H₂S is released from the complex(es) and than it releases NO from GSNO.

Acknowledgement

This work was supported by the Slovak Science Grant Agency VEGA 2/0150/10.

References

[1] Z. Tomaskova, A. Bertova, K. Ondrias, *Curr. Pharmac. Biotech.* 12 (2011) 1394-1405.

O4

Effect of pH, thiols and oxygen on the H₂S/HS⁻ induced NO release from S-nitrosoglutathione

M. Grman^{1,2}, A. Mišák², K. Ondriaš²

¹ Department of Nuclear Physics and Biophysics, FMFI UK, Mlynská dolina F1, 842 48 Bratislava, Slovak Republic

² Institute of Molecular Physiology and Genetics, Slovak Academy of Sciences, Vlárská 5, 833 34 Bratislava, Slovak Republic

e-mail: grman.marian@gmail.com

Hydrogen sulfide (H₂S) and nitrogen oxide (NO) are gaseous transmitters involved in many (patho)physiological processes [1]. Interaction of NO with thiol group of glutathione leads to formation of S-nitrosoglutathione (GSNO). S-nitrosothiols may serve as bioreservoir for NO in physiological conditions [2]. We measured spectrophotometrically (by UV-VIS absorption spectroscopy) decomposition of GSNO and by Griess reaction NO oxidation product NO₂⁻. We found that H₂S donor Na₂S or NaHS released NO from GSNO. This release was pH dependent (in order 8.0>7.4>6.0) and modulated by low molecular thiols. At pH 7.4, L-cysteine (Cys), L-glutathione (GSH) and N-acetyl-Lcysteine (NAC) decreased the rate of NO release from GSNO induced by H₂S (in the order of potency NAC>GSH>Cys), L-methionine (Met) and oxidized L-glutathione (GSSG) did not have any effect. On the other side, at pH 6.0, Cys, GSH and NAC increased NO release from GSNO induced by H₂S (in the order Cys>GSH>NAC). Measurements in nitrogen deaerated solutions revealed that oxygen (O₂) is not necessary for H₂S induced NO release, although the rate of release was significantly lower. We suppose that the interaction of thiol group with H₂S/HS⁻ is responsible for these effects. Presented results indicate involvement of H₂S and low molecular thiols in NO signaling pathway and redox regulation of many physiological processes and our results may contribute to understand a biological role of H₂S and NO in living organisms.

Acknowledgement

This work was supported by the Slovak Science Grant Agency VEGA 2/0150/10.

References

- [1] Z. Tomaskova, A. Bertova, K. Ondrias, *Current Pharmaceutical Biotechnology*. 12 (2011) 1394-1405.
- [2] J.S. Stamler et al., *Proc. Nat. Acad. Sci. USA* 89 (1992) 7674-7677.

O5

Cysteines in the extracellular loop in domain I of the Ca_v3.1 channel are essential for channel opening.

M. Karmazinova¹, S. Beyl², N. Klugbauer³, S. Hering², L. Lacinova¹

¹Institute of Molecular Physiology and Genetics, Slovak Academy of Sciences, Bratislava, Slovakia, e-mail: lubica.lacinova@savba.sk

²Institut für Pharmakologie und Toxikologie, University of Vienna, Vienna, Austria

³Institut für Experimentelle und Klinische Pharmakologie und Toxikologie, Albert-Ludwigs Universität, Freiburg, Germany

Low-voltage activated (LVA) calcium channels activate at more negative membrane voltages than high-voltage activated (HVA) channels. The molecular basis of the gating peculiarities of LVA channels is largely unknown. All voltage-gated calcium channels are composed of four homologous domains, each containing six transmembrane segments S1-S6 and a pore loop (P) between segments S5 and S6. Four voltage-sensing domains each composed of the transmembrane segments S1 - S4 are arranged around a central pore domain formed by four sets of S5-P-S6. LVA calcium channels contain a unique conserved large external domain located between the IS5 region and the pore loop. In HVA calcium channels this loop is smaller and not well conserved. Six cysteines located within this region are conserved among all three Ca_v3 channels. Disulfide bonds between these cysteines may stabilize the conformation of this large extracellular region. Considering that this region is linked to the conducting pore, it might contribute to the modulation of the channel gating.

We investigated the role of six cysteines of Ca_v3.1 in channel gating by mutating each of them (C241, C271, C282, C298, C313 and C323) to alanine. The resultant channels were expressed in HEK293 cells and their gating properties were studied by patch clamping. C298A and C313A mutants conducted calcium currents. The other mutants were not functional. This defect was not caused by defect in targeting of channel proteins into the cell membrane, as confirmed by confocal microscopy. C298A and C313A as well as double mutation C298/313A significantly reduced the amplitude of the calcium currents, shifted the activation curve in the depolarizing direction and slowed down channel inactivation. Redox agents dithiothreitol (DTT) and 5,5'-dithiobis(2-nitrobenzoic acid) (DTNB) shifted the current activation curve of wild type channel in the hyperpolarizing direction. Activation curve for all mutated channels was shifted in hyperpolarizing direction by DTT while DTNB caused a depolarizing shift. Our study reveals that the cysteines we studied have an essential role in Ca_v3.1 gating. We hypothesize that cysteines in the large extracellular loop of Ca_v3.1 form bridges within the loop and/or neighboring channel segments that are essential for channel gating.

Acknowledgement

This work was supported by the Slovak Grant Agency VEGA, project No. 2/0195/10

O6

Gating behavior of coupled cardiac ryanodine receptors is not altered by luminal calcium

M. Gaburjaková, J. Gaburjaková

Institute of Molecular Physiology and Genetics, Vlárská 5, 833 34 Bratislava, Slovakia,
e-mail: marta.gaburjakova@savba.sk

In cardiac muscle, ryanodine receptor (RyR2) channels play a pivotal role in the excitation-contraction coupling. The opening of RyR2 channels results in a large Ca^{2+} release from intracellular Ca^{2+} stores that drives cardiac contractility. RyR2 channels in intact cardiomyocytes are packed into regular, two-dimensional arrays that exhibit a unique “checkerboard-like” organization. By forming a close contact, neighboring RyR2 channels might interact with each other and operate as a functional unit. Indeed, two or more RyR2 channels reconstituted into an artificial system - a bilayer lipid membrane (BLM) - can open and close simultaneously (coupled gating). Although the physiological relevance of coupled gating phenomenon is still not understood, it has been considered as one of mechanisms required for termination of local Ca^{2+} release in the cardiac muscle [1].

The objective of our work was to further characterize the functional profile of the coupled RyR2 channels to advance our knowledge of the tightly synchronized regime of channel functioning. We focused on the effect of luminal Ca^{2+} on gating parameters since luminal Ca^{2+} has been shown to significantly modify the gating behavior of the single RyR2 channel [2]. Employing the method of reconstitution of an ion channel into a BLM we showed that coupled RyR2 channels isolated from the rat heart exhibited flicker gating inside main open events that was less intensive in the presence of luminal Ca^{2+} (8 mM). In contrast, we did not observe such behavior for the single RyR2 channel implying that it is solely a result of coupling between RyR2 channels and it likely reflects the strength of coupling in a given functional state.

When flickering was ignored we were able to determine the gating behavior of coupled RyR2 channels as one functional unit. This analysis revealed that the average open and closed times determined for coupled RyR2 channels were similar in the absence and presence of luminal Ca^{2+} (8 mM). This implies that luminal Ca^{2+} does not affect the gating profile of coupled RyR2 channels that is; however, in contrast to the single RyR2 channel where luminal Ca^{2+} significantly prolonged the average open and closed times [2]. It seems that Ca^{2+} binding site located on the luminal face of each RyR2 channels could be somehow protected by the functional interaction between channels recruited into the functional complex and therefore luminal Ca^{2+} is not able to exert the effect on gating behavior. We tested this hypothesis by examining the caffeine sensitivity of coupled RyR2 channels in the absence and presence of luminal Ca^{2+} (8 mM) because we have previously reported that luminal Ca^{2+} substantially shifted EC_{50} for caffeine sensitivity of the single RyR2 channel to lower concentrations [2]. We showed that coupled RyR2 channels responded to caffeine in a similar way as the single RyR2 channel in respect to luminal Ca^{2+} and this result implies that luminal Ca^{2+} binding sites on coupled RyR2 channels are likely functional.

Acknowledgement

This work was supported by the Slovak Grant Agency VEGA, projects No. 2/0033/11 and 2/0102/12.

References

- [1] M.D. Stern, H. Cheng, *Cell Calcium* 35 (2004) 591-601.
- [2] J. Gaburjakova, M. Gaburjakova, *J. Membr. Biol.* 212 (2006)17-28.

O7

pH-modulation of single-channel properties of anion channels derived from inner mitochondrial membranes of the rat heart

A. Mišák¹, M. Grman^{1,2}, Ľ. Máleková¹, Z. Tomášková¹, K. Ondriaš¹

¹ Institute of Molecular Physiology and Genetics, Slovak Academy of Sciences, Vlárská 5, 833 34 Bratislava, Slovak Republic

² Department of Nuclear Physics and Biophysics, FMPI CU, Mlynská dolina F1, 842 48 Bratislava, Slovak Republic

e-mail: anton.misak@savba.sk

The inner mitochondrial membrane (IMM) possesses an anion channel (IMAC), which was first time studied by light scattering on swelling mitoplasts (mitochondria deprived of outer membrane). Based on these experimental measurements, IMAC has been described as anion-selective channel exhibiting inhibition of channel activity by matrix Mg^{2+} ions ($IC_{50} = 38 \mu\text{mol/l}$ at 7.4 pH) and by matrix protons ($pIC_{50} = 7.7$) [1]. Moreover, IMAC pharmacological profiles have been identified by monitoring the swelling of mitochondria incubated with different drugs. Beside Mg^{2+} and H^+ , IMAC activity is inhibited by many different cationic amphiphiles, including amitriptyline, propranolol, dibucaine, amiodarone, 4'-chlorodiazepam and others [2].

To better understand and characterize anion channels of IMM, many electrophysiological experiments have been performed, involving patch-clamping mitoplasts and reconstitution of submitochondrial particles (SMP) into artificial lipid membrane. The first patch-clamp report on 107 pS anion-selective channel, called "centum pS channel" (mCS), with some properties similar to IMAC has led to the suggestion that both of them are one and the same process [3]. Existence of some reports of different observation between IMAC and mCS, together with the fact that molecular identity of IMAC being still unknown, keeps the hypothesis of the same identity still under investigation and debate.

The functional role of IMAC in mitochondrial biology is not clearly understood and must be clarified, but it has been proposed to contribute to mitochondrial volume homeostasis regulation, to oscillatory behavior of the $\Delta\Psi_m$ and to so-called ROS-induced ROS-release under oxidative stress conditions [4].

In our study, we were measuring the net chloride currents across single chloride channel after incorporation of SMP into artificial lipid membrane (BLM method). We focused also on the best possible purification of mitochondria in order to eliminate the contamination by other membranous structures such as sarcoplasmic reticulum or lysosomes. We aimed especially at the conductance characteristics of the measured chloride channels and its regulation by pH changes. By means of Western Blot analysis we didn't observe any significant contamination by the tested non-mitochondrial membranous structures, thus, we supposed that all recorded channels came from IMM. The mitochondrial origin of the membranous fraction was confirmed also by electron microscopy. Chloride channels ($N = 62$) had mean conductance 129 ± 3 pS under our standard conditions (250/50 mmol/l KCl asymmetric solution, 7.4 pH). After pH dropping to the value of 6.5, mean conductance increased relatively to 120 % (decrease of pH on *cis* side of the membrane) or to 220 % (decrease of pH on *trans* side of the membrane). On the other hand, increase of pH to 8.5 caused the conductance decrease to 76 % (on both side of the membrane). One probable explanation for the pH-sensitive conductance might lie in the change of chemical or conformational pore properties by H^+ concentration. The second parameter investigated in our records was channel activity evaluated as open probability (P_o). As P_o reference we took the channel activity under standard conditions (defined earlier).

After application of HCl into *cis/trans* compartment and consequent pH decrease to 6.5, the P_o was significantly changed to lower values for both compartments. After using of Trizma base to increase the pH to 8.5, there was no significant change in P_o . Observation of the pH- dependent profile of chloride channel at lower pH is in good agreement with the results of the light scattering IMAC studies. However, at higher pH, we have got ambiguous results. To provide better evidence for the possible IMAC identity of recorded chloride channels, we plan to perform other experimental studies.

Acknowledgement

This work was supported by the Slovak Science Grant Agency VEGA 2/0150/10.

References

- [1] A.D. Beavis, J. Bioenerg. Biomembr. 24 (1992)77-90.
- [2] B. O'Rourke, Mitochondrial ion channels. in D. Julius (Ed.) pp. 19-49, 2007.
- [3] J. Borecký, P. Ježek, D. Siemen, J. Biol. Chem. 272 (1997) 19282-19289.
- [4] D.B. Zorov, M. Juhaszova, S.J. Sollott, Biochim. Biophys. Acta - Bioenergetics 1757 (2006):509-517.

O8

SpikeAnalyzer – the MATLAB-based analysis software for calcium spikes

R. Janíček, M. Hořka, A. Zahradníková, Jr., A. Zahradníková, I. Zahradník

Institute of Molecular Physiology and Genetics, Slovak Academy of Sciences, Vlárská 5, 833 34 Bratislava, Slovakia. e-mail: radoslav.janicek@savba.sk

Calcium release in cardiac myocytes during excitation-contraction coupling is the result of elementary calcium release events activated by the calcium current. These release events can be observed as calcium spikes, using combination of confocal microscopy and patch clamp on isolated cardiac myocytes [1]. Calcium spikes provide information about the kinetics, the time and the location of the local calcium fluxes. Due to low signal to noise ratio it is often difficult to estimate the parameters of calcium spikes correctly. In this work we present original analysis software for calcium spikes, which enables us to describe the fluorescent time course of calcium spikes with a theoretical function and to determine their parameters accurately and exactly.

We developed the SpikeAnalyzer program (Fig.1) with the use of the tools provided by MATLAB to increase the productivity and reliability of the analysis of calcium spikes in the x-t images obtained by laser scanning confocal fluorescence microscopy synchronized with patch clamp experiments on isolated cardiac myocytes. This program provides control over the whole course of analysis, from selection of the analyzed sites to approximation of the fluorescent time profiles of the selected sites by the theoretical function [2].

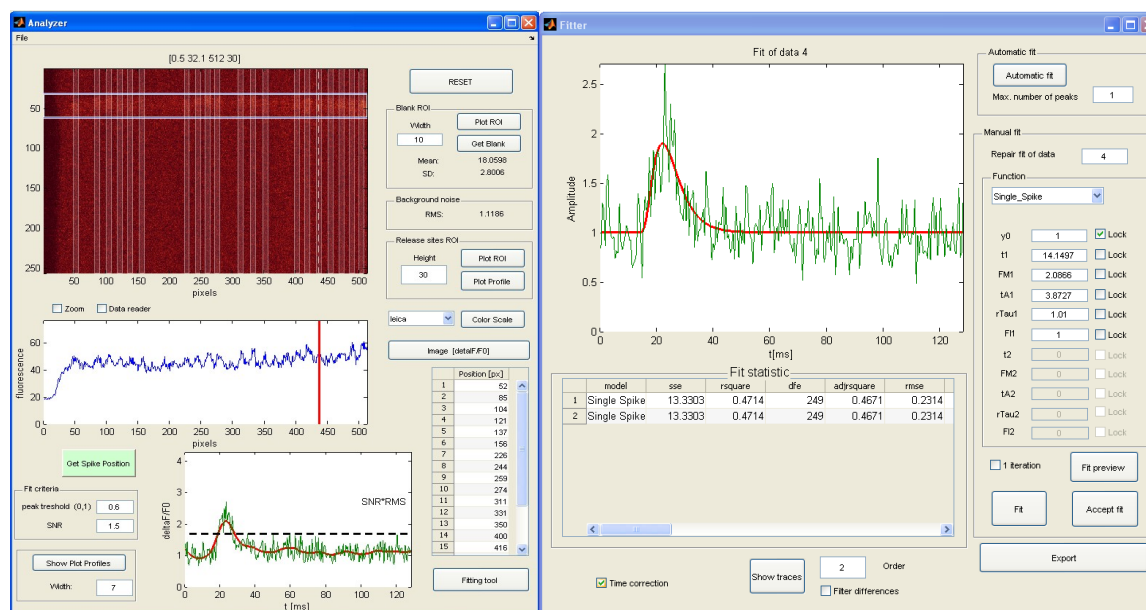


Fig. 1. Dialog windows of the SpikeAnalyzer.

In comparison with the previously used data analysis procedure that was based on three software packages (Scion Image, Excel and Origin), analysis with SpikeAnalyzer is performed much faster (analysis of an x-t image with 20 spikes lasts under 5 minutes from upload to export of results). Moreover, the analysis parameters are automatically initialized upon loading the electrophysiological and confocal data in their respective proprietary formats. The analysis starts with interactive selection of spike positions. At each position, the temporal profile for the selected region is displayed, and the signal to noise ratio (SNR), which can be further used as a criterion for automatic fitting, is computed. The data

approximation uses an automatic fitting procedure with visual control over the process and the quality of the fit, including statistical measures. SpikeAnalyzer is equipped with an original pixel time correction algorithm, introduced to account for the exact time of acquisition of individual pixels of the object in the image. SpikeAnalyzer also features spurious noise reduction routine based on a modified median filter for noisy signals.

Due to its semiautomatic character with visual control and formatted output, the time cost of the analysis and the fatigue are substantially reduced, by about an order of magnitude. Integration of whole process of analysis to the MATLAB environment provided an effective tool to perform calcium spike analysis faster, more reliably and much more easily.

Acknowledgement

This work was supported by the Slovak Grant Agency VEGA, project No. 2/0917/11 and 2/0203/11, and by the Slovak Research and Development Agency under the contract No. APVV-0721-10.

References

- [1] L.S. Song, J.S.K. Sham, M.D. Stern, E.G. Lakatta, H. Cheng, *J. Physiol.* 512 (1998) 677-691.
- [2] A. Zahradníková, Jr, E. Poláková, I. Zahradník, A. Zahradníková, *J. Physiol.* 578 (2007) 677-691.

O9

Software suite for analysis of fluctuations in electrical properties of cells

M. Hořka, I. Zahradník

Institute of Molecular Physiology and Genetics, Slovak Academy of Sciences, Vlárská 5., 833 34, Bratislava, Slovak Republic, e-mail: matej.hotka@savba.sk

Time dependent variability of constitutive properties of biological objects leads to fluctuations in their measured parameters. Fluctuations of passive electrical properties of cardiac muscle cells, measured in isolated cells by the whole cell patch clamp technique is expected to be a rich source of information about dynamics of their surface membrane-plasmalemma. Recently, we have shown that the high resolution impedance measurements on isolated cardiac myocytes are technically feasible by means of the Q-method [1] and that the impedance parameters of cardiac myocytes unlike their equivalent electrical models display spontaneous fluctuations. The original Q-method software (PCP Analyzer) was designed to operate in real-time with available technologies. That limited the continuity of stimulation and made the interpretation and further analyzes difficult.

In this work we present new Matlab-based software suite, the Fluctuation Analyzer, which involves 5 functions (Fig.1, Fig.2). First, it performs integration of the membrane current responses of a myocyte to continuous square wave stimulation, evaluates the parameters of cell impedance, and outputs their time series.

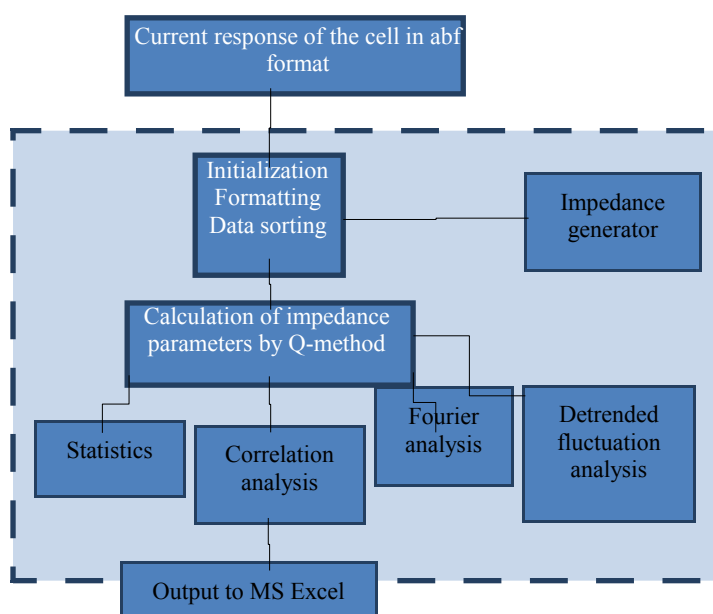


Fig. 1. Block diagram of Fluctuation Analyzer

For this function, the program reads the proprietary binary files (abf) produced by the commercially available data acquisition software pClamp (Molecular Devices, USA), containing the raw data and the metafile that serve for the automatic configuration and

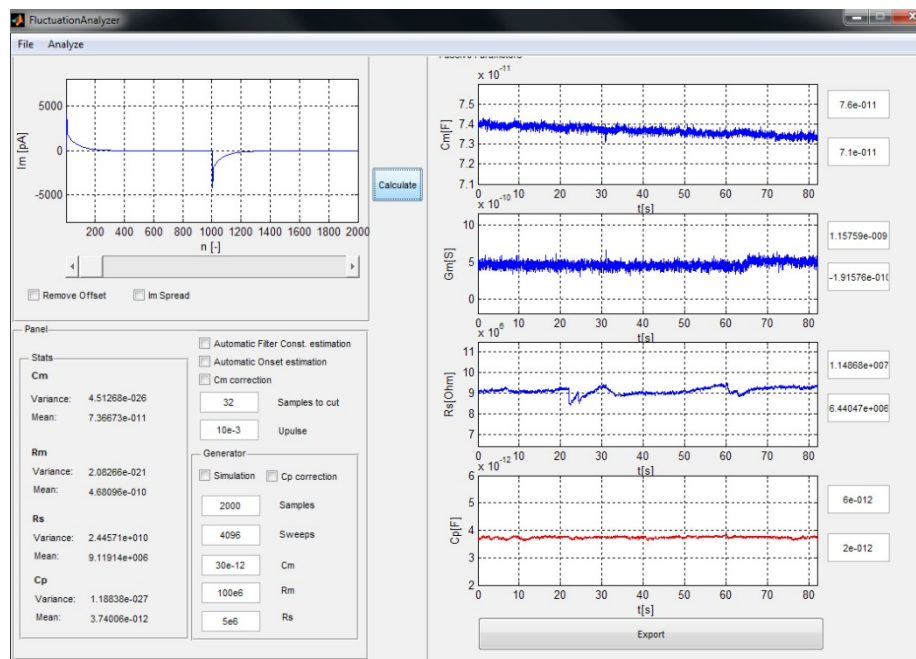


Fig. 2. The main dialog window of the Fluctuation Analyzer

initialization of the analysis. Second, the evaluated impedance parameters, the membrane capacitance and membrane conductance together with the series resistance and parasite capacitance of the measurement are analyzed in the frequency domain via Fourier analysis. The spectra of power densities are approximated with theoretical functions to estimate contribution of various processes. Third, the Fluctuation Analyzer performs the detrended fluctuation analysis of different orders, for determining the fractal characteristics. This analysis is of significant importance for non-stationary signals for which the spectral analysis may provide misleading results. Fourth, the fluctuation vs. scale plots of the detrended fluctuation analysis are approximated with linear polynomials and their slopes are compared with the low-frequency part of the power spectral density. Fifth, the Fluctuation Analyzer offers generator of the exponential current responses to voltage stimuli that simulates cell responses with user defined values of impedance parameters. The artificial responses may be used for comparative analysis to estimate the effect of independent or coupled changes in impedance parameters.

The implementation of the Fluctuation Analyzer in Matlab environment provided essential features of flexibility and adaptability to increase the functionality or to change the methods of analysis according to the needs of specific projects.

Acknowledgement

This work was supported by the Slovak Grant Agency VEGA, 2/0203/11

References

[1] P. Novák, I. Zahradník, *Ann. Biomed. Eng.* 34 (2006) 1201-1212.

O10

Inhibitors of protein amyloid aggregation

Z. Gazova¹, K. Siposova^{1,2}, Antosova¹, D. Fedunova¹, J. Bagelova¹, J. Imrich²

¹ Department of Experimental Physics SAS, Watsonova 47, 040 01, Kosice, Slovakia

² Institute of Chemistry, Faculty of Sciences UPJS, Moyzesova 11, 040 01, Kosice, Slovakia
gazova@saske.sk

Introduction: Protein misfolding and the accumulation of amyloid deposits are prominent features in a vast array of human diseases [1]. Amyloid fibrils are insoluble, highly ordered aggregate and the major component of amyloid deposits found in different part of the human body. Lysozyme forms massive amyloid aggregates in the liver and kidney of individuals affected by lysozyme hereditary systemic amyloidosis. Amyloid deposits of insulin have been observed in patients with diabetes after repeated subcutaneous insulin injection in the site of application. Amyloid fibrils from all proteins are defined by a cross- β structure where the β -sheets run perpendicular to the fibril axis [2]. Thus, it is likely that they have a similar structure and mechanism of fibril formation. Currently, amyloid-related diseases are incurable and the treatment is only symptomatic without feasibility to stop or substantially delay the progressive consequences of the disease [3]. Recent data indicate that pathogenesis of amyloid-related diseases is associated with cell impairment and death due to protein amyloid aggregation [4]. These facts correlate with the findings suggesting that reduction of amyloid aggregates is beneficial for cells and animals [5]. We have studied a library of structurally distinct low-molecular acridine derivatives for their effect on amyloid aggregation of both the lysozyme and insulin proteins.

Materials and Methods: Protein amyloid aggregation was achieved by incubation of protein (10 μ M) in 70 mM glycine containing 80 mM NaCl, pH 2.7 (for lysozyme) or in 100 mM NaCl, pH 1.6 (for insulin). The solution was incubated at 65°C and stirred constantly (1200 rpm) for 120 min. Formation of the amyloid fibrils was detected by ThT fluorescence assay, the presence of amyloid aggregates is associated with significant increase of fluorescence intensity which is not observed for native protein. The morphology of the amyloid aggregates was investigated by microscopic techniques (TEM, AFM). The effect of compounds on protein fibrillization was investigated by adding the acridine compound to the soluble protein (insulin or lysozyme) (10 μ M) before starting the process of amyloid aggregation (described above). Depolymerizing activity was observed after overnight incubation of 10 μ M insulin/lysozyme fibrillar aggregates with studied compounds (200 μ M).

Results: We have studied the effect of low-molecular compounds on the amyloid aggregation of insulin/lysozyme to investigate the structure-activity relationship. To make primary screening we tested the effect of acridine derivatives on process of amyloid aggregation in presence of 200 μ M of compounds by ThT fluorescence assay. As the fluorescence intensity is positively correlated to the extent of amyloid aggregation, the lower fluorescence values indicate more effective anti-aggregation compound. We have found that the efficiency of compounds to affect amyloid aggregation of amyloids was strongly dependent on the type of derivatives (Fig 1A).

Conclusions: The present data indicate that the structure of acridine derivatives is an important factor in determining their effect on insulin/lysozyme amyloid aggregation. We suppose that tricyclic core is significant in accordance with the findings that many compounds with ring structure are able to affect the amyloid aggregation very effectively. The loss of acridine core planarity and transformation of the reactive nucleophilic thiosemicarbazide into more stable heterocycles leads to significant decrease of the acridine

inhibiting and depolymerizing abilities [6]. For the most effective compounds the IC50 and DC50 values, cell viability and interaction with DNA were specified (data not shown). We have identified three planar acridine derivatives with high anti-amyloid activities, low cytotoxicity and weak ability to interfere with the processes in the cell. We assume that present findings represent a starting point for the application of the selected active planar acridines in the treatment of amyloidosis in general.

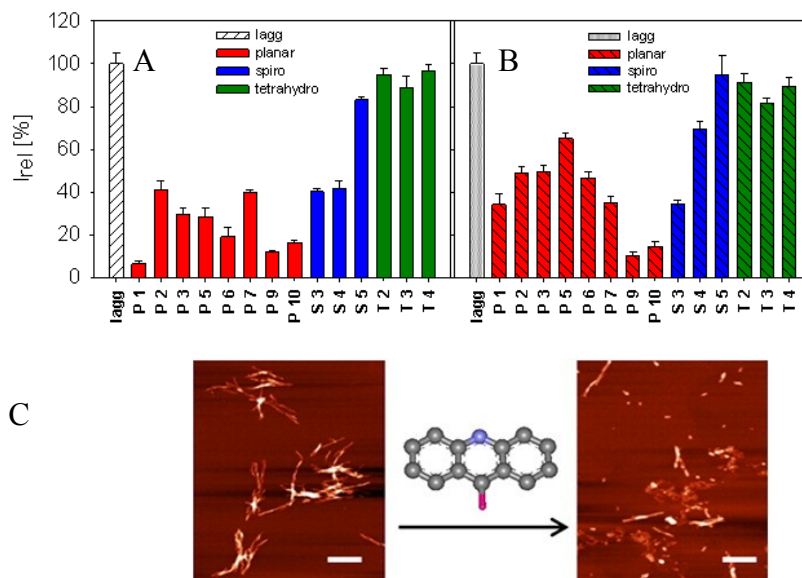


Fig. 1. Inhibiting (A) and depolymerizing activity (B) of acridine derivatives (200 μ M) on amyloid aggregation of insulin. (C) AFM images represent ability of planar acridines to destroy preformed lysozyme amyloid fibrils. Bars represent 1 μ m.

Acknowledgement

This work was supported within the projects 26220220005 and 2622012033 in the framework of the Structural Funds of European Union, Centre of Excellence of SAS Nanofluid, VEGA 0041, 0079, 0077, Slovak Research and Development Agency—contract No. APVV-0171-10 and SK RO-0012-10 and project SAS NSC Taiwan—Computational approaches to study structure, folding and interactions of biopolymers and VVGS 38/12-13.

References

- [1] F. Chiti, C. M. Dobson, *Annu. Rev. Biochem.* 439 (2006) 333–366.
- [2] J. D. Sipe, M. D. Benson, J. N. Buxbaum, et al. *Amyloid* 17 (2010) 101–104.
- [3] H. Kim, B. S. Park, K. G. Lee, C. Y. Choi, S. S. Jang, Y. H. Kim, *J. Agric. Food Chem.* 53 (2010) 8537–8541.
- [4] C. M. Dobson, *Phil. Trans. R. Soc. B* 356 (2001) 133–145.
- [5] I. Khlistunova, J. Biernat, Y. Wang, P. Pickhardt, M. von Bergen, Z. Gazova, E. Mandelkow, E. M. Mandelkow, *J. Biol. Chem.* 281 (2006) 1205–1214.
- [6] A. Antosova, B. Chelli, E. Bystrenova, K. Siposova, F. Valle, J. Imrich, M. Vilkova, P. Kristian, F. Biscarini, Z. Gazova, *Biochim. Biophys. Acta* 1810 (2011) 465–474.

O11

Functional equivalence of as „isolated“ and “high-energy” metastable states of the oxidized mitochondrial cytochrome c oxidase

D. Jancura^{1,2}, V. Berka³, J. Stanicova^{2,4}, M. Fabian²

¹Department of Biophysics, Safarik University, Kosice, Slovakia

²Department of Biochemistry and Cell Biology, Rice University, Houston, USA

³Department of Internal Medicine, University of Texas Health Science Center, Houston, USA

⁴Institute of Biophysics and Biomathematics, University of Veterinary medicine, Kosice, Slovakia

e-mail: jancura@upjs.sk

Mitochondrial cytochrome c oxidase (CcO) is the terminal enzyme of the respiratory electron-transfer chain in mitochondria of the eukaryotic cells. This molecular complex catalyzes reduction of dioxygen to water and converts the released free energy into an electrochemical proton gradient across the inner mitochondrial membrane [1]. The created proton-motive force is consequently used as a driving force for the ATP synthesis and for other energy-requiring processes. Two processes contribute to the development of this gradient. The first is the oxidation of ferrocytochrome c from the intermembrane side of the inner mitochondrial membrane coupled to proton consumption for water formation from the matrix compartment of mitochondria. The second process is proton pumping, during which protons are transported from the matrix to the intermembrane space of mitochondria. Both processes, the reduction of oxygen and proton pumping, lead to a transfer of totally eight charges through the membrane during reduction of one molecule of oxygen. However, the exact mechanism of coupled electron-proton transfer and proton pumping in CcO has not been determined yet and this remains one of the major unresolved problems of current molecular bioenergetics [for recent reviews about CcO see ref. 2-4].

The current model of the proton pumping, formulated in Marten Wikström's laboratory, presumes the existence of a "high-energy" metastable \mathbf{O}_H state, which is formed immediately after oxidation of the fully reduced CcO with oxygen [4-6]. It has been suggested that the energy needed for proton pumping is stored in this activated form. Two-electron reduction of \mathbf{O}_H state and transfer of these electrons to the catalytic site of CcO drives a translocation of two protons across the membrane. In the absence of external electron donor, the "high-energy" \mathbf{O}_H form relaxes to the "resting" oxidized form with dissipation of the energy and the subsequent reduction of CcO does not lead to proton pumping. It was proposed that there exist differences in ligation and protonation states of the catalytic site of \mathbf{O}_H and the "resting" state of the oxidized CcO [5,6].

However, our previous study did not reveal differences either in the spectral characteristics (optical, EPR) or the kinetics of electron transfer to the catalytic site during the reductive phase of the catalytic cycle in these two forms of the oxidized CcO [7].

In the present work, the reactions of as "isolated" fast form (\mathbf{O}) and "high-energy" metastable state (\mathbf{O}_H) of the oxidized CcO with hydrogen peroxide (H_2O_2) have been investigated by multi-wavelength stopped-flow spectroscopy. The rate constants for the binding of H_2O_2 to the catalytic site are almost identical for both forms of the fully oxidized CcO. Using phenol red as a pH indicator we have found that a relaxation of \mathbf{O}_H to \mathbf{O} state and the binding of H_2O_2 to the catalytic site of both forms are not coupled with an apparent proton uptake or release.

Altogether, our findings again indicate that there is no difference in the ligation and protonation states of the catalytic site of \mathbf{O} and \mathbf{O}_H forms of the oxidized mitochondrial CcO. The recently proposed alteration in the water content surrounding the catalytic site in these two forms [4] needs to be evaluated by further studies.

References

- [1] M. Wikström (Ed.), *Biophysical and structural aspects of bioenergetics*, RSC Publishing, 2006.
- [2] P. Brzezinski, R.B. Gennis, *J. Bioenerg. Biomembr.* 40 (2008) 521-531.
- [3] I. Belevich, M.I. Verkhovsky, *Antioxidant & Redox Signaling* 10 (2008) 1-29.
- [4] V.R.I. Kaila, M.I. Verkhovsky, M. Wikström, *Chem. Rev.* 110 (2010) 7062- 7081.
- [5] M.I. Verkhovsky, A. Jasaitis, M.L. Verkhovskaya, J.E. Morgan, M. Wikström, *Nature* 400 (1999) 480-483.
- [6] I. Belevich, D.A. Bloch, N. Belevich, M. Wikström, M.I. Verkhovsky, *Proc. Natl. Acad. Sci. USA* 104 (2007) 2685-2690.
- [7] D. Jancura, V. Berka, M. Antalík, J. Bagelova, R.B. Gennis, G. Palmer, M. Fabian, *J. Biol. Chem.* 281 (2006) 30319-30325.

O12

The stability of the p53 protein complexes with DNA substrates against salt-induced dissociation

P. Šebest, H. Pivoňková, M. Fojta

Institute of Biophysics, v.v.i., Academy of Sciences of the Czech Republic, Kralovopolska 135, Brno 612 65, e-mail: besta@ibp.cz

The tumor suppressor protein p53 is transcription factor involved in regulation of crucial processes, such as DNA repair, cell proliferation and apoptosis [1, 2]. It protects cells from malignant transformation by regulating the responses of cell growth and death to genotoxic stress and maintains genetic integrity of cells [3, 4].

The functions of p53 are closely related with its ability to interact with DNA. The protein is organized into several domains [5]. The N-terminal domain (amino acids 1-100) contains transactivation region and mediates interaction with other transcription factors. The core domain (aa 100-300) is involved in sequence-specific binding to the p53 response elements in promoters of downstream genes [6]. The C-terminal region contain the C-terminal DNA binding site (CTDBS) (aa 363-382) which is responsible for non-sequence specific binding and structure selective binding to supercoiled DNA or *cis*-platinated DNA [7-10]. Mutated p53 was found in more than 50 % of human cancers. The majority of these mutations are located within the core domain [11], which is responsible for sequence specific binding to consensus sequence (two copies of the sequence 5'-RRRC(A/T)(T/A)GYYY-3' separated by 0–13 bp) [6].

We studied interactions of wild type and p53 mutants with different DNA substrates (supercoiled, sc; or linear, lin; open circular, oc DNA containing or lacking specific p53 target sequence – p53CON) towards increased salt concentrations using an immunoprecipitation assay on magnetic beads functionalized with G-protein [12]. The preformed immunocomplexes of p53-DNA with DO-1 antibody (mapping to N-terminus of p53) or Bp53-10.1 antibody (mapping to C-terminus of p53) were exposed to various salt concentrations. We found that the complexes of p53 with DNA substrates without free ends (supercoiled, open circular) captured via DO-1 antibody were more stable than complexes with free ends (linear DNA). The complexes of wtp53 with linDNA containing p53CON (sequence specific binding) were relatively more stable than complexes with linDNA lacking p53CON (non-sequence-specific binding) regardless of the used antibody.

Acknowledgement: This work was supported by GACR (P301/11/2076)

References

- [1] A.J. Levine, *Cell*, 88 (1997) 323.
- [2] T.R. Hupp, *Cell. Mol. Life Sci*, 55 (1999) 88.
- [3] B. Vogelstein, D. Lane, A.J. Levine, *Nature*, 408 (2000) 307.
- [4] E. Appella, C.W. Anderson, *Eur. J. Biochem.* 268 (2001) 2764.
- [5] P. Wang, M. Reed, Y. Wang, G. Mayr, J.E. Stenger, M.E. Anderson, J.F. Schwedes, P. Tegtmeyer, *Mol. Cell. Biol*, 14 (1994) 5182.
- [6] W.S. Eldeiry, S.E. Kern, J.A. Pietenpol, K.W. Kinzler, B. Vogelstein, *Nat. Genet*, 1 (1992) 45.
- [7] M. Fojta, H. Pivonkova, M. Brazdova, L. Kovarova, E. Palecek, S. Pospisilova, B. Vojtesek, J. Kasparikova, V. Brabec, *Biochem Pharmacol*, 65 (2003) 1305.
- [8] M. Fojta, H. Pivonkova, M. Brazdova, K. Nemcova, J. Palecek, B. Vojtesek, *Eur. J. Biochem.* 271 (2004) 3865.
- [9] M. Brazdova, J. Palecek, D.I. Cherny, S. Billova, M. Fojta, P. Pecinka, B. Vojtesek, T.M. Jovin, E. Palecek, *Nucleic Acids Res.* 30 (2002) 4966.
- [10] H. Pivonkova, M. Brazdova, J. Kasparikova, V. Brabec, M. Fojta, *Biochem Bioph Res Co*, 339 (2006) 477.
- [11] S.P. Hussain, C.C. Harris, *Mutat Res-Fund Mol M*, 428 (1999) 23.
- [12] H. Pivonkova, P. Sebest, P. Pecinka, O. Ticha, K. Nemcova, M. Brazdova, E.B. Jagelska, V. Brazda, M. Fojta, *Biochem. Bioph. Res. Comm*, 393 (2010) 894.

O13

Electrochemical immunoprecipitation assays for DNA-protein interactions

H. Pivoňková, K. Němcová, P. Šebest, M. Fojta

Institute of Biophysics, v.v.i., Academy of Sciences of the Czech Republic, Kralovopolska 135, Brno 612 65, e-mail: hapi@ibp.cz

In this contribution we present novel label-free and label-based structure-sensitive electrochemical DNA sensing techniques combined with immunoprecipitation at magnetic beads (MBIP) for the probing of DNA interactions with tumor suppressor protein p53. The label-free technique [1] relies on capture of the p53-DNA complexes at MB via anti-p53 antibodies, followed by salt-induced selective dissociation of linear DNA from the complex and its voltammetric detection. We show that competitive binding of p53 to various plasmid DNA substrates, including lin or scDNAs with or without a specific target site, can easily be followed by *ex-situ* electrochemical analysis of DNA recovered from the immunoprecipitated complexes. Compared to a conventional analysis of the p53-DNA binding by gel electrophoresis the electrochemical detection is faster and allows simpler quantitation of DNA containing free ends at submicrogram levels. Alternatively, the p53-DNA binding activities have been analyzed using competition MBIP with oligonucleotide probes labeled with an osmium complex with 2,2'-bipyridine (Os,bipy) [2]. Os,bipy modifies thymine residues in a single-stranded oligo(dT) tail [3] attached to a double stranded segment containing or not containing a p53 binding sequence. The labeled probe produces a specific electrochemical signal due to the osmium marker, allowing selective determination of the probe in the presence of unlabeled competitor DNA. Thus, relative affinities of the protein to various unlabeled competitor DNAs, differing in nucleotide sequence, secondary and/or higher-order structure, can easily be evaluated using the labeled probes as reference substrates. Both techniques were applied in combination with different antibodies specifically modulating the p53-DNA binding.

Acknowledgement

This work was supported by GACR (P301/11/2076), IAA400040901

References

- [1] K. Němcová, L. Havran, P. Šebest, M. Brazdova, H. Pivonkova, M. Fojta, *Anal. Chim. Acta* 668 (2010) 166.
- [2] K. Němcová, P. Šebest, L. Havran, P. Orsag, M. Fojta, H. Pivonkova,, Submitted to *Anal Chem* (2011)
- [3] M. Fojta, L. Havran, H. Pivonkova, P. Horakova, and M. Hocek, *Curr. Org. Chemi.* 15 (2011) 2936.

O14

Hypericin fluorescence in bilayer lipid membranes.

A. Strejčková¹, G. Bánó¹, J. Staničová², K. Štroffeková¹, G. Fabriciová¹, P. Miškovský¹

¹ Department of Biophysics, P. J. Šafárik University in Košice, Slovak Republic, e-mail: alena.strejckova@student.upjs.sk

² Institute of Biophysics and Biomathematics, UVMF, Košice, Slovak Republic

Hypericin (Hyp) – the natural photosensitizing pigment of the plants of genus *Hypericum* – has been extensively studied because of its antiviral properties and a possible application in photodynamic therapy of cancer. The transport of Hyp through the cell membrane is of major importance for the delivery of Hyp into target tumor cells [1]. Artificial membranes can be used to study the interaction of Hyp with lipid bilayers.

Hyp forms non-fluorescence aggregates in aqueous solutions, and dissolves as a monomer in the lipid membrane. It follows, that the presence of Hyp in the membrane can be detected by measuring its fluorescence. It is the aim of the present work to get information on the interaction of Hyp with bilayer lipid membranes by means of fluorescence and/or absorption measurements.

Bilayer lipid membrane (BLM) of 100 μm diameter is formed by Montal-Mueller method [2] using DPhPC. The membrane quality is monitored by capacitance measurements. After forming the BLM Hyp dissolved in DMSO is added to the membrane surroundings on both sides. Magnetic stirrers are used to promote Hyp mixing with the electrolyte. The final concentration of DMSO in the electrolyte is kept below 0,1%. The optical setup is depicted in Figure 1. Hyp monomers incorporated into the BLM are detected by time-resolved auto-fluorescence measurements using 488, 532 or 594 nm laser excitation. The fluorescence signal is measured either by a photomultiplier tube or by a spectrograph. The absorption of Hyp is detected by the PD2 photodiode (see Fig. 1).

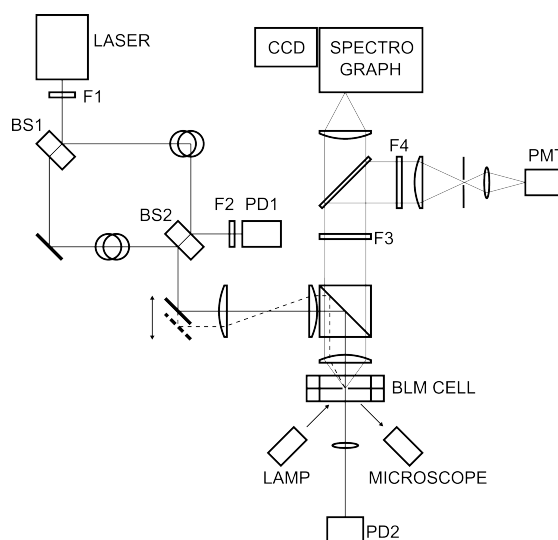


Fig. 1. The schematic view of the experimental setup. F1, F2 – neutral density filters, BS1, BS2 – beam samplers, PD1, PD2 – photodiodes, F3 – edge filter, F4 – bandpass filter, PMT – photomultiplier tube operated in photon counting mode.

Typical time-dependence of Hyp fluorescence (detected by the PMT) during the incorporation of the drug into the BLM is shown in Fig. 2a. The fluorescence onset is driven by two processes. First, there is a diffusion of the studied drug across the boundary layer near

the BLM surface, due to the reduced flow rate of the electrolyte at the surface [3]. Second, there is the time needed for the incorporation of the adsorbed molecules into the BLM. The fluorescence spectra of incorporated Hyp molecules (measured by the spectrograph) are shown in Fig 2b.

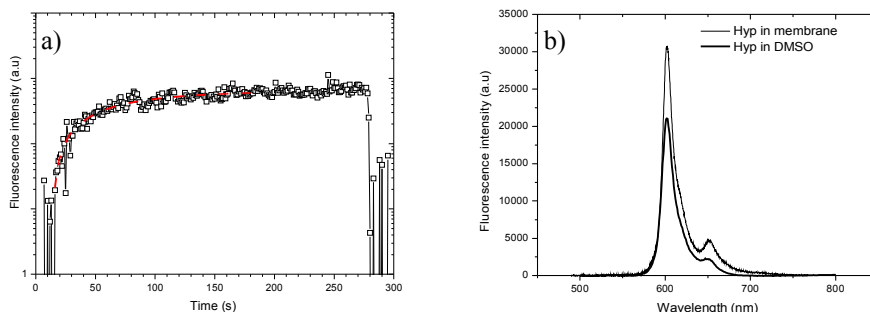


Fig. 2. a) Typical time-dependence of Hyp fluorescence signal (488 nm excitation) during the incorporation process. The concentration of Hyp in the electrolyte is $2 \cdot 10^{-6}$ M. b) Fluorescence spectra of Hyp incorporated into the bilayer membrane and in 100% DMSO.

The experimental setup allows one to get information on the orientation of Hyp molecules in the membrane by changing the angle of laser irradiation using two perpendicular polarizations of the excitation laser beam. The absorption data can be used to evaluate the density of Hyp molecules in the membrane.

Acknowledgement

This work was supported by Slovak Ministry of Education VEGA No. 1/1154/11, and by the Slovak Research and Development Agency, project No. LPP-0290-09.

References

- [1] Š. Bálint, S. Sánchez, V. Huntošová, P. Miškovský, D. Petrov, J. Biomed. Opt. 15 (2010) 027005/1 – 7.
- [2] M. Montal and P. Mueller. Proc. Nat. Acad. Sci. USA, 69 (1972) 3561-3566.
- [3] C. T. Everit, W. R. Redwood, D. A. Haydon., J. Theoret. Biol. 22 (1969) 20-32.

O15

Competition of anti-apoptotic protein kinase C α and pro-apoptotic protein kinase C δ in hypericin induced photodynamic action in U-87 MG

L. Dzurová¹, V. Huntošová^{1,2}, D. Petrovajová¹, P. Miškovský¹

¹ Department of Biophysics, University of Pavol Jozef Safarik, Kosice, Slovak Republic

² EPFL SB ISIC GR-VDB2, Lausanne, Switzerland, e-mail: lenka.dzurova@upjs.sk

Hypericin (Hyp) is a highly hydrophobic pigment and can be extracted from plants of the genus *Hypericum*. In generally Hyp displays antiproliferative and cytotoxic effects after light activation towards various cancerous cell-lines and is suitable initiator of apoptotic program in many cell cultures. Photoactivated Hyp has effect on activation or inhibition of PKC isoforms.

U-87 MG glioma cell line, which are characterized by higher expression of Protein Kinase C α (PKC α), Protein Kinase C δ (PKC δ) and Protein Kinase C ϵ (PKC ϵ) isoforms where used as a model in this study. PKC α has anti-apoptotic function and PKC δ with PKC ϵ are known as pro-apoptotic proteins. The equilibrium of these three isoforms is essential in life cycle of U-87MG cells.

The study was performed for 500 nM Hyp incubated with U-87MG glioma cells. Confocal fluorescence microscopy, flow-cytometry and specific fluorescence labeling were used as main experimental techniques. Our results show that Hyp photoaction strongly affects apoptotic response of the cells. The photo-damage results in mitochondria degradation: depolarization of the membrane, decrease of membrane potential ($\Delta\Psi$), aggregation and granulation of their structure. We also observed failure of nuclear membrane able to penetrate of Sytox Green, relocalization of PKC α from cytoplasm to perinuclear area and inhibition effect of Hyp on PKC α as was presented by our group before. PKC δ was localized 5h after Hyp photo-treatment in the nucleus and at longer time releases from nucleus to cytoplasm.

It can be concluded that Hyp photo-treatment causes not only relocalization of PKCs but also time dependent mode of their activation/inhibition.

Acknowledgments

This work was supported by the Slovak Research and Development Agency under contract num. APVV-LPP-0072-07, by the Scientific Grant Agency of the Ministry of Education of Slovak VEGA 1/0241/09, by the projects "Center for excellent research of atherosclerosis" (034/2009/2.1/OPR&D) (20%) and "Network of excellent laboratories in oncology" (26220120024) (20%) Operation Program Research and Development funded by European Regional Development Fund.

O16

***In situ* SERS detection of natural organic dyes and pigments in Cultural Heritage objects**

Z. Jurašková^{1,2}, C. Domingo¹, J. V. García-Ramos¹, S. Sánchez-Cortés¹

¹ Instituto de Estructura de la Materia, CSIC, Serrano 121, 280 06 Madrid, Spain

² Department of Biophysics, Faculty of Sciences, P. J. Šafárik University, Jesenná 5, 041 54 Košice, Slovakia, e-mail: zuzana.jurasekova@upjs.sk

Detection of natural organic dyes and pigments employed to colour Cultural Heritage objects is a challenge for scientists and conservators. The analytical methods currently employed are based on chromatographic techniques [1], which are highly sensitive and selective, but imply sampling and performing chemical extraction. Raman microscopy is nowadays used as a non-destructive, and even *in situ*, technique for identification of different materials, ranging from inorganic pigments to biomaterials, employed in artifacts so different as manuscripts, paintings, textiles, ceramics, glasses, sculptures stone monuments, and even mummies or underwater cannonballs, where degradation products can also be assessed [2]. Nevertheless, the application of this technique in the characterization of organic pigments and dyes has been limited by two main drawbacks: (1) the intense fluorescence emission from organic pigments, which normally covers the corresponding Raman spectra; and (2) the minute quantities of coloured material, which, in general, are below the detection limit of the low-sensitivity Raman technique. Removing or reducing the fluorescent background is accomplished either employing a longer wavelength laser (1064 nm) and interferometric detection (FT-Raman) [3] or applying changes in wavelength excitation with posterior mathematical procedures, as in SERDS (Shift-excitation Raman difference spectroscopy) and SSRS (Subtracted shifted Raman spectroscopy) [4, 5]. There is another Raman technique, SERS (Surface-Enhanced Raman Spectroscopy), which overcome the intrinsic problems above mentioned, because, when the sample under study is in close proximity to nanostructured metal surfaces, its fluorescence is quenched and its Raman spectrum is enhanced several orders of magnitude [6].

The research group in Madrid has pioneered the application of such technique to the characterization of the two most important families of natural organic pigments (anthraquinones [7, 8] and flavonoids [9]) which, due to their high dyeing capacity, are used in minute quantities not detectable by conventional Raman; a new method of production of silver nanoparticles (AgNPs) “on the dyed textile” (Figure) through laser photoreduction of a silver nitrate water solution in contact with the sample was developed [10, 11]. In this work we present the success application of the technique in the extractionless non-hydrolysis SERS detection of historical mordant dyes on model textiles fibres dyed according original old recipes (Fig., [11]). This *in situ* SERS study not only allowed the detection of the flavonoids luteolin and apigenin, but also the estimation of the relative amounts, the structural changes occurring on the adsorbed dyes upon interaction with the substrate, and their spatial distribution throughout the substrate. The reproducibility and suitability of the method was also successfully examined by *in situ* analysis of other flavonoid compounds detected on wool fibres dyed by different flavonoid-containing dyestuffs according the dyeing recipes range from traditional Mediterranean methods to pre-Columbian Central and South America ones [12]. In addition, a real archeological Coptic textile (6th-8th AD) from Egyptian origin was also inspected, and the anthraquinone alizarin has been clearly identified [12].

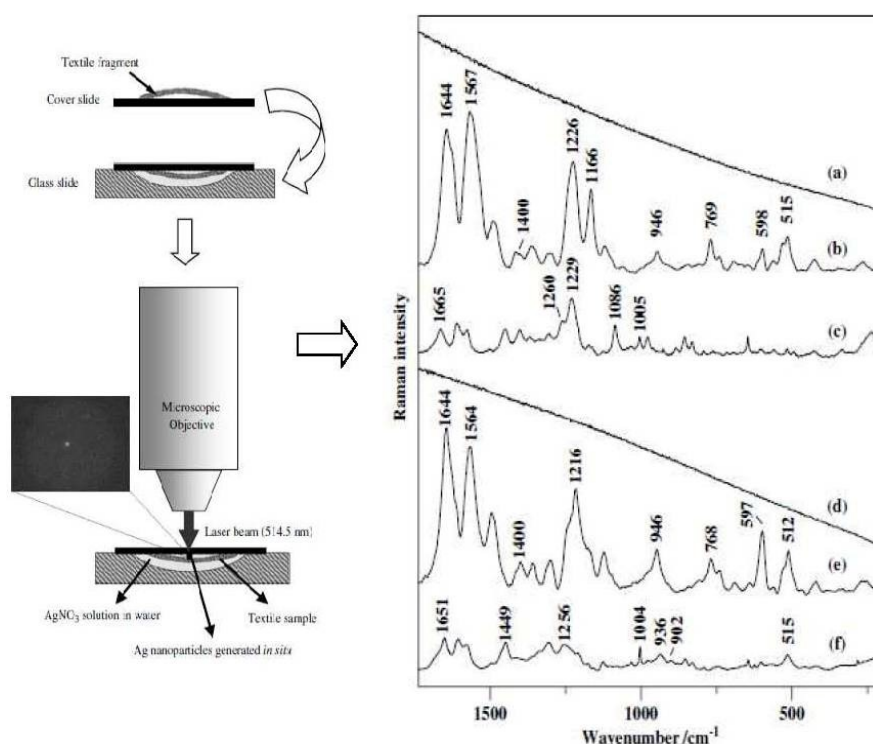


Figure: (Left) *In situ* preparation of photoreduced Ag nanoparticles (AgNPs) on textile fibres. This scheme was also used for the Raman spectra recording. The laser line at 514.5 nm was used both to create AgNPs and to excite SERS spectra from the fibre. The bright spot in the microscopic window displays the light reflection due to the presence of created AgNPs. (Right) Raman spectra of weld-dyed silk (a) and wool (d) obtained in the absence of AgNPs by exciting at 514.5 nm, 2 mW. Raman of weld-dyed silk (c) and wool (f) obtained by exciting at 785 nm, 2 mW. SERS spectra of weld-dyed silk (b) and wool (e) obtained after *in situ* fabrication of AgNPs (excitation at 514.5 nm, 2 mW). The SERS spectra were baseline corrected to withdraw the fluorescence background. Spectra were normalized by using the band at 1564 - 1567 cm^{-1} as a reference. [11]

Acknowledgement

This work was supported by European Community's Sixth Framework Programme (contract No. MEST-CT-2004-513915). Z.J. also acknowledges P. J. Šafárik University for the postdoctoral research fellowship.

References

- [1] X. Zhang, R. Boytner, J.L. Cabrera, R. Laursen, *Anal. Chem.* 79 (2007) 1575-1582.
- [2] P. Vandenameele, H.G.M. Edwards, L. Moens, *Chem. Rev.* 107 (2007) 675-686.
- [3] H.G.M. Edwards, L.F.C. de Oliveira, M. Nesbitt, *Analyst* 128 (2003).187-193.
- [4] I. Osticioli, A. Zoppi, E.M.J. Castellucci, *Raman Spectrosc.* 37 (2006) 974-980.
- [5] F. Rosi, M. Paolantoni, C. Clementi, B. Doherty, C. Miliani, B.G. Brunetti, A. Sgamellotti, *J. Raman Spectrosc.* 41 (2010) 452-458.
- [6] M. Fleischmann, P.J. Hendra, A.J. McQuilla, *Chem. Phys. Lett.* 26 (1974) 163-166.
- [7] M.V. Cañamares, J.V. Garcia-Ramos, C. Domingo, S. Sanchez-Cortes, *J. Raman Spectrosc.* 35 (2004) 921-927.
- [8] M.V. Cañamares, J.V. Garcia-Ramos, C. Domingo, S. Sanchez-Cortes, *S. Vibr. Spectrosc.* 40 (2006) 161-167.
- [9] Z. Jurasekova, J.V. Garcia-Ramos, C. Domingo, S.J. Sanchez-Cortes, *J. Raman Spectrosc.* 37 (2006) 1239-1241.
- [10] M.V. Cañamares, J.V. Garcia-Ramos, J.D. Gomez-Varga, C. Domingo, S. Sanchez-Cortes, *S. Langmuir* 23 (2007) 5210-5215.
- [11] Z. Jurasekova, C. Domingo, J.V. Garcia-Ramos, S. Sanchez-Cortes, *J. Raman Spectrosc.* 39 (2008) 1309-1312.
- [12] Z. Jurasekova, E. del Puerto, G. Bruno, J.V. Garcia-Ramos, S. Sanchez-Cortes, C. Domingo, *J. Raman Spectrosc.* 41 (2010) 1455-1461.

O17

Time-resolved measurements of endogenous NAD(P)H fluorescence in living systems

J. Horilová¹, M. Bučko², A. Illésová², D. Chorvát³, A. Chorvátová³

¹ Department of Nuclear Physics and Biophysics, FMFI UK, Mlynská dolina F1, 842 48 Bratislava, Slovakia, e-mail: j.horilova@gmail.com

² Institute of Chemistry, Slovak Academy of Sciences, 845 38 Bratislava, Slovakia

³ International Laser Centre, Ilkovičova 3, 841 04 Bratislava, Slovakia

Evaluation of the mitochondrial metabolic state is crucial for understanding of cellular energetics. Currently there is a lack of non-invasive techniques that would allow monitoring of the cell metabolism directly in living systems. Spectral characteristics of endogenous fluorophores, namely NAD(P)H, are unique and can therefore provide their specific identification and separation. Moreover, time-resolved fluorescence decay patterns are additional effective means of fluorophore separation (as spectrally-overlapping signals can often be segregated by distinct fluorescence lifetimes), or of its “free” and/or “bound” forms [1]. In recent years, advanced optical methods based on time-resolved measurements were developed for detection of mitochondrial oxidative state in living systems. Ratio of the “free/bound” NAD(P)H fluorescence amplitude was proposed to correspond to NADH/NAD⁺ reduction/oxidation pair and thus to mitochondrial NAD(P)H/NAD(P)⁺ in living systems [2, 3].

We have chosen time-resolved measurements of endogenous NAD(P)H fluorescence to evaluate mitochondrial metabolic state in living systems. NAD(P)H fluorescence was recorded using SPC-830 Time-Correlated Single Photon Counting (TCSPC) system from Becker-Hickl following excitation by 375 nm pulsed laser diode with detection of photon counts at emission wavelengths between 410 – 450 nm. *In vitro* measurements of NADH (Fig. 1) confirmed exponential rise of the fluorescence intensity with NADH concentration, with little modification in the fluorescence lifetimes.

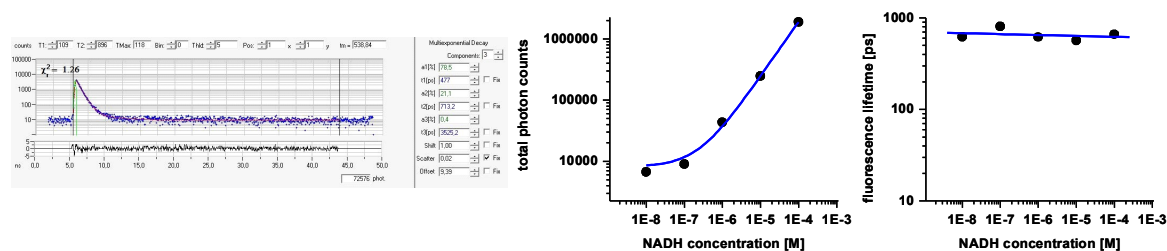


Fig. 1. Time-resolved fluorescence of NADH (10^{-6} M) in water (left; original recording), with concentration-dependence of total photon counts (centre) and fluorescence lifetimes (right).

We have decided to use the bacterial strain *Gluconobacter oxydans* as a model system. The genus *Gluconobacter* comprises some of the most frequently used microorganisms when it comes to biotechnological applications [4]. It has been involved in several processes, such as vinegar production and, in the last decades, many bioconversion routes for special and rare sugars as well as natural flavours involving *Gluconobacter* have been developed. The genus *Gluconobacter* belongs to the group of acetic acid bacteria, which are characterized by their ability to incompletely oxidize a wide range of carbohydrates and alcohols resulting in production of NAD(P)H in electron transport chain [5]. In most cases, the reactions are catalyzed by dehydrogenases connected to the respiratory chain.

Our goal was to evaluate whether NAD(P)H fluorescence can be recorded in

Gluconobacter oxydans and whether this parameter can be used for evaluation of the oxidative capacity and sensitivity of the oxidative metabolic state of this bacterial strain. Endogenous NAD(P)H fluorescence of *Gluconobacter oxydans* was measured in bacteria in cuvette (**Fig. 2**) resuspended at different concentrations in phosphate buffer (50 mM, pH 7). We have evaluated concentration dependence of the total photon counts of the bacterial endogenous fluorescence at room temperature (22°C) of either fresh bacteria (up to 5 hours after isolation) or defrosted after one week of congelation at -20°C. Temperature-dependent changes were also analyzed when the cuvette temperature was increased by temperature bath (RE106, Lauda) from 22°C to 30°C. We have observed clear rise in the endogenous fluorescence with the concentration of bacteria, which remained almost unaffected by the congelation. We have noted some increase in total photon counts at 30°C, but this observation still needs to be verified. Fluorescence lifetimes were little affected by the procedures at higher bacterial concentrations, indicating that the rise in the fluorescence intensity at these concentrations seems primarily related to the increase in the amount of bacteria and thus in the NAD(P)H content.

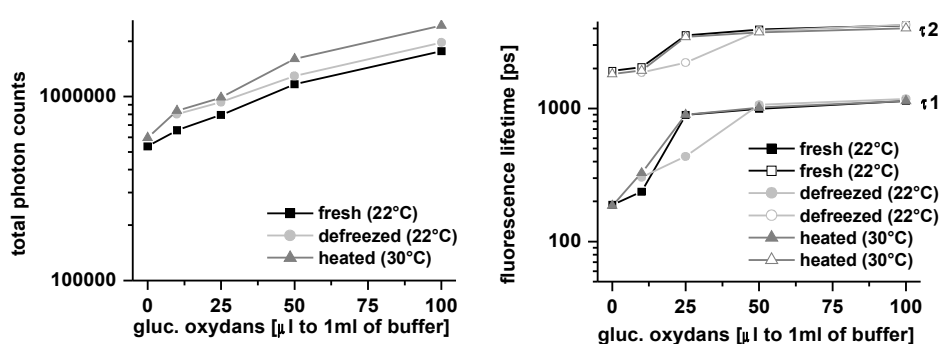


Fig. 2. NAD(P)H fluorescence of *Gluconobacter oxydans* in cuvette in phosphate buffer (50 mM, pH 7): total photon counts (left) and fluorescence lifetimes (right).

Gathered preliminary results demonstrate that endogenous NAD(P)H fluorescence can be successfully recorded in the bacterial strain *Gluconobacter oxydans* using time-resolved measurements. Containing NAD(P)H and basic mitochondrial respiratory chain, *Gluconobacter oxydans* thus represents a useful model system to obtain fundamental information on the functioning of the mitochondrial oxidative metabolism and its eventual changes during biocatalytic production of natural flavours and/or pathophysiological modifications.

Acknowledgement

This publication was supported by VEGA-1/0296/11 and APVV-0302-10.

References

- [1] D. Chorvat Jr. A. Chorvatova, *Laser Phys. Letters* 6 (2009) 175–193.
- [2] D.K. Bird, L. Yan, K.M. Vrotsos, K.W. Eliceiri, E.M. Vaughan, P.J. Keely, J.G. White, N. Ramanujam, *Cancer Res.* 65 (2005) 8766-8773.
- [3] R. Niesner, B. Peker, P. Schlusche, K.H. Gericke, *ChemPhysChem.* 5 (2004) 1141-1149.
- [4] C. Muynck, C.S.S. Pereira, M. Naessens, S. Parmentier, W. Soetaert, E.J. Vandamme, *Crit. Rev. Biotechnol.* 27 (2007) 147-171.
- [5] U. Deppenmeier, M. Hoffmeister, C. Prust, *Appl. Microbiol. Biotechnol.* 60 (2002) 233-242.

O18**LASERLAB-EUROPE working modes and opportunities**

D. Chorvát

International Laser Centre, Ilkovicova 3, 84104 Bratislava, Slovakia, e-mail: dusan@ilc.sk

Lasers are undoubtedly one of the key element of research across various disciplines, from life science to material research. To strengthen the role of Europe in laser science, LASERLAB-EUROPE project has been launched as an Integrated Initiative of European Laser Laboratories, operated under the 7th FP of the EU. The network of Laserlab Europe is formed from more than 26 laser infrastructures from 19 European countries, covering all areas of different scientific disciplines and creating a powerful network on a global scale for modern laser research. The aims of LASERLAB-EUROPE can be divided into three main working modes:

- Joint Research Activities between the partners,
- Transnational Access providing more than 1100 days per year of access to top-quality laser research facilities open for scientists all over Europe,
- Networking Activities that allows fostering collaboration, best practices, exchanges and user training, as well as public outreach activities.

User training activities in LASERLAB-EUROPE are focused at increasing the experience of Access Users providing special experimental and theoretical skills that are instrumental in specific areas of laser science, and expand the pool of prospective Users in new areas of science. These actions are mostly targeted to:

- i) new research groups, e.g. from new members states within the EC or groups from other scientific disciplines (biology/medicine) whose participation in the Access program is gradually increasing;
- ii) younger scientists, at the doctoral or post-doctoral level, while respecting the diversity and specific needs for different levels of collaboration with LASERLAB-EUROPE infrastructures.

The LASERLAB-EUROPE provides not only exclusive technical infrastructure, but also fruitful base for mentoring and collaboration in various fields of photonics/ laser research. Institutions and personnel participating in the User Training Schools has been subjected to number of joint discussions and brainstorming activities at different occasions, with the common goal of gradual optimization of the form and content of the Training. These include close collaboration with the User representatives and regular visits at User meetings, periodically organized under the cover of LASERLAB Networking Activities.

O19

Inauguration of SPIE Student Chapter in Slovakia

A. Chorvátová

International Laser Centre, Ilkovičova 3, 841 04 Bratislava, Slovakia, alzbeta.chorvatova@ilc.sk

Student Chapters of the International Society for Optical Engineering (SPIE) [1, 2] are an original opportunity offered by SPIE to students working in the fields of optics, photonics and related disciplines. As the students are the future leaders in these fields, SPIE provides an extensive support to students through information exchange, financial assistances and exposure to cutting-edge technology developments.

Student Chapter is designed to give students a voice, while funding and supporting yearly activities thanks to a chapter grant. It also allows applying for the Student Chapter Officer's Travel Grant to attend any SPIE event, invite an industry or research speaker through the Visiting Lecture Program, subscribing to SPIE Journal and to the SPIE Digital Library at a reduced rate with chapter funds, networking with other SPIE International Student Chapters and interacting with SPIE members from industry.



Fig. 1. Logo of the newly established SPIE Student Chapter in Slovakia.

In 2011, International Laser Centre (ILC) has applied to establish the first Student Chapter of the SPIE in Slovakia (**Fig. 1**). We have recently received the good news that our application was successful and that the International Laser Centre SPIE Student Chapter is now approved by the SPIE [3]. Currently, 15 students from institutions such as Slovak Technical University in Bratislava, University of Pavol Jozef Safarik in Kosice, Comenius University in Bratislava, or Zilina University in Liptovsky Mikulas are members of the newly establish chapter. Several activities are eligible for the SPIE support, including organisation of informal lectures, providing snacks at the Chapter meeting, develop workshops and volunteer to supplement science and math education, mentoring secondary science and technology students, inviting an industry or academic speakers, industry tours and many others.

The International Laser Centre SPIE Student Chapter is now looking for students in Slovakia, ideally at the Ph.D. and post-doctorate level that would be interested to take part in the SPIE Chapter activities. Those interested, please contact the chapter advisor.

Acknowledgement

Supported by the SPIE Student Chapter.

References

- [1] <http://spie.org/>.
- [2] <http://spie.org/x1727.xml>.
- [3] http://spie.org/x1742.xml?chapter_id=1059417.

O20**PhD study in Medical Biophysics at Jessenius Faculty of Medicine, Comenius University in Martin**J. Jakuš

Institute of Medical Biophysics, Jessenius Faculty of Medicine, Comenius University, Malá Hora 4, 036 01 Martin, Slovakia, e-mail: jakus@jfmed.uniba.sk

The PhD study in biophysics at Jessenius Faculty of Medicine, Comenius University (JFM CU) in Martin has more than 10 years history. At the beginning it has been connected with participation of Prof.MUDr. Ján Jakuš, D.Sc., a head of the Institute of Medical Biophysics JFM CU, in Joint Scientific Council on Biophysics at Faculty of Mathematics, Physics and Informatics of Comenius University. Only in a framework of the activities in this council it has been possible to finish PhD study of three internal and external doctoral students of JFM CU including Martin University Hospital.

The requirement of more narrow specialization in biomedical sciences resulted in attempts to establish in 2006 a new study program Medical Biophysics at Comenius University. According to the resolution of Ministry of Education of the Slovak Republic in Bratislava on March 19, 2007 it has been given a right to Comenius University in Bratislava to award PhD degree in Medical Biophysics both in the internal and external studies with restriction of 1 year. After evaluation of accredited study No. 7.1.27 „Medical Biophysics“ the Ministry of Education of Slovak Republic on October 14, 2010 passed a right to JLFUK for awarding PhD degree to the students who finished of 4 years internal and 5 years external study with no time restriction. The guarantor of this study program is prof. MUDr. Ján Jakuš, D.Sc. At the same time it has been given the right to JLFUK for habilitations of Assoc. professors and inauguration of Professors in Medical Biophysics.

The necessary condition for entering the PhD study is finished second stage of University education (MUDr, RNDr, MDD, MVDr) or in some engineering study programs (Ing) or the magister study programs (Mgr.), respectively. The study, scientific and administrative duties are managed by Specialized Council that is composed of Professors and Assoc. professors of JFM CU in Martin, FM CU in Bratislava, FM UPJS in Košice, University of Žilina and SHU in Bratislava. The requirements on the students including the study and scientific parts, also the credit system, PhD exams, defense of PhD thesis as well as other issues can be found at the web pages: www.jfmed.uniba.sk/index.php?id=377, www.jfmed.uniba.sk/index.php?id=2311, www.jfmed.uniba.sk/index.php?id=2448 a www.lefa.sk/prof_jakus/

O21

PhD study in biophysics in FMFI UKT. Hianik

Department of Nuclear Physics and Biophysics, Faculty of Mathematics, Physics and Informatics, Comenius University, Mlynska dolina F1, 842 48 Bratislava, Slovakia, e-mail: tiber.hianik@fmph.uniba.sk

Biophysics at Faculty of Mathematics, Physics and Informatics, Comenius University (FMFI UK) has long traditions. The Department of Biophysics has been established in 1979 thanks to the effort of prof. Dusan Chorvat, D.Sc. and former dean of the Faculty of Natural Sciences, prof. Sergej Usačev, D.Sc. However, even before this time the Division of Biophysics existed in Department of Experimental Physics. After prof. Ivan Hubač, D.Sc. joined the faculty in 1980 the Department has been extended also on Division of Chemical Physics and later also thanks to the effort of prof. Chorvat new study program Biomedical Physics, organized jointly by FMFI UK and Medical Faculty of Comenius University has been established. The guarantor of this program is currently prof. Libuša Šikurova, PhD. Later, in 2004, after administrative changes in the faculty the Department of Biophysics became part of newly established Department of Nuclear Physics and Biophysics. Since establishment of master program in biophysics, almost 35 years ago also the PhD program in biophysics has been started and continuing permanently to these days. Important peculiarity of this program is participation of leading scientists from several departments of FMFI UK, but also from faculty of Pharmacy, Medical Faculty as well as from Slovak Academy of Sciences, mostly from Institute of Molecular Physiology and Genetics. The Joint Scientific Council, that is responsible for acceptance of study program, supervisors, topics of the PhD thesis and their defense is composed of leading scientists from several Universities and Scientific Institutions from Slovakia and Czech Republic.

The duration of internal PhD program is 4 years and in external form 5 years. The program is open for students that finished master study in physics, biophysics, biomedical physics, pharmacy, medicine and other programs of natural sciences. The program is open also for foreign students. Currently 15 students are involved in this program. More information on the program can be found on webpage www.fmph.uniba.sk.

P1

Proapoptotic proteins distribution in U-87 MG glioma cells before and after photodynamic action.

L. Balogová, M. Maslaňáková, P. Miškovský, K. Štroffeková

Department of Biophysics, Pavol Jozef Safarik University, Faculty of Science, Jesenna 5, 040 01 Kosice Slovak Republic, e-mail: luba.svk@gmail.com

Introduction: Apoptosis, or programmed cell death, is a physiological process occurring in the embryonic development, tissue renewal, and the maintenance of cell homeostasis [1]. Apoptosis is a highly regulated process, and there is still a lot of unknown about its regulation mechanisms. We focused our attention towards the intrinsic mitochondrial pathway where Bcl-2 family of proteins plays the major role [2-4]. We are particularly interested in two proapoptotic players Bak and Bax from this family. Here we investigated their role in cell death triggered by photodynamic action. Targeted photodynamic therapy (PDT) is a promising approach to diagnose and treat different types of cancer, which are resistant to traditional approaches such as surgery, radiation and chemotherapy [5]. We show the localization of Bax and Bak in U-87 MG human glioma cells incubated with photosensitizer hypericin (Hyp) before and after photodynamic action.

Material and methods: Hyp was bought from Sigma-Aldrich. Stock solution was prepared by dissolving Hyp in 100% dimethyl sulfoxide (DMSO, Sigma-Aldrich). The final concentration was $2 \cdot 10^{-3}$ M. Cell culture medium Dulbecco's modified Eagle medium (D-MEM) with high glucose ($4500 \text{ mg} \cdot \text{L}^{-1}$) was purchased from Gibco-Invitrogen (Life Technologies LTD.). D-MEM was supplied with 10% Fetal Bovine Serum (FBS), Streptomycin ($50 \text{ } \mu\text{g} \cdot \text{mL}^{-1}$) and Penicillin ($50 \text{ } \mu\text{g} \cdot \text{mL}^{-1}$). Ultrosor G (artificial serum substitute without lipids) was from BioSeptra SA (France). Immortal cell line U-87 MG human glioma cells was purchased from CLS (Cell Lines Services, Germany). Primary antibodies: antibody against N-terminus of Bak (anti-Bak NT) was purchased from ψ ProSci Inc., (USA); antibodies purchased from Enzo Life Sciences AG (Switzerland) were: against Bax (anti-Bax 2D2); antibody against active form of Bax (anti-Bax 6A7). Secondary antibodies were purchased from Invitrogen (Life Technologies LTD.): goat anti-rabbit conjugated with Alexa Fluor 488 and goat anti-mouse conjugated with Alexa Fluor 546. Results were obtained by immunocytochemistry and fluorescent confocal microscopy using LSM 700 confocal scanning microscope with 63X oil objective (Zeiss, Germany).

Cell culture: Cell cultures were prepared and plated according propagation protocols onto 35 mm culture dishes with integral No.0 glass cover slip bottoms (MatTek, USA). The U-87 MG human glioma cells were grown in D-MEM supplemented with 10% FBS or serum substitute 2% Ultrosor G, in the presence of 5% CO₂ humidified atmosphere at 37°C. Cells were incubated in dark. For all experiments final content of DMSO was less than 0.1%. After reaching 40-50% confluence, cells were treated according PDT protocol, followed by immunocytochemistry.

PDT protocol: U-87 MG human glioma cells were grown in D-MEM supplemented with 2% Ultrosor G for 24 hours. After that cells were incubated one hour with Hyp (final concentration either 90 or 500 nM), in the presence of 5% CO₂ humidified atmosphere at 37°C. After the incubation with Hyp in Ultrosor G containing media, cell media were changed to D-MEM containing 10% FBS. Cells were then illuminated by light of 590 nm wavelength at the light dose of $4 \text{ J} \cdot \text{cm}^{-2}$. After the illumination, cells were placed in the CO₂ incubator for one hour in dark. After one hour cells were fixed according immunocytochemistry protocol.

Immunocytochemistry protocol: Cell cultures were plated onto 35 mm culture dishes with

integral No.0 glass cover slip bottoms (MatTek, USA). The cells were fixed with 100% methanol at -20°C for a minimum of 20 min. Cells were then incubated 1 hour in PBS (phosphate-buffered saline) containing 1% BSA (bovine serum albumin), 10% goat serum, 0,4 mM Mg^{2+} and 0,2 mM Ca^{2+} to block unspecific labeling. After 3 washes with PBS/BSA (0.2%), cells were incubated with specific primary antibody (Ab) against Bak (anti-Bak NT) overnight at 4°C . Cells were washed out 3 times with PBS/BSA (0.2%), followed by 1 hour incubation with appropriate secondary Ab conjugated with Alexa 488 at 37°C . Cells were then washed 3 times with PBS/BSA (0,2%) to remove unbind secondary Ab. After 3 washes with PBS/BSA (0,2%), cells were incubated with specific primary Ab against Bax (anti-Bax 2D2 or anti-Bax 6A7) for 1 hour at 37°C . Cells were washed out 3 times with PBS/BSA (0.2%), followed by 1 hour incubation with appropriate secondary Ab conjugated with Alexa 546 at room temperature. Cells were then washed 3 times with PBS/BSA (0.2%) to remove unbind secondary Ab, placed in PBS/BSA (0.2%), and assessed with a confocal microscope (LSM 700, Zeiss).

Results:

1. In U-87 MG glioma cells incubated with either 90 or 500 nM Hypericin without irradiation, Bak localizes predominantly in mitochondria which are distributed homogenously throughout the cell. Bax localizes in cytosol and in small portion is peripherally attached to mitochondria similarly to previously published findings [6, 7].
2. After an apoptotic stimulus (PDT), Bak containing mitochondria move predominantly towards plasma membrane, Bax translocates to mitochondria, and mitochondria containing Bax are distributed throughout the cell.
3. Mitochondria containing Bax and Bak simultaneously (see co-localization in Fig.1) are almost exclusively localized near plasma membrane.

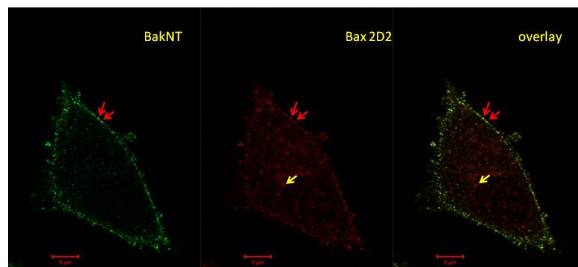


Fig.1. Immunocytochemistry of pro-apoptotic proteins Bak and Bax in U-87 MG glioma cells after PDT.

Green fluorescence represents distribution of Bak and red signal distribution of Bax. Please note, that mitochondria near plasma membrane contain Bax and Bak simultaneously (red arrows). Mitochondria containing Bax only reside throughout of the cell (yellow arrow).

Conclusion: Apoptotic stimulus by photodynamic action at the presence of Hyp causes Bax translocation into mitochondria. However our results suggest, that under these conditions there are two populations of mitochondria, one which contain Bax and Bak simultaneously, and the other which contain Bax only.

Acknowledgement: This work was supported by PIRG06-GA-2009-256580 to KS, Marie Curie Actions FP7-PEOPLE-2009-RG,EU.

References:

- [1] S. Y. Hsu, A. J. W. Hsueh, *Physiol. Rev.* 80 (2002) 593-614
- [2] M. F. van Delft, D. C. S. Huang, *Cell Res.* 16 (2006) 203-213
- [3] L. Zhou, D. C. Chang, *J. Cell Sci.* 121 (2008) 2186-2196
- [4] J. M. Adams, S. Cory, *Curr. Opin. Immunol.* 19 (2007) 488-496
- [5] P. Miskovsky, *Curr. Drug Targets* 3 (2002) 55-84
- [6] A. Schinzel *J. Cell Biol.* 164 (2004) 1021-1032
- [7] S.A. Desagher et al., *J. Cell. Biol.* 144 (1999) 891-901.

P2

Activity of PKC isoforms in U-87MG glioma cells before and after PDT treatment- Western blot study

L. Dzurová, D. Petrovajová, K. Štroffeková, Z. Naďová, P. Miškovský

Department of Biophysics, Pavol Jozef Safarik University, Faculty of Science, Jesenna 5, 040 01 Kosice Slovak Republic, e-mail: dana.petrovajova@student.upjs.sk

Apoptosis (programmed cell death) increase greatly with the identification of some of the major components of the apoptotic programme and the processes regulating their activation. Although apoptosis is an intrinsic process present in all cells, it can be regulated by extrinsic factors, including hormones, growth factors, cell surface receptors and cellular stress. The actions of both pro- and antiapoptotic factors are often affected by modulation of the phosphorylation status of key elements of the apoptotic process [1].

Protein kinases (PKC) participate in the regulation of early stages of apoptosis by phosphorylating key apoptotic proteins or in later events by acting downstream of caspases [2]. PKC δ has a role in the execution of the apoptotic program, while PKC α is frequently associated with cell survival and suppression of apoptosis [3]. U-87 MG glioma cell line are characterized by higher expression of PKC α , PKC δ and PKC ϵ isoforms. The equilibrium of these isoforms is essential for life cycle of U-87MG cells.

From our previous results we know, that hypericin photo-treatment causes not only relocalization of PKCs but also time dependent mode of their activation/inhibition. The opposite role of PKC α and PKC δ isoforms in apoptotic process induced by photodynamic action was examined by Western blot technique in order to quantify concentration ratio of different PKC α and PKC δ isoforms.

Acknowledgement

This work was supported by the Slovak Research and Development Agency under contract num. APVV-LPP-0072-07, by the Scientific Grant Agency of the Ministry of Education of Slovak VEGA 1/0241/09, by the projects within Operation Program Research and Development funded by European Regional Development Fund: "Center for excellent research of atherosclerosis" (034/2009/2.1/OPR&D) (20%), "Network of excellent laboratories in oncology" (26220120024) (20%) and "NanoBioSens" (26220220107) (10%).

References

- [1] T. G. [Cross](#), D. [Scheel-Toellner](#), N.V. [Henriquez](#), E. Deacon, M. [Salmon](#), J. M. [Lord](#), [Exp Cell Res.](#) 256 (2000) 34-41.
- [2] C. Brodie, P. M. Blumberg, *Apoptosis* 8 (2003) 19–27.
- [3] Ch. A. Carter, *Current Drug Targets* 1 (2000) 163-183.

P3

The use chorioallantoic membrane of quail embryo as an *in vivo* model for the study of photodynamically active drugs

I. Čavarga¹, B. Bilčík², P. Výboh², P. Miškovský³, L. Košťál², P. Kasák⁴, B. Čunderlíková⁵, P. Mlkvý¹, A. Mateašík⁵, D. Chorvát⁵, A. Chorvátová⁵

¹ St Elizabeth Oncological Institute, OUSA, Bratislava, Slovakia

² Institute of Animal Biochemistry and Genetics, Slovak Academy of Sciences, Bratislava, Slovakia

³ Department of Biophysics, Faculty of Sciences, Pavol Jozef Šafárik University, Košice, Slovakia

⁴ Polymer Institute, Slovak Academy of Sciences, Bratislava, Slovakia

⁵ International Laser Center, 841 04 Bratislava, Slovakia, alzbeta.chorvatova@ilc.sk

Photodynamic therapy (PDT) is a promising and innovative treatment for small localized tumors, in post-surgical adjuvant protocols, and in palliative treatment of inoperable advanced tumors. PDT is based on the concept that tumor destruction occurs when a photodynamically active molecule, photosensitizer, administered into a human body, accumulates within the tumor and is consequently illuminated by light. However, despite intense PDT research in many laboratories worldwide, there is still shortage of easily accessible *in vivo* models that would allow to study the action of photodynamically active drugs experimentally.

Chorioallantoic membrane (CAM) assay is an established model for evaluating angiogenesis and it has long been a favored system for the study of tumor angiogenesis and antivascular therapy [1-5]. Avian chorioallantoic membrane (CAM) is an extra embryonic membrane formed on day 4 of incubation. It has very thick capillary network. Rapid capillary proliferation continues and the vascular system attains its final arrangement before hatching.

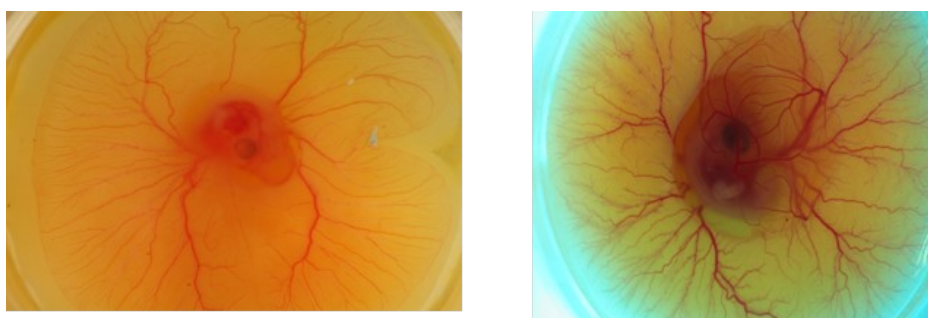


Fig. 1. Embryo isolated using *ex ovo* technique: reflectance image in a white light (Canon EOS 40D, left) and autofluorescence image via emission filter blocking blue excitation light to enhance anatomical structures and vasculature (right).

We have therefore evaluated the possibility to use the chorioallantoic membrane of quail embryo as an *in vivo* model for the study of the effects of photodynamically active drugs. CAMs are cultured either *in ovo*, or *ex ovo* as a shell-less culture. Each of these methods has benefits and disadvantages. Although the chicken CAMs are the most widely used, we have tested the CAM of the Japanese quail. **Fig. 1** illustrates an embryo isolated by the *ex ovo* technique. In this model, tested substances can be applied systemically (intravenously into yolk, or intraperitoneally), or topically into the silicone ring. There is also the possibility to study the tumors grown on the surface of the chorioallantoic membrane in this model.

The new model was tested to evaluate its possible use for the study of photodynamic active drugs, namely Foscan® (temoporfin) *meta*-tetra(hydroxyphenyl)chlorin (*m*THPC) and Hypericin (HYP), 7,14-dione-1,3,4,6,8,13-hexahydroxy 10,11-dimethyl-phenanthrol [1,10,9,8-*opqra*] perylene. Foscan® is a photosensitive drug routinely used in the clinical

practice for photodynamic palliative therapy of patients with advanced squamocellular carcinoma of head and neck, where all the other therapies failed. Foscan® was applied by topical application into quail CAM to study its effects on the vascular damage after 1 hour of PDT (**Fig. 2**).

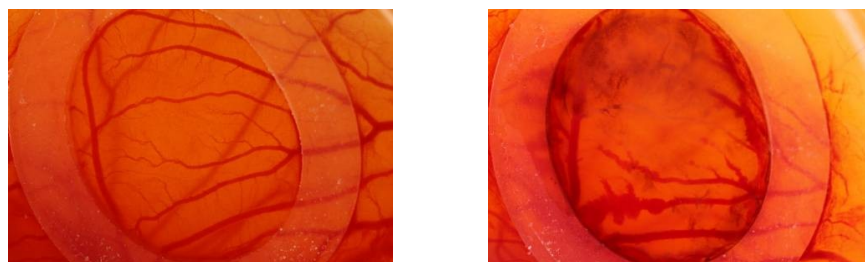


Fig. 2. Quail CAM before Foscan® topical application at a dose 0,5mg/ml into silicone ring (left) and quail CAM vascular damage (thrombosis, disruption, constriction) 1 hour after PDT (right): fluence rate 14mW/cm², fluence 16.8J/cm², excitation at 405nm.

HYP, is a natural photosensitizing pigment occurring in plants of the genus *Hypericum*. HYP under light illumination displays antiproliferative and cytotoxic effects (necrosis as well as apoptosis) in many tumor cell lines and is therefore a promising agent in PDT of cancer. HYP was also applied to the quail CAM by an *ex ovo* technique (**Fig. 3**). Gathered preliminary results indicate that, thanks to the transparency of its tissues, quail CAM model can be useful particularly for development of novel biophotonic techniques for investigation of the effects of photodynamically active drugs, namely in the case of examination of surface mucosal malignancies.



Fig. 3. Quail CAM (*ex ovo* technique) before HYP application. Autofluorescence image (left) and HYP fluorescence (right) in vascular compartment 24 hours after systemic (into yolk sac) application at a dose 2mg/kg.

Acknowledgement

This publication was supported by VEGA-1/0296/11.

References

- [1] Papoutsi M. et al., *Micros. Res.Tech.* 55 (2001) 100.
- [2] Vyboh P. et al., *Acta Vet.* 79 (2010) 13.
- [3] Gottfried V. et al., *J. Photochem. Photobiol. B* 30 (1995) 115.
- [4] Hagedorn M. et al., *PNAS* 102 (2005) 1643.
- [5] Zeisser-Labouebe M. et al., *Nanomedicine* 4 (2009) 135.

P4

Changes in synchronous fluorescence spectra of human urine induced by ovarian tumors

M. Zvarík¹, L. Šikurová¹, E. Hunáková², D. Martinický³

¹ Department of Nuclear Physics and Biophysics, Faculty of Mathematics, Physics and Informatics, Comenius University, Bratislava, Slovakia, e-mail: zvarikmilan@gmail.com

² Cancer Research Institute Slovak Academy of Sciences, Bratislava, Slovakia

³ Department of Gynecological Oncology, National Cancer Institute, Bratislava, Slovakia

Introduction: Analysis of urine is widely used for detection of various medical conditions. As urine contains many intrinsic fluorophores, modern fluorescence techniques are perspective candidates for new routine urine tests [1]. When compared to other methods, fluorescence analysis is fast, safe, highly sensitive, and non-invasive. Also, this method is stressless for patients and cheap enough to be provided routinely. Synchronous fluorescence spectroscopy has been used to resolve many components in a mixture without previous physical separation [2]. Compared with ordinary emission spectra, a synchronous spectrum often has more features and thus provides more information, in part because varying both excitation and emission varies the contribution of more components to the spectrum. In this study, we concentrated on the analysis of changes in synchronous fluorescence spectrum of urine from patients with malignant and benign ovarian tumor in comparison to healthy subjects.

Materials and Methods: 22 morning urine samples from fasting normal volunteers and 76 patients (36 with malignant and 40 with benign ovarian tumor) were used in this study. All of them were analyzed for pH, protein, glucose, bilirubin, nitrate, hemoglobin, ketones, acetone, and urobilinogen. The presence of red blood cells, white blood cells, casts, epithelial cells and crystals was also tested in these samples at the Department of Clinical Biochemistry, National Cancer Institute, Bratislava, Slovakia. 22 samples from volunteers (women aged 23 - 54) showed no abnormal laboratory findings and they were referred to healthy samples, i.e. controls. 76 urine samples were taken from female patients (women aged 36 – 78) before radical surgery for ovarian tumor. The histological examination of removed tissues confirmed ovarian malignant or benign tumors (ICD 10 code C56 or D27). Urine samples were taken before the start of anticancer or antibiotic therapy. Urine samples were centrifuged at 3000 rpm for 10 min at room temperature ($22 \pm 1^\circ\text{C}$) and supernatants were used undiluted for spectral analysis. The detailed fluorescence data of urine samples were obtained on a LS45 (PerkinElmer) luminescence spectrometer using the FL WinLab software. Measurements were taken at room temperature ($22 \pm 1^\circ\text{C}$) in an ultra micro quartz cuvette (5 mm excitation path length and 1 mm emission path length). Both emission and excitation slit widths were set to 10 nm. Synchronous fluorescence spectra (SFS) were collected by simultaneously scanning the excitation and emission monochromator in the excitation wavelength range 250 - 550 nm, with constant wavelength differences $\Delta\lambda$ between them. Our spectra were recorded for $\Delta\lambda = 70$ nm. The Mann–Whitney U test was used to compare mean values of fluorescence of urine samples from healthy and oncological patients.

Result and discussion: Typical synchronous fluorescence spectrum (SFS) for $\Delta\lambda = 70$ nm of undiluted urine sample from healthy human is presented in Fig. 1 (solid line). We can resolve three main bands at 340 nm, 360 nm and 450 nm. All of these spectral characteristics were found in each of the 22 urine samples from healthy controls. According to previously published fluorescence characteristics, the peak at 340 nm can be attributed to several fluorophores; pyridoxic acid is the strongest fluorescent species from this group [2] and other urine compounds, such as uric acid, xantine or hydroxyanthranilic acid might contribute to

this fluorescence, too. The peak at 360 nm may be formed by one or more species, mainly blue-fluorescing pteridines, and perhaps kynurenines [2]. The peak at 450 nm is most likely due to the presence of flavins and their metabolites [2].

The SFS of undiluted urine from oncological patients were different from the SFS from healthy volunteers. We observed pronounced depression of fluorescence peaks at 340 nm and 360 nm in urine samples from benign (dashed) and malignant (dotted) patients. Urine samples from patients with malignant tumor are characterized by domination of the peak at 360 nm in this spectral region (300 nm - 400 nm). We found significant difference ($p < 0.01$) in fluorescence at 340 nm and 360 nm between control samples and samples from malignant patients (Fig. 2). Moreover, the ratio of intensities of the peaks at 360 nm and at 340 nm is statistical significantly ($p < 0.01$) elevated in patients with ovarian malignant tumor compared to healthy persons (Fig. 2). On the contrary, the intensities at 450 nm do not show any significant changes (Fig. 1, 2).

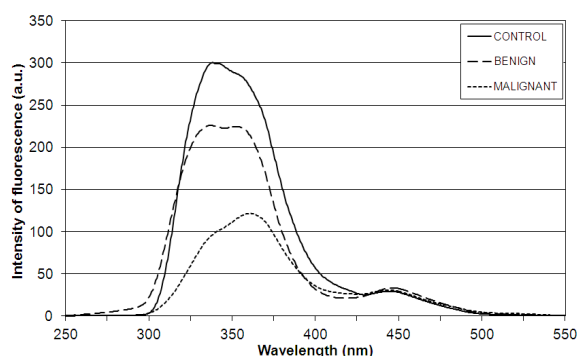


Fig. 1 Representative synchronous fluorescence spectrum of undiluted urine from healthy human (control, solid) and oncological patients with benign (dashed) and malignant (dotted) tumor.

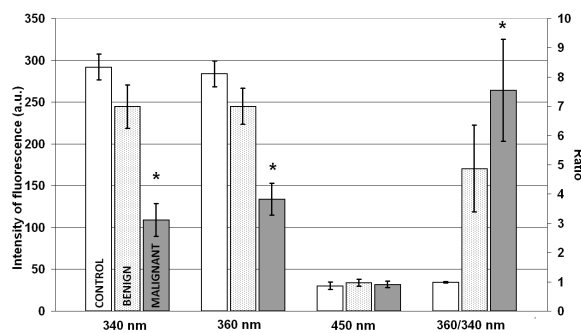


Fig. 2 Mean value (\pm SEM) of fluorescence intensity at 340 nm, 360 nm, 450 nm and ratio of fluorescence between 340 nm and 360 nm of undiluted urine from healthy human (control, white) and oncological patients with benign (dotted) and malignant (grey) tumor.

* - significant difference between control and oncological group ($p < 0.01$).

Conclusion: We focus on the analysis of intrinsic fluorescence of human urine using synchronous fluorescence spectra, comparing healthy persons and oncological patients with benign and malignant tumors. The SFS represents the graphical definition of the urine sample with a characteristic shape and with high sensitivity to pathological changes in urine composition. Consequently, monitoring of urine composition by this method reveals feasibility of a simple, noninvasive, inexpensive approach for the detection of cancer.

Acknowledgement

The authors acknowledge a support provided by VEGA grants 2/0177/11 and 1/0668/11, and by a grant from The Slovak Research and Development Agency under the contract VVCE-0001-07. This publication is also the result of the project implementation: BIOMAKRO2, ITMS: 26240120027 and project No. 26240220004 supported by the Research & Development Operational Programme funded by the ERDF.

References

- [1] E.J. Saude, D. Adamko, B.H. Rowe, T. Marrie, B.D. Sykes, *Metabolomics* 3 (2007) 439–451.
- [2] K. Dubayova, J. Kusnir, L. Podracka, *J. Biochem. Biophys. Methods* 55 (2003) 111–119.
- [3] M.J.P. Leiner, M.R. Hubmann, O.S. Wolfbeis, *Anal. Chim. Acta.* 198 (1987) 13–23.
- [4] V. Masilamani, T. Vijmasi, M.Al Salhi, K. Govindaraj, A.P. Vijaya-Raghavan, B. Antonisamy, *J. Biomed. Opt.* 15 (2010) 057003.

P5

A study of fish oil influence on aorta fluorescence of healthy and diabetic rats

M. Uherek¹, L. Šikurová¹, O. Uličná²

¹Department of Nuclear Physics and Biophysics, Faculty of Mathematics, Physics and Informatics, Mlynská dolina, Bratislava, 842 48, ²Department of Pathology, Faculty of Medicine, Comenius University, Špitálska 24, Bratislava, 813 72, kerehu@gmail.com

Alterations in the arterial wall have been suggested to play a role in the development of macrovascular disease in diabetes mellitus. Arterial wall contains naturally occurring, e.g. endogenous or intrinsic fluorophores: aromatic amino acids, structural proteins, and cofactors. Thus fluorescence-based techniques can be valuable tools for studying cellular structure and function, and interactions of molecules in arteries, including aortas [1,2,3].

Our work is aimed at monitoring of the naturally occurring fluorophores of thoracic aorta (tunica intima) of rats of Wistar strain by fluorescence spectroscopy, while fluorescence alterations induced by diabetes mellitus and its treatment by fish oil are studied.

Segments of aorta (ranged from 1 to 3 cm) were isolated from healthy (control) and diabetic adult male Wistar rats. Diabetes mellitus was induced by streptozotocin. Total number of animals was 100, whereas 60 subjects had diabetes and 40 subjects were healthy controls. We divided rats into ten groups with ten animals. The animals were three times weighted and monitored for blood glucose concentration during the experiment. Control and diabetic animals were treated by two doses of fish oil, 80 mg/kg/day and 400 mg/kg/day for 8 weeks. Fish oil comprises 59% eikozapentaen acid (C20:5) and 41% dokozaheptaen acid (C20:6).

The fluorescence spectra were obtained from the aorta layer known as tunica intima using a LS45 PerkinElmer luminescence spectrometer equipped with an external fibre optic accessory. All the sample preparations and measurements were carried out at 25 ± 2 °C and protected from light. The sample was transferred in a physiological buffer solution for maximally two hours at 4 °C.

The results were subject to the two sample t-test to verify the difference in fluorescence intensity. Data were considered statistically significant at P values < 0.05.

Monitoring of aortic segments using excitation wavelength of 270 nm

The wavelength of 270 nm is the excitation maximum for aromatic amino acids in proteins, specifically tryptophan, tyrosine, and phenylalanine [1,2], that is why we used it for monitoring of protein presence in the tunica intima of aorta. Recorded emission maxima were in the range of interval 332 – 342,5 nm, which is the evidence of mainly tryptophan presence [1].

We found the significant difference in fluorescence intensity of the amino acids of the aortic segments of the diabetic samples and control samples (Fig. 1, Tab. 1). Amount of amino acids (proteins) is higher in case of the aorta of diabetic subjects than that for the control samples.

Application of both doses of fish oil to the healthy rats (controls) did not cause any significant fluorescence changes. Application of 80 mg/kg/day of fish oil to the diabetic rats induced significant decrease in fluorescence intensity of amino acids; however treatment of higher fish oil dose 400 mg/kg/day caused a non-significant decrease in fluorescence intensity of aromatic amino acids in treated samples compared to untreated diabetic aorta segments (Fig. 1, Tab.1). The lower dose of fish oil (80 mg/kg/day) appeared sufficient for suppression of some pathological processes in diabetic aorta.

Monitoring of aortic segments using excitation wavelength of 340 nm

The excitation maximum 340 nm corresponds particularly to collagen and elastin

molecules [1, 2]. We found intensive emission peak in interval from 380 to 389 nm for both investigated groups of aortic segments at excitation 340 nm and it can be considered as collagen fluorescence [1,2]. We observed only a non significant increase in fluorescence intensity of collagen in diabetic aorta segments compared to healthy samples (Fig. 2, Tab.2). Application of both doses of fish oil to the healthy rats (controls) cause significant fluorescence changes. However application of 400 mg/kg/day of fish oil to the diabetic rats induced a lower significant decrease in fluorescence intensity of collagen as compared to untreated diabetic samples.

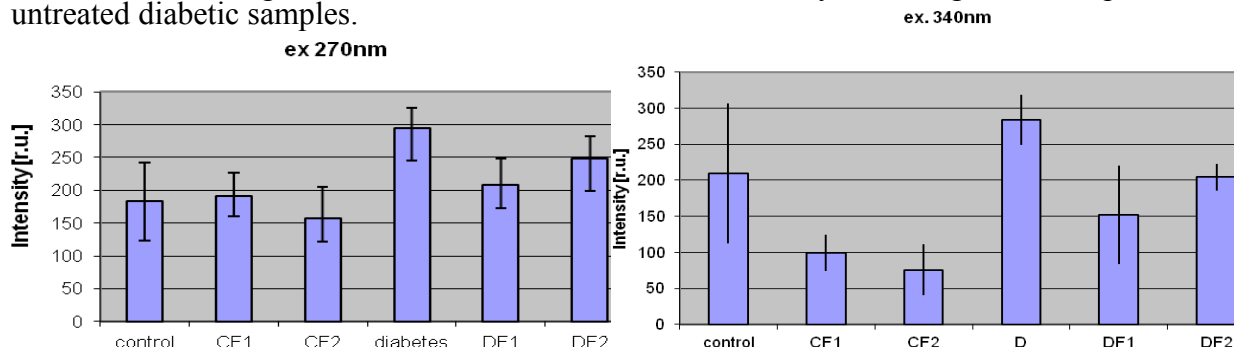


Fig. 1. The fluorescence intensity of aortic segments of rats of Wistar strain at excitation 270 nm, emission at about 338 nm. Statistical significances are presented in Tab. 1.
Fig. 2. The fluorescence intensity of aortic segments of rats of Wistar strain at excitation 340 nm, emission at about 388 nm. Statistical significances are presented in Tab. 2

(control – healthy animals (control group); CF1, CF2 - healthy animals treated with two doses of fish oil, 80 and 400 mg/kg/day; D – animals with diabetes mellitus; DF1, DF2 – animals with diabetes mellitus treated with two doses of fish oil, 80 and 400 mg/kg/day) The data are expressed as the means \pm SD of 8 independent experiments.

Tab.1		P	s/ns
C	D	0,001671	s
D	CF1	0,765382	ns
	CF2	0,192051	ns
	DF1	0,001839	s
	DF2	0,882673	ns

Tab.2		P	s/ns
C	D	0,138359	ns
D	CF1	0,013949	s
	CF2	0,006997	s
	DF1	0,000632	s
	DF2	0,003303	s

Tab. 1. Basic statistical summaries of the data for excitation at 270 nm (Fig. 1).

Tab. 2. Basic statistical summaries of the data for excitation at 340 nm (Fig. 2).

(P - the probability of observing data; s – significant, ns – non-significant; C – healthy animals (control group); CF1, CF2 - healthy animals treated with two doses of fish oil, 80 and 400 mg/kg/day; D – animals with diabetes mellitus; DF1, DF2 – animals with diabetes mellitus treated with two doses of fish oil, 80 and 400 mg/kg/day)

Acknowledgement: The authors acknowledge a support provided by the Comenius University Grant No. UK/579/2011. This publication is the result of the project implementation: BIOMAKRO2, ITMS: 26240120027 and project No. 26240220004, supported by the Research & Development Operational Programme funded by the ERDF

References

- [1] N. Ramanujam, Fluorescence spectroscopy in vivo, Encyclopedia of Analytical Chemistry, John Wiley & Sons Ltd., Chichester, 2000.
- [2] M. Aldrovania, A.M.A. Guaraldob, B. De Campos Vidala, Fluorescence, birefringence and confocal microscopy of the abdominal aorta from nonobese diabetic (NOD) mice, Elsevier, 2007.
- [3] I. Hulin et al., Patofyziológia a klinická fyziológia, Bratislava, SAP 494-498 (2005) 229-239.

P6

Measurement of fluorescence anisotropy as a parameter of membrane fluidity in patients with chronic kidney diseaseM. Morvová¹, L. Šikurová¹¹ Department of Nuclear Physics and Biophysics, FMFI UK, Mlynská dolina F1, 842 48 Bratislava, Slovakia, e-mail: morvova@gmail.com**Introduction**

Chronic kidney disease (CKD) represents diseases in presence of kidney damage or reduced levels of kidney function for more than 3 months [1]. In terminal stages, CKD results in loss of kidney function, dialysis, respectively kidney transplantation. We intended to investigate whether the early stages of CKD (specifically 2. - 3. stage) imply alterations in cell membrane properties. Anisotropy measurements with fluorescence probe are commonly used to measure fluidity of membranes. In biological membranes position of probe restricts the movement of phospholipids, probe oscillates with membrane phospholipids and so it can be used to measure the fluidity of membranes [2]. We chose red blood cells (RBC) membranes, because they represent the simplest usable model to study membrane fluidity since they avoid the contribution of other intracellular structures besides plasma membrane.

Material and methods

Twenty-one patients with stage 2.-3. of CKD and thirty-seven age- and gender-matched healthy volunteers with normal haematological and biochemical values were included in the study. The diagnosis of CKD was based on clinical and laboratory examinations as defined by the K/DOQI criteria [1]. The Ethics Committee of Slovak Medical University approved the study and all participants gave their written informed consent. As a biological sample we used human blood, which was granted from Laboratory of Experimental and Clinical Biochemistry of Slovak Medical University in Bratislava. Blood was taken in tubes containing heparin, subsequently plasma, leukocytes and platelets were removed, and only red blood cells were used for this work. From erythrocyte mass we had isolated red blood cell membranes, we achieved "ghosts" using standard method Hanahan&Ekholm [3] modified in our laboratory to achieve a higher quality of the "ghosts". To measure fluorescence anisotropy we used DPH (1,6-diphenyl-1,3,5-hexatriene) probe. The stock solution of DPH (Serva, Germany), which was used during the measurements was prepared in acetone (Lachema, Czech Republic) and had concentration of 5×10^{-4} mol/L, was stored in the dark and refrigerated at 4°C. Before each measurement we prepared from the stock solution the dye working solution diluting it in TRIS (2 - amino - 2 - hydroxymethyl - propane - 1,3 - diol) (concentration of 20 mmol/L, pH 7.4) in a ratio of 1:250. After shaking (approximately 40 min) acetone was removed from the dye working solution. Measured sample (2000 μ L) was composed of 1840 μ L of TRIS (20 mmol/L, pH 7.4), 10 μ L of "ghost" and 150 μ L of the dye working solution. The final concentration of DPH in the sample was 1.5×10^{-7} mol/L. Stationary fluorescence anisotropy measurements in erythrocyte membranes, using DPH probes were made on a luminescent spectrophotometer Perkin-Elmer LS 45, single-channel method in the L-conformation, which is part of the software program FL WinLab. The sample was excited with linear polarized light and fluorescence was subsequently measured perpendicular to the direction of excitation beam. The experiment was based on time dependence measurements of stationary fluorescence anisotropy DPH probe $r_s(t)$ during incorporating the DPH probe into the erythrocytes membrane, up to 2000 seconds after its addition, with recording fluorescent intensity every 8.55 s. We used a constant excitatory wavelength of 360 nm (probe reaches the maximum absorption) and a constant emission wavelength length of 430 nm (maximum fluorescence). Measurements were conducted at room temperature ($22 \pm 2^\circ\text{C}$). In determining of erythrocyte membrane

fluidity from time evolution of the fluorescence anisotropy of probe DPH (at least 2000 s) we achieve the value of the stationary anisotropy by fitting with exponential curve in first order.

Results and discussion

We were interested in the fact whether CKD influences the membrane fluidity of red blood cells. To solve this problem we measured the value of DPH fluorescence anisotropy incorporated into the membrane after stabilization (approximately 2000 s). The process of DPH incorporation was fitted by exponential curve, do shown in Figure 1.

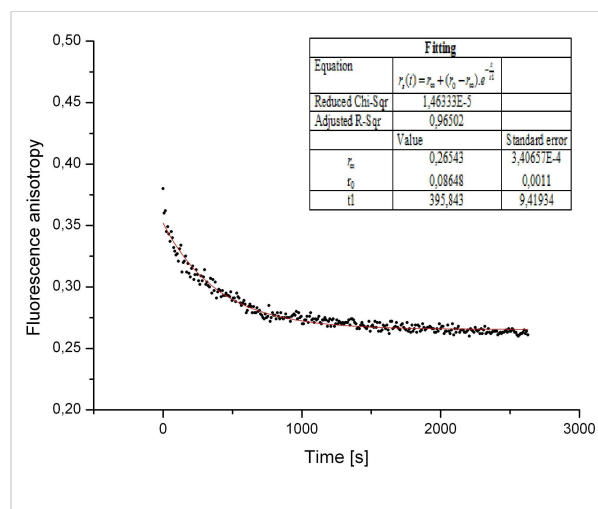


Figure 1: Typical time course of incorporation of probe DPH into the erythrocyte membrane in patient with chronic kidney disease with fitting curve, when r_∞ represent stationary fluorescence anisotropy, r_0 anisotropy in moment of adding DPH probe and τ is a kinetic parameter of incorporating DPH probe.

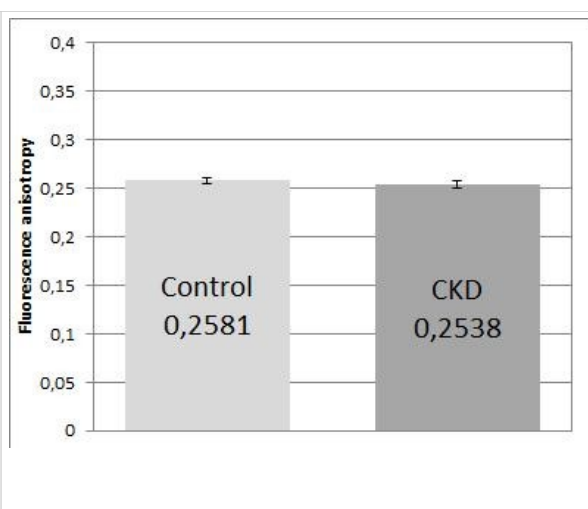


Figure 2: Comparison central value of fluorescence anisotropy by probe DPH in the column graph for control (n = 37) and CKD group (n = 21) with handed down by standard errors of mean (SEM)

The object of our interest is r_∞ parameter describing the fluorescence probe DPH at steady state, which gives us information on membrane fluidity. Graphic representation of mean values of fluorescence anisotropy using the DPH probe for CKD and control group in column format with standard errors of mean (SEM) gives us Figure 2. We assess that we found no significant difference of fluorescence anisotropy in patients with chronic kidney disease in 2. and 3. stage compared with the control group of healthy volunteers at the significance level $\alpha = 0.05$. It means that the level of motion of membrane phospholipids hydrophobic chains is not significantly different between CKD patients and healthy donors, at least in the early stages of CKD. It was previously shown that RBC from end stage CKD patients demonstrate reduction in membrane deformability, possibly as a result of increased RBC cellular calcium level [4]. Probably the changes in cell deformability occur only in the later stages of the disease.

Acknowledgement

The authors acknowledge a support provided by VEGA grant 1/0668/11, and UK grant UK/159/2012. This publication is also the result of the project implementation: BIOMAKRO2, ITMS: 26240120027 and project No. 26240220004, supported by the Research & Development Operational Programme funded by the ERDF.

References

- [1] K/DOQI, Am. J. Kidney Dis. 42 (Suppl 3) (2003) S1-S201
- [2] W.T. Mason, Academic press, London, 1999.
- [3] D. J. Hanahan, J. E. Ekholm, [Methods Enzymol.](#) 31 Pt A (1974) 168-172.
- [4] D. Polak-Jonkisz, L. Purzyc, K. Laszki-Szcza, K. Musiał, D. Zwolinska, Nephrol. Dial. Translant. 25 (2010) 438-444

P7

Thioflavin as probe for different biophysical processesD. Fedunová¹, P. Huba², J. Bágel'ová¹, M. Antalík^{1,2}¹ Institute of Experimental Physics, Slovak Academy of Sciences, Watsonova 47, 040 01 Košice, Slovakia,² Department of Biochemistry, PF UPJŠ, Moyzesova 11, 040 01 Košice, Slovakia, Slovakia,e-mail: fedunova@saske.sk

Thioflavin T (ThT) – 3,6-dimethyl-2-(4-dimethylaminophenyl)-benzothiazolium cation – is a fluorescence dye, generally used for staining amyloid tissues or detection of amyloid fibrils in solutions [1]. This dye has a high selectivity for amyloid fibrils. The binding of ThT to amyloid aggregates causes occurrence of fluorescence emission in the 475-600 nm region after excitation in the 440-450 nm region. In contrast, very low emission quantum yields of ThT are observed in the presence of native proteins as well as unfolded or partially folded monomeric protein conformations [2]. Since ThT binding only slightly affects the early stages of fibrillization [3], this method is also suitable for *in situ* fibril detection and monitoring of kinetics of fibril formation.

Several studies on the mechanism of ThT-fibril interactions have been reported [3-5]. β -sheets, as major components of amyloid fibrils, contain cavities and channels which can serve as possible ThT binding sites. ThT emission changes after binding to amyloids were, at first, attributed to formation of highly fluorescent dimers, excimers, or micelles [5]. However, repulsion of positively charged ThT molecules will probably prevent formation of dimers or micelles especially in nonpolar environment of fibrils [6]. Recently it was found that ThT

fluorescence quantum yield depends mainly on viscosity. This quantum yield significantly increases with increasing viscosity or rigidity of microenvironment [6]. It has been suggested that photoinduced intramolecular charge transfer occurs in ThT molecule, which is typical behavior for the specific

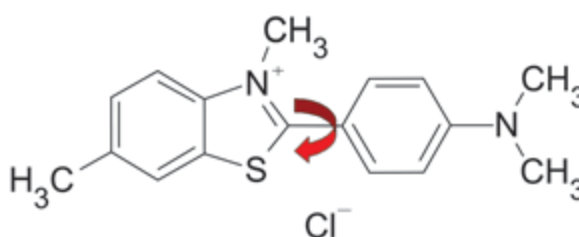


Fig. 1: Scheme of Thioflavine T.

class of fluorophores known as molecular rotors [7]. For the molecular rotors the significant fluorescence increase is observed in high viscosity media due to the decreased torsional relaxation in the molecule. Free rotation of benzothiazole and benzaminic rings around shared C-C bond (Fig. 1) is blocked in ThT-amyloid complexes, leading to significant increase of fluorescence yield. In environment where the internal rotation is not prevented, the nonfluorescent twisted internal charge transfer state is formed [6].

With the aim of clarifying the photophysical processes of this dye, we have studied the effect of different solvents on ThT spectroscopic characteristics – absorption and circular dichroism spectra and fluorescence emission. In the wide pH range (0.5-13) we have observed two transitions. At acidic pH the protonated conformation is formed with pK equal to 1.4. At alkaline pH range the hydroxylated ThT occurs with pK equal to 11.3. OH⁻ group is probably bound to the benzothiazole group involving loss of a positive charge and mutual rotation of fragments [8]. The hydroxylation therefore affects the fluorescence intensity, which could be taken into account for using this probe at alkaline pH. We have also studied the effect another negatively charged groups on ThT spectral properties, chaotropic ions KI and NaClO₄. Upon increasing concentration of salt the decrease of band intensity at 412 nm and slight shift of maxima to 415 nm is observed for both ions, with larger impact of NaClO₄

ion as the strongest chaotrop. On the contrary, cosmotropic sulphate salt has no effect on ThT absorption spectra.

Denaturants are frequently used for amyloid preparations *in vitro*. Therefore, we have tested the effect of GdnHCl, urea and ionic liquids on the urea basis on absorption spectra of ThT. The shift of maximum absorption band to 426 or 422 nm is observed, accompanied with increase of band intensity with increasing concentration of denaturants.

The synergistic effect of negatively charged groups on ThT spectral characteristic was studied in ThT complexes with polyanions – heparin and polystyrene sulphate as well as amyloids. We have observed strong CD signals in the visible region for ThT- heparin complex, whereas no fluorescence signal occurs at the same conditions. On the other hand, polystyrene sulphate does not induce any CD signal, but significant increase of fluorescence signal is observed at excitation of 440 nm. Relations between optical activity and fluorescence of complex system of ThT and biopolymers and other models will be discussed.

Acknowledgement

This work was supported by the Slovak Grant Agency VEGA, projects Nos. 2/0155/11, 2/0025/12, by the Slovak Research and Development Agency under the contract No. APVV-0171-10 and ESF projects 26220220061 and 2622012003.

References

- [1] S. Waldrop, H. Puchtler, S. N. Meloan, J. Histotechnol. 7 (1984) 123-126.
- [2] H. Naiki, K. Higuchi, M. Hosokawa, T. Takeda, Anal. Biochem. 177 (1989) 244-249.
- [3] V. Fodera, F. Librizzi, M. Groenning, M. van de Weert, M. Leone, J. Phys. Chem. B. 112 (2008) 3853-3858.
- [4] M. Groenning, M. Norman, J. M. Flink, M. van de Weert, J. T. Bukurinsky, G. Schluckebier, S. Frokjaer, J Struct. Biol. 158 (2007) 483-497.
- [5] R. Khurana, C. Coleman, C. Ionescu-Zanetti, S. A. Carter, V. Krishna, R. K. Grover, R. Roy, S. Singh, J. Struct. Biol. 151 (2005) 229-238.
- [6] V. I. Stsiapura, A. A. Maskevich, V. A. Kuzmitsky, V. N Uversky, I. M. Kuznetsova, K. K. Turoverov, J Phys. Chem. B 112 (2008) 15893-15902.
- [7] V. I. Stsiapura, A. A. Maskevich, V. A. Kuzmitsky, K. K. Turoverov, I. M. Kuznetsova, J. Phys. Chem. A 11 (2007) 4829-4835.
- [8] V. Fodera, M. Groenning, V. Vetri, F. Librizzi, S. Spagnolo, C. Cornett, L. Olsen, M. van de Weert, M. Leone. J. Phys. Chem. B 112 (2008) 15174 -15181.

P8

Magnetic fluid targets insulin-related amyloidosis

K. Šipošová^{1,2}, M. Kubovčíková¹, Z. Bednáriková², A. Antošová¹, M. Koneracká¹, V. Závašová¹, P. Kopčanský¹, Z. Daxnerová³, Z. Gažová¹

¹ Department of Experimental Physics, Watsonova 47, 040 01, Košice, Slovakia

² Institute of Chemistry, Faculty of Science, UPJŠ, Moyzesova 11, 040 01, Košice, Slovakia

³ Institute of Biology and Ecology, Faculty of Science, UPJŠ, Moyzesova 11, 040 01, Košice, Slovakia
e-mail: katkaposova@gmail.com

Amyloids are insoluble fibrillar aggregates of poly/peptides. Accumulation of these aggregates in organs is often associated with a large variety of human diseases such as type 2 diabetes mellitus, dialysis-related amyloidosis or Alzheimer's, Parkinson's and Huntington's diseases [1]. Insulin amyloid deposits containing intact molecules, including disulfide bridges, have been reported in a patient with insulin-dependent diabetes undergoing treatment by injection of various kinds of insulin (porcine or recombinant human insulin, insulin analogues) [2]. The recent data confirm the toxic effect of aggregates on the cells, however, it was found that reduction of amyloid aggregates plays important role in prevention as well as therapy of amyloidosis. Recent works report the ability of nanoparticles (NPs) to affect amyloid aggregation of proteins [3-5].

We have studied the ability of a series of 18 magnetic fluids (MF) consisting of magnetite nanoparticles (Fe_3O_4) stabilized by sodium oleate and modified by different amounts of bovine serum albumin (BSA) to depolymerise insulin amyloid fibrils.

Material and Methods: The insulin amyloid aggregates (Iagg) were achieved by incubation of the soluble protein (10 μM) in 50 mM phosphate buffer, pH 7.5 at 65°C and constant stirring of the solution for 2 h. Formation of amyloid aggregates was observed by characteristic changes in thioflavin T (ThT) fluorescence and visualized by AFM.

The magnetic Fe_3O_4 particles were synthesized by a chemical co-precipitation procedure method and stabilised by the procedure described in paper [5]. MF modification by BSA was done by adding varying amounts of BSA stock solution. We prepared 18 MFBSA samples with defined w/w BSA/ Fe_3O_4 ratios from 0.005 to 15.0 at a constant value of magnetite concentration of 30 mg ml^{-1} [5].

Results and Discussion: We have investigated the depolymerizing activity of magnetic fluids modified by different amounts of albumin (MFBSAs). We were interested to find out if the changes in the amount of BSA influence both the magnetic fluid properties and the interference of MFBSA with amyloid aggregates. The depolymerizing activities (A_{dep}) of MFBSAs were determined after overnight incubation of the insulin amyloid fibrils (10 μM Iagg) with MFBSAs for two different Iagg : MFBSA ratios (1:1 and 1:2) by ThT assay. Decline of fluorescence intensity indicates the ability of the magnetic fluid to reduce the amount of amyloid aggregates (Fig.1A). The destruction of amyloid fibrils by MFBSA was confirmed by microscopic technique, the AFM figures are shown in representative figure 1B. The significant depolymerizing activities - A_{dep} (higher than 50%) were observed for all studied MFBSAs at both protein : MFBSA ratios (data not showed). The most effective magnetic fluids (A_{dep} 80-90%) were detected for low values of BSA/ Fe_3O_4 ratio (from 0.005 to 0.1).

For the most effective MFBSAs (MFBSA0.01 and MFBSA0.02) characteristic of 90% reduction of amyloid aggregates the half-maximal depolymerization concentration DC_{50} was determined. The obtained DC_{50} values equal to 21.98 $\mu\text{g ml}^{-1}$ and 38.58 $\mu\text{g ml}^{-1}$ imply that these MFBSAs interfere with insulin fibrils already at stoichiometric concentrations.

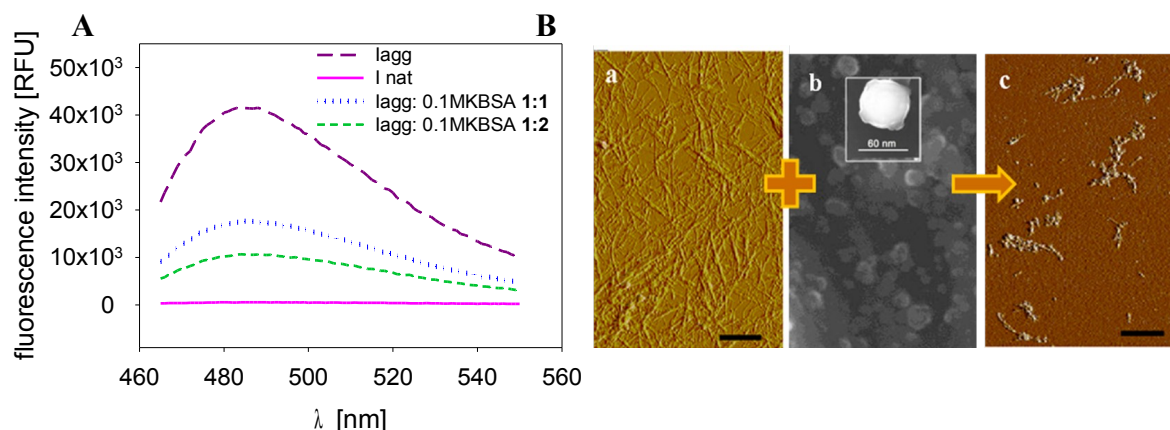


Fig 1 A - fluorescence intensities of native insulin, insulin amyloid fibrils alone and in presence of MFBSA. B - AFM images of insulin amyloid fibrils (a), SEM image of MFBSA (b), and AFM image of insulin amyloid fibrils in presence of MFBSA (lagg : MFBSA ratio 1:2). Bars in all AFM images represent 1μm.

Results indicate that the physical–chemical features of studied MFBSAs, such as hydrodynamic diameter, zeta potential and isoelectric point, were influenced by the amount of BSA used for MF’s functionalization and significantly affected the extent of MFBSA depolymerizing activity [5]. Incubation of insulin amyloid fibrils with albumin-modified magnetic fluid leads to the significant destruction of aggregates. The extent of the depolymerizing activity was affected by the amount of albumin used for magnetic fluid modification and mainly depends on the size of nanoparticles. We assume that the present findings represent a starting point for the application of the selected active MFBSAs as therapeutic agents targeting insulin-associating amyloidosis.

Acknowledgement

This work was supported within the projects 26220220005 and 2622012033 in the framework of the Structural Funds of European Union, Centre of Excellence of SAS Nanofluid, VEGA 0041, 0079, 0077, Slovak Research and Development Agency—contract No. APVV-0171-10 and SKRO-0012-10 and project SAS NSC Taiwan—Computational approaches to study structure, folding and interactions of biopolymers and VVGS 38/12-13.

References

- [1] E. Mandelkow, M. von Bergen, J. Biernat, E. M. Mandelkow, *Brain Pathol.* 17 (2007) 83–90.
- [2] S. Yumlu, R. Barany, M. Eriksson, C. Rocken, *Hum. Pathol.* 40 (2009) 1655–1660.
- [3] S. Linse, C. Cabaleiro-Lago, W. F. Xue, I. Lynch, S. Lindman, E. Thulin, S. E. Radford, K. A. Dawson, *Proc. Natl Acad. Sci.* 104 (2007) 8691–8696.
- [4] A. Bellova, E. Bystrenova, M. Koneracka, P. Kopcansky, F. Valle, N. Tomasovicova, M. Timko, J. Bagelova, F. Biscarini, Z. Gazova, *Nanotechnology* 21 (2010) 065103.
- [5] K. Siposova, M. Kubovcikova, Z. Bednarikova, M. Koneracka, V. Zavisova, A. Antosova, P. Kopcansky, Z. Daxnerova, Z. Gazova, *Nanotechnology* 23 (2012) 055101.

P9

Implementation of the method of correlative light/electron microscopy on the same cell

J. Sukeřová¹, Z. Nichtová^{1,2}, M. Novotová¹, I. Zahradník¹

¹ Institute of Molecular Physiology and Genetics, Slovak Academy of Sciences, Vlárská 5, 833 34 Bratislava, Slovakia

² Department of Pharmacology and Toxicology, Faculty of Pharmacy CU, Kalinčiakova 8, 832 32 Bratislava, Slovakia

e-mail: juliana.sukelova@savba.sk

For general understanding of the function of mammalian cardiac myocytes in various physiological and pathological situations it would be beneficial to know the spatial and temporal dynamics of their plasma membrane. The sarcolemma of isolated cells can be studied by confocal fluorescence microscopy, which allows *in vivo* observation of even very fast structural changes; however, at a relatively low resolution of about 0.5 micrometers that may not be sufficient for many purposes. In addition, this approach requires the use of specific fluorescent labels that limit the number of simultaneously observed structures to less than four. Much more detailed information about the structure of the sarcolemma can be obtained by means of electron microscopy, which uses different contrasting and processing methods to visualize the cells. The resolution approaches 1 nanometer but at the expense of very long processing time and observation of non-living preparations. One of recently developed approaches combines the two techniques to the advantage of both, the fast *in vivo* and the detailed *in vitro* structural view - the correlative light/electron microscopy (CLEM) [1, 2].

We adopted the CLEM principle for studies on isolated cardiac myocytes by laser scanning confocal fluorescence microscopy and by transmission electron microscopy. Cardiac myocytes were isolated by enzymatic digestion from the left ventricles of 12 weeks old male Wistar rats. After isolation, the suspension of cells was placed in a calcium free medium in small plastic dishes. The cells were stained by 5 μ M solution of di-8-ANEPPS in calcium-free medium for 10 - 20 minutes and then transferred to a fresh ANEPPS-free solution.

For identification of a specific cell in both, the confocal and the electron microscope image, we used 200 mesh copper grids, marked at some places for easier orientation, covered with a thin formvar membrane to prevent toxic effects of copper on myocytes in suspension. The copper grids were placed on coverslips that were then covered with a layer of laminin and transferred to a plastic chamber. The stained isolated cells were layered over the laminin and allowed to adhere for 40 minutes. Then the cells were observed, measured and recorded using a Leica TCS SP2 AOBS confocal microscope with a 63 \times oil immersion objective. The position of the measured cells relative to the copper grid was recorded.

In the next step, the observed cells adhering to the coverslip with the grid were processed for electron microscopy by fixation with 2% glutaraldehyde solution in cacodylate buffer for 30 minutes. Then the cells were postfixed by 1% OsO₄ solution in cacodylate buffer and contrasted by a saturated solution of uranyl acetate in water. Then, the cells on the coverslips were dehydrated in a series of alcohols, saturated by a mixture of acetone and durcupan and cured for 24 hours at 60 °C. The resulting blocks with grids were inspected under low magnification with a binocular stereo microscope to identify the cells in the grid that have been observed in the confocal experiment and to make them available for longitudinal sectioning. Ultrathin longitudinal sections were prepared by the ultramicrotome Power-Tome MT-XL. Finally, the sections were contrasted with lead citrate and studied using a transmission electron microscope JEM 1200. The images were recorded using a Gatan Dual Vision 300W CCD camera and compared with confocal images.

Our method successfully combines two different approaches, electron microscopy and confocal fluorescence microscopy, for studies of the dynamics and the ultrastructure of the plasma membrane of the same cell. The method allows us to correlate the changes in the sarcolemma of cardiac myocytes due to specific experimental interventions. In the future it will be extended for use with the patch clamp electrophysiological technique to correlate the dynamics of electrical properties with the structural characteristics of the sarcolemma.

Acknowledgement

We would like to thank Ladislav Novota for technical assistance. This work was supported by the Slovak Grant Agency VEGA, project No. 2/0116/12 and 2/0203/11 and by the Slovak Research and Development Agency under the contract No. APVV-0721-10.

References

- [1] R. S. Polishchuk, E. V. Polishchuk, P. Marra, S. Alberti, R. Buccione, A. Luini, A. A. Mironov, *J. Cell. Biol.* 148 (2000), 45-58.
- [2] K. Cortese, A. Diasporo, C. Tacchetti, *J. Histochem. Cytochem.* 57 (2009) 1103 - 1112.

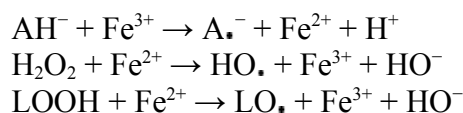
P10

Interaction of magnetic nanostructures with antioxidants: Risks, benefits, and possible therapeutic applications

H. Vrbovská, A. Olas, M. Babincová

Department of Nuclear Physics and Biophysics, FMFI UK, Mlynská dolina F1, 842 48 Bratislava, Slovakia, e-mails: h.vrbovska@gmail.com, adamolas@gmail.com

Iron is an essential nutrient for mammals and most life forms and iron oxide nanoparticles were generally assumed to be safe, however this type of nanoparticle can be toxic in some cell types and their nano-toxicity in yet another type of cell suggests that these particles may not be as safe as we had once thought. Iron oxide nanoparticles are considered promising because they are maneuverable by remote magnetic fields, and can be functionalized with various molecules to make them stick selectively to tumors and other targets within the body [1]. The particles can also be made to deliver anti-cancer drugs or radioactive materials directly to a tumour. Magnetic nanoparticles designed to attach to cancerous tissue can also be made to heat up by using a remote, alternating magnetic field, thereby selectively killing cancer cells in a process called magnetic fluid hyperthermia [2]. For the biocompatibility, as well as stability of iron magnetic core are magnetic nanoparticles covered by protecting sheet form lipids, fatty acids, saccharides, and other polymers. Although in nanoparticles the iron is in the “safe” insoluble Fe^{3+} oxidation state, as in the ferritin, it is always possible that some compounds can reduce this form of iron into the Fe^{2+} state, which is soluble, and is a risk for the organism [3]. Paradoxically, such a compounds is also the best known antioxidant - ascorbic acid which can reduce iron and form toxic free radicals via the Fenton reaction, which can lead to peroxidation of lipid in cell membranes:



For these reasons we have studied interaction of well stabilized magnetic nanoparticles with L-ascorbic acid H_2A as a reducing agent (being a donor of two H^+ and two e^-). The oxidation of H_2A involves outer sphere electron transfer from ascorbic acid to MF. H_2A first dissociates to HA^- and releases a proton. MF ($\text{Fe}^{\text{II}}\text{OFe}_2^{\text{III,III}}\text{O}_3$) reacts with HA^- in the rate-determining step k involving an outer sphere one-electron transfer from HA^- to MF to form an intermediate reduced species $[\text{Fe}^{\text{II}}\text{OFe}_2^{\text{II,III}}\text{O}_3]^-$ and ascorbate radical $\text{HA}\cdot$. Ionic strength dependence also confirmed that the rate-determining step involves the interaction of neutral MF and HA^- . A rapid electron transfer from $\text{HA}\cdot$ to $[\text{Fe}^{\text{II}}\text{OFe}_2^{\text{II,III}}\text{O}_3]^-$ gives the reduced MF $[\text{Fe}^{\text{II}}\text{OFe}_2^{\text{II,II}}\text{O}(\text{OH})_2]$ and A. Time dependent measurements monitoring the reactions at temperature 45°C (Fig. 1) were performed on a UV/VIS spectrophotometer (Shimadzu

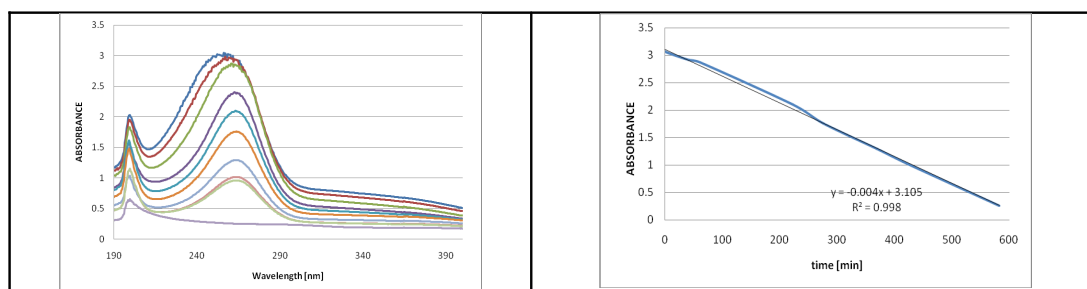


Fig. 1. Time dependence of the absorbance at 45°C .

UVmini 1240). As it is clear from our results, higher doses of ascorbic acid when combined with application of magnetic nanostructures are a risk factor due to the possible oxidative cell injury. Nevertheless, since e.g. neuroblastoma cells contain elevated iron levels (stored in ferritin) and produce high amounts of H_2O_2 , conditions for pro-oxidative cell injury can be generated by application of ascorbic acid. This may be used as a new approach in cancer therapy of this hardly curable tumor, especially in combination with some cytostatic drugs [4].

Because magnetic nanostructures are often stabilized by lipids, e.g. in magnetoliposomes, we have also proposed to use α -lipoic acid for their protection. Lipoic acid is one of the most effective antioxidant used in the prevention of Alzheimer disease, a progressive neurodegenerative disorder that destroys patient memory and cognition, and the Fe^{2+} ions are most harmful for neurons and glial cells. As is shown in Fig. 2, already at low concentrations of lipoic acid, peroxidation index is almost corresponding to the liposomes without oxidation.

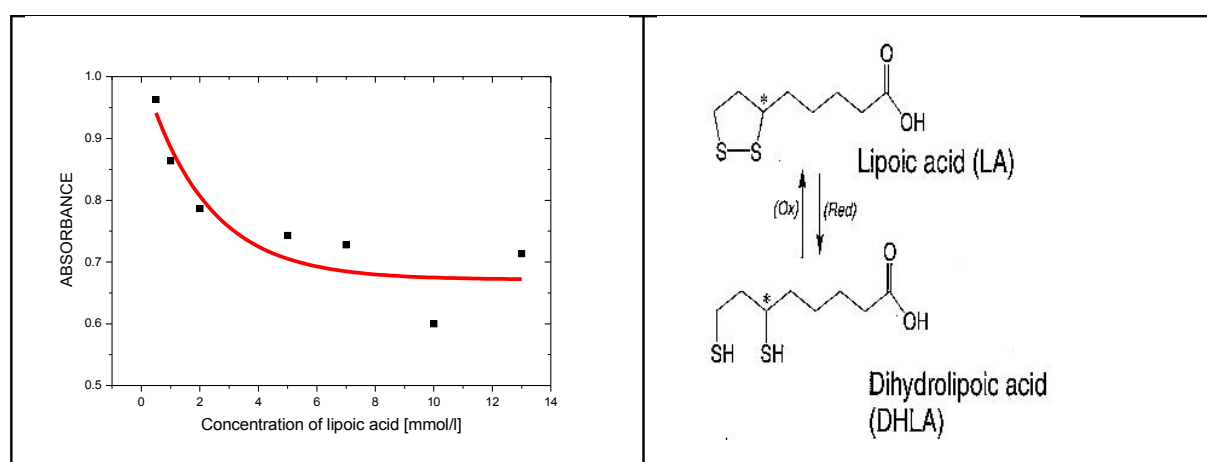


Fig. 2. Dependence of lipid peroxidation index on the concentration of lipoic acid. The reduced form of LA, dihydrolipoic acid (DHLA), is probably the active compound responsible for these beneficial antioxidant effects.

Lipoic acid *in vivo* effects seems primarily to induce the oxidative stress response rather than directly scavenge free radicals [5], nevertheless its OH radical scavenging capability is also remarkable, therefore its application during magnetic drug targeting to the brain, or during MRI scan with magnetic nanoparticles as a contrast agent would be beneficial for protection of glial cells.

In conclusion, we can say that the interaction of antioxidants with magnetic nanostructures is an interesting field with many potential therapeutic applications [6].

Acknowledgement

This work was supported by the Slovak Grant Agency VEGA, project No. 1/0642/11.

References

- [1] M. Babincová, P. Babinec, Biomed. Papers 153 (2009) 243-250.
- [2] M. Babincová, V. Altanerová, Č. Altaner, C. Bergemann, P. Babinec, IEEE Trans. Nanobiosci. 7 (2008) 15-19.
- [3] M. Babincová, P. Babinec, J. Magn. Magn. Mater. 293 (2005) 394-399.
- [4] M. Babincová, V. Altanerová, Č. Altaner, Z. Bačová, P. Babinec, Eur. Cells Mater. 3 (2002) 140-141.
- [5] L. Holmquist, G. Stuchbury, K. Berbaum, Pharmacol Ther. 113 (2007) 164-174.
- [6] M. Babincová, P. Babinec, Medical Hypotheses 54 (2000) 177-179.

P11

Partial Molecular Volumes of DMPC and Cholesterol in Mixed Bilayers

J. Gallová, C. Ďurčovičová, P. Balgavý

Department of Physical Chemistry of Drugs, FaF UK, Odbojárov 10, 832 32 Bratislava, Slovakia.
e-mail: gallova@fpharm.uniba.sk

Molecular volume per lipid for lipid bilayers is a very important datum which supplements neutron and X-ray structural data. Values for most frequently used phospholipids could be found in literature at least for several temperatures. But information on the influence of additives on the molecular volumes of lipids in bilayers is rare.

In this work, molecular volumes of dimyristoylphosphatidylcholine (DMPC) and cholesterol in mixed bilayers were studied at different temperatures.

To prepare samples, weighted amounts of DMPC and cholesterol were dissolved in chloroform. Appropriate volumes of DMPC and sterol solutions were mixed and the solvent was evaporated to dryness. The dry lipid was hydrated by deionized water to obtain final concentration of lipid 0.15% (w/w). Multilamellar liposomes were formed in nitrogen atmosphere during vortexing and brief sonication in a bath sonicator. Degassed samples were measured using densitometer DMA 4500M (Anton Paar) in a temperature range 13-50 °C.

The specific volume of lipid part of the sample was calculated from the density of the sample and density of water supposing that water phase in multilamellar suspension undergoes the same temperature changes as in pure water. Mixed molecule was defined as one DMPC molecule together with particular part of cholesterol molecule at different molar ratios of cholesterol to DMPC. The temperature dependence of the volume of a mixed molecule $V(X_C)$ can be seen on Fig. 1 for different molar fractions of cholesterol $X_C = n_C / (n_C + n_{DMPC})$, where n_C and n_{DMPC} are number of moles of cholesterol and DMPC respectively.

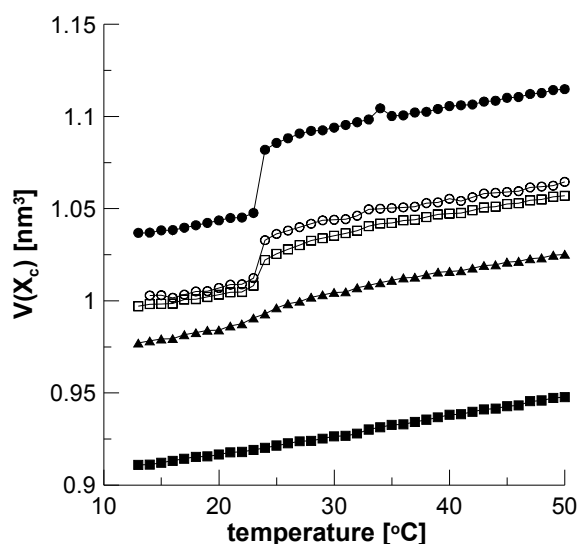


Fig. 1: Temperature dependence of the mixed molecule volume $V(X_C)$ at different cholesterol mole fraction: 0-● (pure DMPC), 0.11 -○, 0.12-□, 0.20-▲, 0.50-■.

Fig. 1 shows that the phase transition from solid ordered to fluid disordered phase diminishes with increasing of cholesterol mole fraction and above $X_C=0.3$ is practically not visible. This is probably connected with the formation of a liquid ordered phase which is stable in a broad temperature range.

We have utilized a formalism of partial volumes known from thermodynamics and

used earlier in [1,2]. Partial volumes of cholesterol v_{CHOL} and DMPC v_{DMPC} are defined as follows:

$$v_{DMPC}(X_c) = \left(\frac{\partial V(X_c)}{\partial N_{PC}} \right)_{N_{CHOL}}, \quad (1)$$

where N_{CHOL} and N_{DMPC} are total numbers of cholesterol and DMPC molecules in the sample.

$$V(X_c) = X_c v_{CHOL}(X_c) + (1 - X_c) v_{DMPC}(X_c) \quad (2)$$

The volume of mixed molecule decreases linearly with mole fraction at temperatures well above the main phase transition (Fig. 2). It means that the molecular volume of DMPC is not influenced by the presence of cholesterol at higher temperatures. The value of molecular volume of DMPC determined in this work is in good agreement with results of other authors [1, 3, 4]. We found that molecular volume of cholesterol is about 10% lower compared to [1].

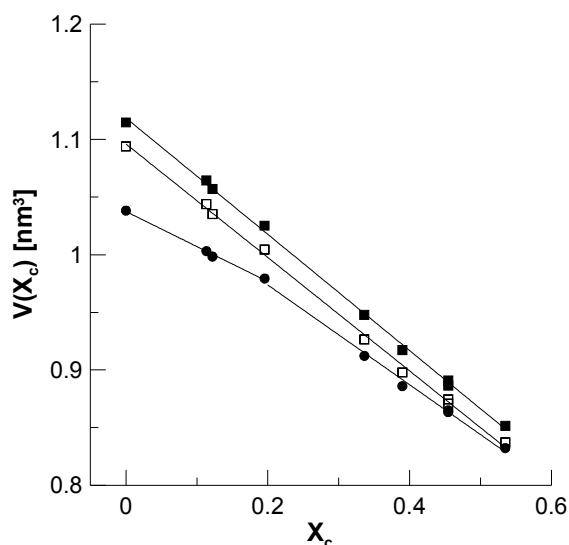


Fig. 2: Dependence of the volume of mixed molecule on the cholesterol mole fraction at different temperatures. 15 °C-●, 40 °C-□, 50 °C-■.

It is seen from Fig. 2 that at temperatures below the main phase transition the molecular volume decreases less steep with increasing X_c . We suppose that this is a consequence of disturbing effect of cholesterol on lipid bilayer in gel phase. This effect is not present at higher concentrations because the gel phase is transformed to liquid ordered phase.

Acknowledgement

This work was supported by the Slovak Grant Agency VEGA, project No. 1/0159/11 and by the Dubna JINR 07-4-1069-09/2011 project.

References

- [1] A. I. Greenwood, S. Tristram-Nagle, J. F. Nagle, Chem. Phys. Lipids. 143 (2006) 1-10.
- [2] M. Klacsová, P. Westh, P. Balgavý, Chem. Phys. Lipids. 163 (2010) 498-505.
- [3] R. Krivánek, P. Rybár, E. J. Prenner, R. N. McElhaney, T. Hianik, Biochim. Biophys. Acta 1510 (2001) 452-463.
- [4] D. Uhríková, P. Rybár, T. Hianik, P. Balgavý, Chem. Phys. Lipids. 145 (2007) 97-105.

P12

Fluorescence anisotropy measurements of lipid vesicles incorporated calixarenes

Z. Garaiová¹, D. Wrobel², I. Waczulíková¹, M. Ionov², M. Bryszewska², T. Hianik¹

¹ Department of Nuclear Physics and Biophysics, FMFI UK, Mlynská dolina F1, 842 48 Bratislava, Slovakia, e-mail: zuzana.garaiova@fmph.uniba.sk

² Department of General Biophysics, University of Lodz, Banacha 12/16, 90-237, Lodz, Poland

The vesicles as a convenient model of biological membranes can be modified by various receptors and thus serve as a recognition device for medical diagnosis. Therefore, substantial effort is put into developing efficient synthetic receptors for molecular recognition. Calixarenes - aromatic macrocyclic molecules - have gained a lot of attention due to their versatility and sensitivity to various ligands. Hydrophobic cavity formed by phenol subunits of these vase-like shape molecules can selectively bind a wide range of compounds such as proteins, e.g. cytochrome c [1]. Obviously, their efficacy would depend on the composition and stability of the vesicles.

The aim of this work was therefore to study the lipid ordering and to monitor membrane fluidity of the vesicles with incorporated calix[6]arene (CX) sensitive to cytochrome c (Fig.1). Large unilamellar vesicles (LUV) composed of 1,2-dimyristoyl-sn-glycero-3-phosphocholine (DMPC) alone or in the mixture with CX (1, 3, 10 mol%) were prepared by an extrusion method and characterized by size and zeta potential measurements [2].

Fluorescence anisotropy measurements were carried out with a LS-50B (Perkin-Elmer, UK) spectrofluorimeter. In order to analyze membrane fluidity across the bilayer, two fluorescent probes were used. 1,6-diphenyl-1,3,5-hexatriene (DPH) is an apolar molecule, which is incorporated in the hydrophobic area of the membrane and N,N,N-trimethyl-4-(6-phenyl-1,3,5-hexatrien-1-yl) phenylammonium p-toulenesulfonate (TMA-DPH) with the positively charged amino group is anchored in the hydrophilic region of the lipid bilayer. The excitation and emission wavelengths were 348 nm and 443 nm, respectively. The experiments were carried out at 30°C.

The average (\pm standard deviation) steady-state anisotropy values of pure DMPC liposomes were 0.151 (\pm 0.004) and 0.053 (\pm 0.003) probed with TMA-DPH and DPH, respectively. Increasing molar content of CX in the vesicles led to an increase in the anisotropy; at 10 mol% of CX it reached 0.182 (\pm 0.002) and 0.092 (\pm 0.007) for TMA-DPH and DPH, respectively. Observed anisotropy increase has indicated a decrease in fluidity as a result of the enrichment of the lipid bilayer with CX that made the membrane more rigid in both - hydrophilic and hydrophobic parts.

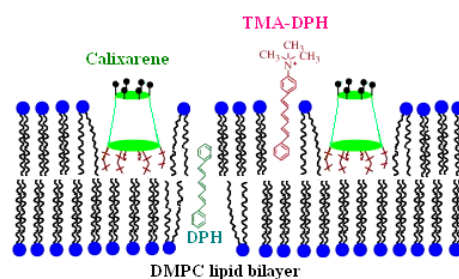


Fig. 1. Schematic representation of calixarene modified lipid membrane with incorporated fluorescence probes TMA-DPH and DPH

Acknowledgement

This work was supported by the Slovak Grant Agency VEGA, project No. 1/0785/12, by the Slovak Research and Development Agency under the contracts No. APVV-0410-10, LPP-0250-09, SK-PL-0034-09. This publication is also the result of the project implementation: BIOMAKRO2, ITMS: 26240120027, supported by the Research & Development Operational Programme funded by the ERDF.

References

- [1] T. Oshima, H. Higuchi, K. Ohto, K. Inue, M. Goto, *Langmuir* 21 (2005) 7280-7284
- [2] Z. Garaiová, M.A. Mohsin, V.Vargová, F.G. Banica, T. Hianik, *Bioelectrochemistry* , in press (2012)

P13

AFM imaging of lipid layers containing calixarenes after addition of cytochrome c

A. Poturnayová¹, M. Šnejdárková¹, I. Neudlinger², A. Ebner², T. Hianik³

¹Institute of Animal Biochemistry and Genetics, SAS, Moyzesova 61, 900 28 Ivanka pri Dunaji, Slovakia

²Biophysics Institute, Johannes Kepler University Linz, Altenbergertrasse 69, 4040 Linz, Austria

³Department of Nuclear Physics and Biophysics, FMFI UK, Mlynská dolina F1 84248 Bratislava, Slovakia
email: alexandrapoturnayova@gmail.com

The vesicles and supported bilayer lipid membranes are convenient models of biomembranes. The lipid films could be modified by proteins or synthetic receptors and serve as a recognition devices for medical diagnosis. Calixarenes (CX) are being used for detection of a wide range of compounds such as metal ions, amino acids or proteins. The CX can therefore serve as a recognition element in sensor for detection cytochrome c (cyt c). Cyt c participates in electron transport and it is responsible for activation of the apoptotic pathway through releasing from mitochondria into the cytosol. In particularly it has been shown that cyt c induced transition of lamellar phase composed of phosphatidylcholine, which is favorable for transport of cyt c through hydrophobic part of the membrane. The detection of endogenous concentration of cyt c is of high importance for diagnosis of possible pathological processes in the organism. By atomic force microscopy we studied the topography of the self assembled lipid films contained CX and formed on freshly cleaved mica surface. The height difference between mica surface and upper part of DMPC layer was between 3 and 4 nm, which correspond to the lipid bilayer and agrees well with results published earlier. Interesting result were obtained for the layers incubated with 30 nM cyt c. The roughness of CX layer was about 5 times higher in comparison with that of DMPC, probably due to formation of monolayers and even multilayers of CX. Novel and surprising result has been obtained for mixed DMPC-CX layers at presence of cyt c. Incubation of these layers with 30 nM of cyt c resulted in transformation of rather rough multilayers into the relatively flat layers contained sharp fibers of cyt c.

Acknowledgement

This work was financially supported by Slovak Research and Development Agency (Projects VVCE-0064-07 and APVV -0410-10), by Slovak Academy of Sciences (Project MNT-ERA.NET, IntelliTip ID 431, AN 234989 and Centre of Excellence SAS for Functionalized Multiphase Materials (FUN-MAT)) and by FFG (MNT-ERA.NET, IntelliTip, project No. 823980). This publication is also the result of the project implementation: BIOMAKRO2, ITMS: 26240120027, supported by the Research & Development Operational Programme funded by the ERDF. We thank to Dr. T. Oshima for generous gift of calixarenes.

P14

DNA-aptamers: sensitive tool for thrombin detection by quartz crystal microbalance.

M. Šnejdárková¹, A. Poturnayová¹, I. Neundlinger², A. Ebner², T. Hianik³

¹Institute of Biochemistry and Animal Genetics, SAS, Moyzesova 61, 900 28 Ivanka pri Dunaji, Slovakia

²Biophysics Institute, Johannes Kepler University Linz, 4040 Linz, Austria

³Department of Nuclear Physics and Biophysics, FMFI UK, Mlynská dolina F1 842 48 Bratislava, Slovakia

Email: maja.snejdarkova@savba.sk

Thrombin is a highly specific serine protease involved in the coagulation cascade, which converts soluble fibrinogen into insoluble strands of fibrin which is a matrix of the blood clot. The thrombin is not present in the blood under physiological conditions but appears in pathological processes including deep vein thrombosis, myocardial infarction, stroke and in central nervous system injury. Under coagulation the concentration of the thrombin in blood varied from nM to μ M levels. Development of the sensitive method of the thrombin detection in nanomole level is important for clinical practice. The traditional methods of thrombin detection are based on the antigen-antibody immunoassay, clotting – based assay or synthetic-substrate-based enzymatic assays. Alternative method of thrombin detection is based on biosensors using DNA aptamers as receptors.

In this work we used thickness shear mode method to study the interaction between thrombin and DNA aptamers immobilized at the surface of quartz crystal transducer. We used 30-mer biotinylated DNA aptamer (BF) of following composition: 5'-GGT TGG TGT GGT TGG TTT TTT TTT TTT TTT - 3'- biotin. The immobilization of the aptamers to the surface is crucial and we compared two types of the surfaces formed on the gold electrode. First surface was formed from neutravidin on which BF was attached. Second surface was formed from the DNA tetrahedron DS3BT1 for oriented attachment of neutravidin and for subsequent BF binding. We studied the kinetics of the changes of the series resonant frequency, f_s , and the motional resistance, R_m , of the quartz crystal transducer following addition of thrombin. The decrease of f_s and increase of R_m , following addition of thrombin has been observed. The changes of both parameters started already at 50 nM of thrombin. The increase of R_m suggests on increase of surface viscosity. The kinetics analysis of aptamer-thrombin system was performed. Binding experiments carried out using BF immobilized on neutravidin layer at gold surface showed that constant of dissociation is $K_d = 114$ nM. This constant is measure of the affinity of the interactions. The lower K_d , the higher affinity. However, lower affinity of thrombin to the aptamer was observed when DS3BT1 structures were used for aptamer immobilization ($K_d = 151$ nM). The reasons of these differences are discussed.

Acknowledgment

This work was financially supported by Slovak Research and Development Agency (Projects VVCE-0064-07 and APVV -0410-10), by Slovak Academy of Sciences (Project MNT-ERA.NET, IntelliTip ID 431, AN 234989 and Centre of Excellence SAS for Functionalized Multiphase Materials (FUN-MAT)) and by FFG (MNT-ERA.NET, IntelliTip, project No. 823980). This publication is also the result of the project implementation: BIOMAKRO2, ITMS: 26240120027 and project No. 26240220004, supported by the Research & Development Operational Programme funded by the ERDF. We thank to Dr. T. Oshima for generous gift of calixarenes.

P15

Functionalization of multiwalled carbon nanotubes with dendrimers for aptamer-based biosensor sensitive to human cellular prions

G. Castillo¹, A. Miodek², H. Dorizon², H. Korri-Youssoufi², T. Hianik¹

¹ Department of Nuclear Physics and Biophysics, FMFI UK, Mlynská dolina F1, 842 48 Bratislava, Slovakia, e-mail: gabriela.castillo@fmph.uniba.sk

² UMR – CNRS 8182, Institut de Chimie Moléculaire et des Matériaux d'Orsay ICMMO, University Paris-Sud, Bat 420, 91405 Orsay, France

Prion diseases, a group of rare and fatal brain disorders, result from the transformation of cellular prion (PrP^C) into the pathological isoform (PrP^{Sc}) [1]. PrP^{Sc} aggregates in the nervous system forming amyloid plaques in the neocortex, cerebellum and subcortical nuclei that provokes a rapid degeneration of neuronal tissues [2]. Since prion detection in blood is limited down to pico molar (pM) levels [3], the development of an effective, high-sensitive and reliable approach of recognition is of fundamental importance in the diagnosis and treatment of neurodegenerative diseases, meanly in countries facing ageing problems which are closely related to them.

The aim of this work was to develop a label-free electrochemical aptamer-based nanoarray for *in vitro* detection of PrP^C, that can be potentially used also for detection of PrP^{Sc} as a biomarker of prion disease. The biosensor consisted on multiwalled carbon nanotubes (MWCNTs) modified with polyamidoamine dendrimers of fourth generation (PAMAM G4) functionalized by amino-groups. These amino groups allow by one side to link the aptamer as bioreceptor, as well as, to incorporate the ferrocenyl group, a redox marker that makes possible the electrochemical measurements. A schematic representation of the array is shown in Fig. 1.

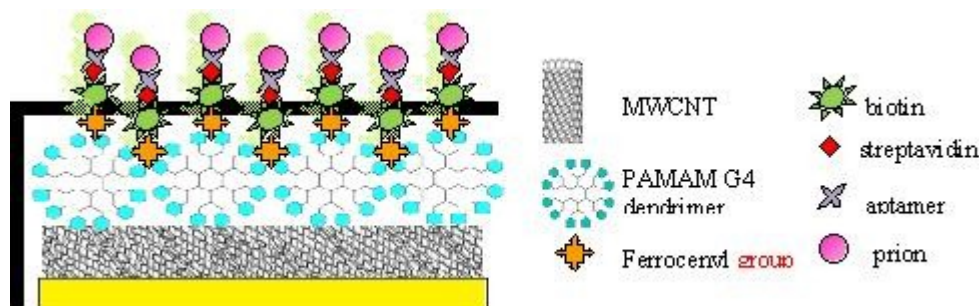


Fig. 1 Nanoarray for prion recognition consisting on a gold support that contains functionalized COOH-MWCNTs linked to PAMAM G4 dendrimers, followed by the covalent attachment of ferrocenyl redox marker subsequently attached to a biotin-modified aptamer by means of biotin-streptavidin chemistry.

Using electrochemical methods such as differential pulse voltammetry (DPV) and cyclic voltammetry (CV), we demonstrate that the interaction between aptamers and prion proteins leads to variation in electrochemical signal of the ferrocenyl group. Biosensor characterization also includes an analysis by infrared spectroscopy (FT-IR) for illustrating the different conjugation steps of MWCNTs with dendrimers, prior assembling of whole sensor.

Biosensor's wide linear response, ranging from 1 pg/ml up to 10 µg/ml, is an evidence of the platform high sensitivity. Additionally, PrP^C limit of detection (LOD) corresponding to 1 pg/ml, corroborates the sensor utility even for prion levels found in human plasma.

Acknowledgements

The group of Human Rezaï from INRA of Jouey en Josas (France) is acknowledged for giving the purified prion protein Pr^{Sc}. This work was supported by the Slovak Research and Development Agency and France government (PHC Stephanic)(contracts No. APVV-0410-10, SK-FR-0025-09). by Grant Agency VEGA (project No. 1/0785/12) This publication is also the result of the project implementation: BIOMAKRO2, ITMS: 26240120027, supported by the Research & Development Operational Programme funded by the ERDF, by Centre of Excellence SAS for Functionalized Multiphase Materials (FUN-MAT) and by the Grant of Education and research ministry of French government.

References

- [1] J. Bratosiewicz-Wasik, T.J. Wasik, P.P. Liberski, *Folia Neuropathol.* 42 (2004) Suppl A:33-46.
- [2] S. B. Prusiner, K. K. Hsiao, *Ann Neurol.* 35 (1994) 385-95.
- [3] M. Panigaj, A. Brouckova, H. Glierova, E. Dvorakova, J. Simak, J. G. Vostal, K. Holada, *Transfusion* 51 (2011) 1012–1021.

P16

Binding of p53 (wt/mut), p63 and p73 to different DNA substratesL. Navratilova¹, M. Adamik¹, M. Brazdova¹, H. Pivonkova¹, M. Fojta¹¹Institute of Biophysics, Academy of Sciences of the Czech Republic v.v.i., CZ-612 65 Brno, Czech Republic
e-mail: luna@ibp.cz

Protein p53, in its standard form (wtp53), is a tumor suppressor involved in regulation of main processes in cells, such as cell cycle, DNA repair, apoptosis, proliferation, differentiation and many others. Unique two DNA binding domains (central core domain and C-terminal) are necessary for its functions as guardian of genome [1]. P53 belongs to a family composed of proteins p53, p63 and p73. The other two proteins share significant structural (Fig. 1) and functional homologies with p53, mainly in DNA binding core domain, and they can specifically bind to p53-response elements and also directly activate specific wtp53 target genes [2]. About 50 % of all human cancer contains mutation in *TP53* gene and almost 80% of alterations of the *TP53* gene are point mutations [3]. Mutant p53s (mutp53s) lost their function as tumor suppressors and as transcription regulators of wtp53 target genes. Majority of mutations are located within the sequence specific DNA-binding domain (core domain) and they are called hot spots [4].

Firstly, in our work we focused on comparison of wtp53 and hot spots mutp53 proteins binding to topologically different DNA substrates (supercoiled and linear forms) by electrophoretic mobility shift assay (EMSA). Our results indicated preferential binding to sc DNA by both wt and mutp53s *in vitro* [5].

Secondly, we studied interactions of p53, p63 and p73 core domains with different DNA substrates (various wt p53-response elements (p53CONs), supercoiled and linear DNA) by EMSA. Sensitivity of protein/DNA complex to different heavy metals and thermal stability of protein/DNA complexes were investigated by EMSA and immunoblots. Overall, the molecular details of the mechanism of p53 family recognition of DNA will leads to better understanding the tumor suppressor functions of p53 family and mutp53 and could provide good background for p53-dependent cancer therapeutics.

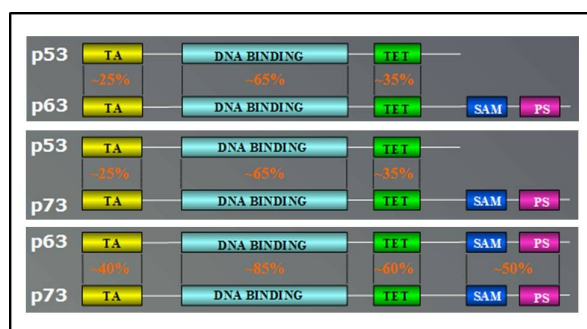


Fig. 1. Sequence identity between p53, p63, p73 proteins (from Courtois at al., 2010)

Acknowledgement

This work was supported by P301/10/2370 (Grant Agency of Science of CR) to M.B and P301/11/2076 to H.P.

References

- [1] A.C. Joerger, A.R. Fersht, Cold Spring Harb Perspect Biol. (2010) 2:a000919.
- [2] M. Dohn, S. Zhang, X. Chen, Oncogene 20 (2001)3193-3205.
- [3] M. Olivier, R. Eeles, M. Hollstein, M.A. Khan, C.C. Harris, P. Hainaut, Hum Mutat. 19 (2002) 607-614.
- [4] A. Petitjean, M.I. Achatz, A.L. Borresen-Dale, P. Hainaut, M. Oliveir, Oncogene 26 (2007)2157-2165.
- [5] M. Brazdova, L. Navratilova, K. Nemcova, V. Tichy, P. Pecinka, M. Lexa, E. Palecek, W. Deppert, B. Vojtesek, M. Fojta, In prepatrin.

P17

Effect of moving average window width on integration of EMG signal

M. Veterník, M. Šimera, J. Jakuš, I. Poliaček

Institute of Medical Biophysics, Jessenius Faculty of Medicine, Comenius University, Malá Hora 4, 037 54 Martin, Slovakia, e-mail: marcelveternik@gmail.com

Introduction

Nerves conduct signals in form of action potentials. Action potential is a basic manifestation of excitatory tissues activity. It represents an essential element of encoding and transmission of informations in neural system and it also represents the first stage of muscle contraction triggering. It is generally assumed (in the field of nerve modeling as well) that the nerve compound activity (multipotential) is a linear superposition of single fiber action potentials [1]. Elektromyogram (EMG) usually represents a complex electrical biosignal, the results of superposition of action potential trains recorded from muscle fibers located near the electrode and generated by active motor units. The motor unit consists of the motor neuron and the muscle fibres innervated by its axonal branches. The number of muscle fibres in the motor unit ranges widely across human (and animal) muscles. The muscle fibres of each motor unit are intermingled with fibres of other motor units so fibres belonging to several different motor units are close to each other [2]. In this paper, we attempted to study effect of moving average window width on integration of EMG signal using computer theoretical model. We hypothesized that variability of integrated EMG signal depends on frequency of action potentials and on the width of integrated windows.

Methods

The model consisted of five waveforms. Four of these waveforms simulated single unit EMG signals and the fifth waveform represented algebraic summation of the four single units. A three phase shape of action potential (single units) was chosen. It corresponded to the in vivo recordings [3] and lasted 5 ms (the 1st and the 3rd waveform) and 7 ms (the 2nd and the 4th waveform) [3]. All waveforms were shifted in time from the 1st one. The second started 4 ms, the third 1 ms and the fourth waveform 5 ms after the 1st one. The frequency of their incidence was 5 - 75 Hz (the 1st and the 3rd one) and 9 - 135 Hz (the 2nd and the 4th one) [4]. The integrated waveform represented rectified (absolute values) and averaged signal. We employed 3 windows widths - 1 s, 200 ms and 40 ms. Moving average window (MA) was shifted by 0,01 ms each step. Theoretical model was built and simulations were performed in PC environment MATLAB.

Results

We tested an impact of the width of moving average window on the interval wherein values of integrated waveform can fall. We used moving average window widths 200 ms and 40 ms. Superposed waveform was rectified and integrated. Then, we found minimal and maximal values in the entire range of integration. These values (the differences maximum minus minimum) were determined for all frequencies and for both moving average window widths. This way 2 sets of intervals were obtained (Figure 1a). The variability of differences (maximum minus minimum) with 200 ms moving average window was 3.2 fold less than that with 40 ms moving average window. Subsequently we attempted to express the inaccuracy of integration performed using 200 ms and 40 ms windows at superposed waveform. Reference (the accurate) value was obtained with integration of the signal using the window width of 1 s (all action potentials were taken). The values obtained with 200 ms and 40 ms, which differed the most from the reference value were calculated and these deviations were expressed in

percentage. We determined the deviations for all 15 pairs of frequencies. The deviation at 40 ms window and the lowest frequency of incidence of action potentials was 259 %, while using 200 ms window the deviation was only 17 %. The deviations decreased with higher frequency of action potentials in the waveforms in both cases (200 ms and 40 ms moving average window), and at the highest frequency it was 1,55 % for 200 ms window and 10,2 % for 40 ms window (Figure 1b).

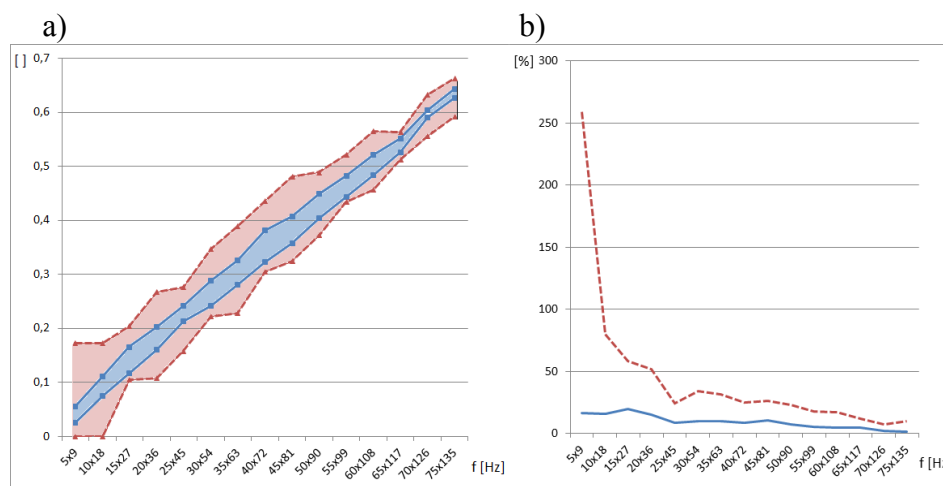


Fig. 1: Inaccuracy of moving average values (deviations) related to different moving average window width and frequency of action potentials. a) The width of interval with 200 ms window (blue) was 3.2 fold narrower than using the with of 40 ms window (red). b) With the increasing frequency of incidence of action potentials the deviation was decreasing in both cases, 200 ms window - blue unbroken line, 40 ms window - red broken line.

Conclusions

Our simulations demonstrated that the width of moving average window significantly influences the range (dispersion) of integrated values. Approximately three fold higher variability was found for the moving average window width of 40 ms compared to that for 200 ms window. The accuracy of the determination of integrated EMG signal increases with the number of action potentials taken and with the width of moving average window. Our results are consistent with experiences obtained during experiments and analyses of data on animals (reference; our own data).

Acknowledgement

This work was supported by the Slovak Grant Agency VEGA, project No. 1/0038/09.

References

- [1] X. Shaojun et al. Experimental Verification of Nerve Conduction Linearity, 18th Annual International Conference of the IEEE Engineering in Medicine and Biology Society. 1996.
- [2] R. Merletti, D. Farina, J. Phil. Trans. of The Royal Society A. 367 (2009) 357-368.
- [3] S.C. Day, M. Hulliger, J Neurophysiol. 86 (2001) 2144-2158.
- [4] P.A. McNulty, K.J. Falland, V.G. Macefield, J. Physiol. 526 (2000) 445-456.
- [5] I. Poljacek et al., J. Physiol. Pharmacol. 60, Suppl 5 (2009) 105-110.

P18

Effect of confinement on molecular mobility and free volume as seen by computer simulations and positron annihilation lifetime spectroscopy

D. Račko

Polymer Institute of the Slovak Academy of Sciences, Dúbravská cesta 9, 845 41 Bratislava, Slovakia,
e-mail: dusan.racko@savba.sk

Glycerol is an important substance in biological processes and as such it has been a subject of extensive scientific investigations [1]. The glycerol molecule is flexible, with three alcohol groups giving rise to a rich conformational behavior and formation of complex hydrogen bonding networks. As a result of the hydrogen bonding glycerol exhibits higher density. Increased density implies a decreased mobility of molecular bodies, what has been confirmed by experimental measurements of mean square displacements $\langle u^2 \rangle$ (from neutron scattering) or self-diffusivity [2]. Based on the *Free volume theory*, [3] originally developed to explain viscosity of liquids, the decreased mobility of molecules should be related with a decreased free volume amounts in the structure. This has been indeed confirmed by experimental free volume measurements by positron annihilation lifetime spectroscopy PALS [4] and a developed computational modeling method [5-9].

In this contribution the former computational study in glycerol condensed phases [5] is extended by including the effect of confinement, by enclosing glycerol molecules into a narrow channel of silica. It is well known, that confinement affects thermodynamic properties, such as glass transition temperature [10]. By imposing a confinement to a molecular system it is possible to define relationship between molecular structure and thermodynamic properties. Thanks to an increasing computational power of present computers, the atomistic studies of molecules in confinement well fit into the scale of the problem and allow studying effects of confinement on molecular level. As results show, the confined glycerol exhibits larger portions of the free volume as compared to pure bulk system. The increased free volume amounts well agree with the experimental measurements by PALS [11]. The large portions of the free volume are probably a result of less effective packing of molecules in confinement and lower coordination number as compared to the bulk. The different packing of molecules is probably also related to self-arranging of molecules along the silica surface. On the other hand, despite an increased free volume the system exhibits a decreased mobility of molecules as observed by self-diffusivity of molecules. This might be result of layering of molecules along the surface of the channel.

Acknowledgement This work was supported by the Slovak Grant Agency VEGA, project No. 2/0144/10 and 2/0093/12.

References

- [1] R Chelli, P Procacci, G Cardini, RG Della Valle, S Califano, *Phys Chem Chem Phys* 1 (1999) 871.
- [2] R Chelli, P Procacci, G Cardini, S Califano, *Phys Chem Chem Phys* 1 (1999) 879.
- [3] AJ Batschinski, *Z Phys Chem* 84 (1913) 643.
- [4] J Bartos, O Sausa, P Bandzuch, J Zrubcova, J Kristiak, *J Non-Cryst Sol* 307 (2002) 417.
- [5] D Račko, R Chelli, G Cardini, J Bartos and S Califano, *Eur Phys J D* 32 (2005) 289.
- [6] D Račko, R Chelli, G Cardini, S Califano, J Bartos, *Theo Chem Acc*, 118 (2007) 443.
- [7] D Račko, S Capponi, F Alvarez, J Bartos, J Colmenero, *J Chem Phys*, 133 (2009) 064903.
- [8] D Račko, S Capponi, F Alvarez, J Colmenero, *J Chem Phys*, 134 (2011) 044512.
- [9] D Račko, *Mat Sci Forum*, 666, 16, (2011).
- [10] GB McKenna, *Eur Phys J Special Topics* 189 (2010) 285.
- [11] D Kilburn, EP Sokol, VG Sakai, AM Alam, *Appl Phys Lett* 92 (2008) 033109.

Quantitative proteomics and integration of systems biology models - our first experience

C. Uličná, J. Uličný

Department of Biophysics, PF UPJŠ, Jesenná 5, 041 54 Košice, Slovakia, e-mail: jozef.ulicny@upjs.sk

Very recently, quantitative proteomics data were published for human U2OS and HeLa cell lines[1,2]. Thus, for the first time it is possible to address systematically one of the shortcomings of the present mathematical models - lack of comprehensive quantitative experimental data obtained on the single cell line under consistent experimental conditions.

We used this opportunity to take a fresh look at known generic predictive models of apoptotic processes initiated through TNF-alpha, including our own modifications[3,4]. According to our first experience, straightforward introduction of the experimentally estimated molecular concentrations into established models leads to some surprises, but only moderate tweaking of the models is required to restore the model properties.

In the process of model refinement, additional understanding of the processes characteristic for the cell line can be obtained. Although quantitative proteomics data are at the limits of current experimental capabilities, they still do not provide complete information necessary for the construction of mathematical models. On the other side, the data significantly reduce uncertainties inherently present in all models and in combination with available microarray data provide ground for very promising predictive models tailored to particular cell line.

Acknowledgement

The presented work was supported from VEGA grant 1/4019/07, OPVaV project ITMS - 26220120024 and OPVaV project - 2009/2.1/02-SORO.

References

- [1] M. Beck, A. Schmidt, J. Malmstroem, M. Claassen, A. Ori, A. Szymborska, F. Herzog, O. Rinner, J. Ellenberg, *Mol Syst Biol* 7 (November 8, 2011). <http://dx.doi.org/10.1038/msb.2011.82>
- [2] N. Nagaraj, J.R. Wisniewski, T. Geiger, J. Cox, M. Kircher, J. Kelso, S. Paabo, M. Mann. *Mol Syst Biol* 7 (November 8, 2011). <http://dx.doi.org/10.1038/msb.2011.81>
- [3] J. G. Albeck, J. M. Burke, B. B. Aldridge, M. Zhang, D. A. Lauffenburger, P. K. Sorger, *Molecular Cell* 30 (2008) 11–25.
- [4] S. Legewie, N. Bluthgen, H. Herzel, , *PLoS Computational Biology* 2 (2006) 1061–1073.
- [5] T. Tokár, J. Uličný Computational study of the mechanism of Bcl-2 apoptotic switch <http://arxiv.org/abs/1110.5225> , submitted to *Physica A*, 2011



UV-2700 – UV-VIS Spectrophotometer

Surfing different waves

Applying different wavelengths, the new compact UV-2600/2700 series of research grade UV-VIS spectrophotometers enables high-precision spectral analysis. It is based on the Shimadzu LO-RAY-LIGHTTM diffraction gratings optical system and covers a wide range of applications such as organic and inorganic compounds, biological samples, optical materials and photovoltaics.

- **Wide wavelength range**
of up to 1,400 nm enables expanded research of photovoltaics with UV-2800
- **High absorbance level**
of the UV-2700 double monochromator optics allows measurement of high density samples up to 8 Abs.

- **Ultra low stray light**

Shimadzu gratings offering "best in class" performance

- **User-friendly economic design**

with smallest footprint in its class, energy saving electronics, comprehensive system control software including validation, USB connection as well as the widest scope of accessories

www.shimadzu.eu

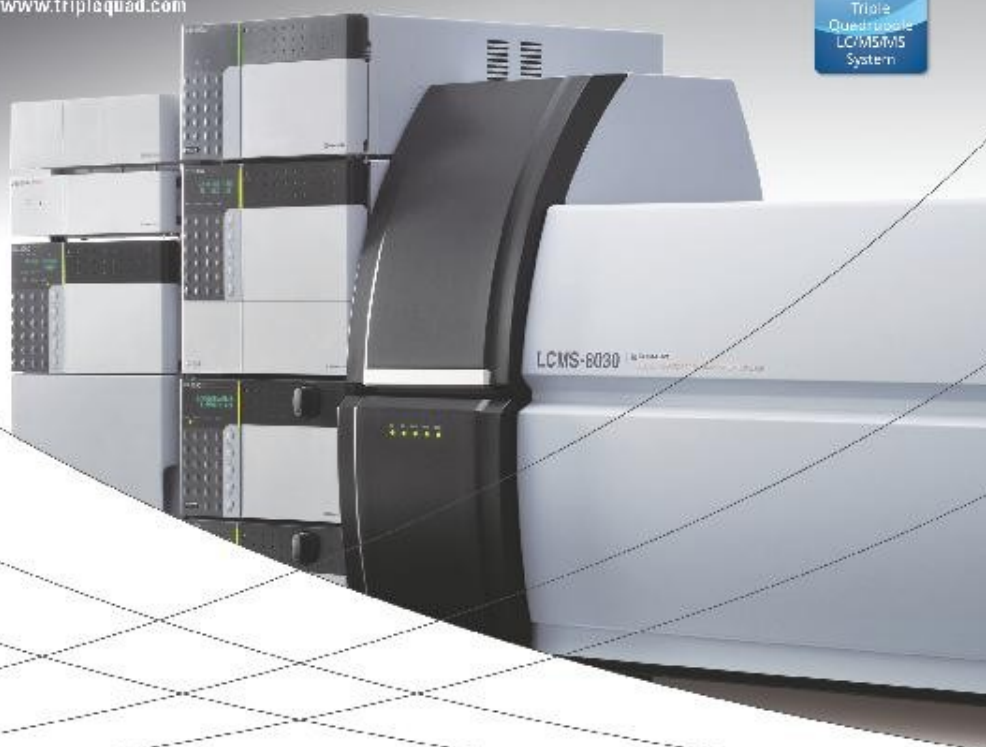


Supersonic flow

LCMS-8030's triple quadrupole technology enables ultra-fast mass spectrometry. Combined with the class-leading Nexera UHPLC, both systems facilitate seamless LC/MS/MS analyses in a high performance, high-speed flow, steadily and reliably.

- The fastest triple quadrupole mass spectrometer available**
 providing a fast passage speed, ultra-fast polarity switching with up to 500 VPM transitions in one second.
- Highly reliable results**
 through UF sweeper technology effectively sweeps trailing ions out of the cell scan cell and minimizing cross talk.
- Ease of use**
 enabled by a single vendor solution supported by LabSolutions software for seamless quantitative and qualitative analysis.
- Wide range of applications for various industries**
 such as pharmaceutical, environmental, food and chemical.

www.triplaquad.com



 **SHIMADZU**

www.shimadzu.eu

List of Participants

Balogová Lucia, RNDr.

Department of Biophysics PF UPJŠ
Jesenna 5
040 01 Košice, Slovakia
e-mail: luba.svk@gmail.com

Banó Gregor, Mgr. PhD.

Department of Biophysics PF UPJŠ
Jesenna 5
040 01 Košice, Slovakia
e-mail: gregor.bano@upjs.sk

Baumruk Vladimír, Prof.RNDr.DrSc.

Institute of Physics
Faculty of Mathematics and Physics
Charles University in Prague
Ke Karlovu 5, 121 16 Prague 2
Czech Republic,
e-mail: baumruk@karlov.mff.cuni.cz

Belej Dominik, Mgr.

Department of Biophysics PF UPJŠ
Jesenna 5
040 01 Košice, Slovakia
e-mail: belej.dominik@gmail.com

Castillo Gabriela, RNDr.

Department of Nuclear Physics and Biophysics
FMFI UK
Mlynská dolina F1
842 48 Bratislava, Slovakia
e-mail: gabriela.castillo@fmph.uniba.sk

Dzúrová Lenka, RNDr..

Department of Biophysics PF UPJŠ
Jesenna 5
040 01 Košice, Slovakia
e-mail: lenka.dzurova@upjs.sk

Fedunová Diana, RNDr., PhD.

Institute of Experimental Physics
Slovak Academy of Sciences
Watsonova 47
040 01 Košice, Slovakia
email: fedunova@saske.sk

Frečer Vladimír, RNDr.CSc.

Department of Physical Chemistry of Drugs
FAF UK
Odbojárov 10
832 32 Bratislava, Slovakia
e-mail: frecer@fpharm.uniba.sk

Gaburjaková Marta, RNDr.PhD.

Institute of Molecular Physiology and Genetics
Slovak Academy of Sciences
Vlárska 5
833 34 Bratislava, Slovakia

e-mail: marta.gaburjakova@savba.sk

Gallová Jana, Doc.RNDr.PhD.

Department of Physical Chemistry of Drugs
FAF UK
Odbojárov 10
832 32 Bratislava, Slovakia
e-mail: gallova@fpharm.uniba.sk

Garaiová Zuzana, Mgr.

Department of Nuclear Physics and Biophysics
FMFI UK
Mlynská dolina F1
842 48 Bratislava, Slovakia
e-mail: garaiova.zuzana7@gmail.com

Gažová Zuzana, RNDr. PhD.

Department of Biophysics
Institute of Experimental Physics
Slovak Academy of Sciences
040 01 Košice, Slovakia
e-mail: gazova@saske.sk

Grman Marian, Mgr.

Department of Nuclear Physics and Biophysics
FMFI UK
Mlynská dolina F1
842 48 Bratislava, Slovakia
e-mail: grman.marian@gmail.com

Hianik Tibor, Prof.RNDr.DrSc.

Department of Nuclear Physics and Biophysics
FMFI UK
Mlynská dolina F1
842 48 Bratislava, Slovakia
e-mail: tibor.hianik@fmph.uniba.sk

Horilová Júlia, Bc.

Department of Nuclear Physics and Biophysics
FMFI UK
Mlynská dolina F1
842 48 Bratislava, Slovakia
e-mail: j.horilova@gmail.com

Hořka Matej, Ing.

Institute of Molecular Physiology and Genetics
Slovak Academy of Sciences
Vlárska 5
833 34 Bratislava, Slovakia
e-mail: matej.hotka@savba.sk

Chorvát Dušan, RNDr.PhD.

International Laser Center
Ilkovičova 3
812 19 Bratislava, Slovakia
e-mail: dusan@ilc.sk

Chorvátová Alžbeta, PhD.
International Laser Center
Ilkovičova 3
812 19 Bratislava, Slovakia
e-mail: alzbeta.chorvatova@ilc.sk

Jakuš Ján, Prof.MUDr.DrSc.
Institute of Medical Biophysics JLF UK
Malá Hora 4
037 54 Martin, Slovakia,
e-mail: jakus@jfmmed.uniba.sk

Jancura Daniel, Doc.RNDr.PhD.
Department of Biophysics PF UPJŠ
Jesenná 5
041 54 Košice, Slovakia
e-mail: jancura@upjs.sk

Janiček Radoslav, Mgr.
Institute of Molecular Physiology and Genetics
Slovak Academy of Sciences
Vlárska 5
833 34 Bratislava, Slovakia
e-mail: radoslav.janicek@savba.sk

Jurášeková Zuzana, RNDr. PhD
Department of Biophysics PF UPJŠ
Jesenná 5
041 54 Košice, Slovakia
e-mail: zuzana.jurasekova@upjs.sk

Kopáni Martin, RNDr.PhD
Department of Pathology LFUK
Sasinkova 4
811 08 Bratislava, Slovakia
e-mail: martin.kopani@fmed.uniba.sk

Lacinová Lubica, Doc.RNDr.DrSc.
Institute of Molecular Physiology and Genetics
Slovak Academy of Sciences
Vlárska 5
833 34 Bratislava, Slovakia
e-mail: lubica.lacinova@savba.sk

Maslaňáková Mária, Mgr.
Department of Biophysics PF UPJŠ
Jesenná 5
040 01 Košice, Slovakia
e-mail: maria_maslanakova@yahoo.com

Mišák Anton, Mgr.
Institute of Molecular Physiology and Genetics
Slovak Academy of Sciences
Vlárska 5
833 34 Bratislava, Slovakia
e-mail: anton.misak@savba.sk

Miškovský Pavol, Prof.RNDr.DrSc.
Department of Biophysics PF UPJŠ
Jesenná 5
040 01 Košice, Slovakia
e-mail: misko@kosice.upjs.sk

Morvová Marcela, Mgr.
Department of Nuclear Physics and Biophysics
FMFI UK
Mlynská dolina F1
842 48 Bratislava, Slovakia
e-mail: morvova@gmail.com

Navrátilová Lucie, Mgr.
Institute of Biophysics
Academy of Sciences of Czech Republic
Královopolská 135
612 65 Brno, Czech Republic
e-mail: luna@ibp.cz

Olas Adam, Bc.
Department of Nuclear Physics and Biophysics
FMFI UK
Mlynská dolina F1
842 48 Bratislava, Slovakia
e-mail: adamolas@gmail.com

Ondriaš Karol, RNDr.D.Sc.
Institute of Molecular Physiology and Genetics
Slovak Academy of Sciences
Vlárska 5
833 34 Bratislava, Slovakia
e-mail: karol.ondrias@savba.sk

Petrovajová Dana, RNDr.
Department of Biophysics PF UPJŠ
Jesenná 5
041 54 Košice, Slovakia
e-mail: dana.petrovajova@student.upjs.sk

Pivoňková Hana, Mgr.PhD.
Institute of Biophysics
Academy of Sciences of Czech Republic
Královopolská 135
612 65 Brno, Czech Republic
e-mail: hapi@ibp.cz

Poliaček Ivan, Doc. RNDr.PhD.
Institute of Medical Biophysics
JLF UK
Malá Hora 4
037 54 Martin, Slovakia
e-mail: poliacek@jfmmed.uniba.sk

Poturnayová Alexandra, Ing
Institute of Animal Biochemistry and Genetics
Slovak Academy of Sciences
900 28 Ivanka pri Dunaji, Slovakia
e-mail: alexandrapoturnayova@gmail.com

Račko Dušan, Ing.PhD.
Polymer Institute
Slovak Academy of Sciences
Dúbravská cesta 9
842 36 Bratislava, Slovakia
e-mail: dusan.racko@savba.sk

Rybár Peter, RNDr.PhD.
Department of Nuclear Physics and Biophysics
FMFI UK
Mlynská dolina F1
842 48 Bratislava, Slovakia
e-mail: peter.rybar@fmph.uniba.sk

Strejčková Alena, RNDr.
Department of Biophysics PF UPJŠ
Jesenná 5
040 01 Košice, Slovakia
e-mail: alena.strejckova@student.upjs.sk

Súkeľová Juliana, Mgr.
Institute of Molecular Physiology and Genetics
Slovak Academy of Sciences
Vlárska 5
833 34 Bratislava, Slovakia
e-mail: juliana.sukelova@savba.sk

Šebest Peter, Mgr.
Institute of Biophysics
Academy of Sciences of Czech Republic
Královoposlá 135
612 65 Brno, Czech Republic
e-mail: besta@ibp.cz

Šimera Michal, RNDr.
Institute of Medical Biophysics JLF UK
Malá Hora 4
037 54 Martin, Slovakia
e-mail: simera@jfmed.uniba.sk

Šipošová Katarína, Mgr.
Department of Biophysics PF UPJŠ
Jesenná 5
040 01 Košice, Slovakia
e-mail: katkasiposova@gmail.com

Šnejdárková Maja, Ing. CSc.
Institute of Animal Biochemistry and Genetics
Slovak Academy of Sciences
900 28 Ivanka pri Dunaji, Slovakia
e-mail: Maja.Snejdarkova@savba.sk

Štroffeková Katarína, RNDr.PhD.
Department of Biophysics PF UPJŠ
Jesenná 5
040 01 Košice, Slovakia
e-mail: katarina.stroffekova@upjs.sk

Uherek Martin, Mgr.
Department of Nuclear Physics and Biophysics
FMFI UK
Mlynská dolina F1
842 48 Bratislava, Slovakia
e-mail: kerehu@gmail.com

Uličný Jozef, Doc.RNDr.CSc.
Department of Biophysics PF UPJŠ
Jesenná 5
040 01 Košice, Slovakia
e-mail: jozef.ulicny@upjs.sk

Veterník Marcel, Ing.
Institute of Medical Biophysics JLF UK
Malá Hora 4
037 54 Martin, Slovakia
e-mail: marcelveternik@gmail.com

Víglaský Viktor, Doc.RNDr.PhD.
Department of Biochemistry PF UPJŠ
Moyzesova 11
040 01 Košice
e-mail: viktor.viglasky@upjs.sk

Višňovcová Nadežda, Mgr.
Institute of Medical Biophysics JLF UK
Malá Hora 4
037 54 Martin, Slovakia
e-mail: nvisnovcova@jfmed.uniba.sk

Vrbovská Hana, Bc.
Department of Nuclear Physics and Biophysics
FMFI UK
Mlynská dolina F1
842 48 Bratislava, Slovakia
e-mail: h.vrbovska@gmail.com

Waczulíková Iveta, Doc.RNDr.PhD.
Department of Nuclear Physics and Biophysics
FMFI UK
Mlynská dolina F1
842 48 Bratislava, Slovakia
e-mail: waczulikova@fmph.uniba.sk

Zahradník Ivan, RNDr. PhD.
Institute of Molecular Physiology and Genetics
Slovak Academy of Sciences
Vlárska 5
833 34 Bratislava, Slovakia
e-mail: ivan.zahradnik@savba.sk

Zahradníková Alexandra, Ing. DrSc.
Institute of Molecular Physiology and Genetics
Slovak Academy of Sciences
Vlárska 5
833 34 Bratislava, Slovakia
e-mail: alexandra.zahradnikova@savba.sk

Zvarík Milan, Mgr.
Department of Nuclear Physics and Biophysics
FMFI UK
Mlynská dolina F1
842 48 Bratislava, Slovakia
e-mail: zvarikmilan@gmail.com

Index of Authors

Adamík M.	77	Chorvát D.	44,46,53
Antošová A.	33,63	Chorvátová A.	44,47,53
Antalík M.	51	Illesová A.	44
Babincová M.	67	Imrich J.	33
Bágel'ová J.	33,61	Ionov M.	71
Balgavý P.	69	Jakubovský J.	12
Balogová L.	50	Jakuš J.	10,19,48,78
Banó G.	39	Jakušová V.	19
Baumruk V.	17	Jancura D.	35
Bednáríková Z.	63	Janiček R.	29
Berka V.	35	Jurašeková Z.	42
Beyl S.	25	Karmazinová M.	25
Bilčík B.	53	Kasák P.	53
Boca R.	12	Klugbauer N.	25
Brázdová M.	77	Koneracká N.	63
Bryszewska M.	71	Kopáni M.	12
Bučko M.	44	Kopčanský P.	63
Čaplovičová M.	12	Korri-Youssoufi H.	75
Castillo G.	75	Košťál L.	53
Čavarga I.	53	Kubovčíková M.	63
Čunderlíková B.	53	Lacinová Ľ.	25
Daxnerová Z.	63	Liptaj T.	23
Dekan J.	12	Málek L.	27
Dlháň L.	12	Martinický D.	55
Domingo C.	42	Maslaňáková M.	50
Dorizon H.	75	Mateášik A.	53
Dzurová L.	41,52	Miertuš S.	14
Ďurčovičová C.	69	Miglierini M.	12
Ebner A.	73,74	Miodek A.	75
Fabian M.	35	Mišák A.	23,24,27
Fabriciová G.	39	Miškovský P.	39,41,50,52,53
Fedunová D.	61	Mlkvý P.	53
Fojta M.	37,38,77	Morvová M.	59
Frečer V.	14	Naďová Z.	52
Gaburjáková J.	26	Navrátilová L.	77
Gaburjáková M.	26	Neudlinger I.	73,74
Galandová J.	34	Němcová K.	38
Gallová J.	69	Nichtová Z.	65
Garaiová Z.	71	Novotná M.	65
García-Ramos J.V.	42	Olas A.	67
Gažová Z.	33,63	Ondriaš K.	21,23,24,27
Grman M.	21,23,24,27	Petrovajová D.	41,52
Hering S.	25	Pivoňková H.	37,38,77
Hianik T.	49,71,73,74,75	Poliaček I.	10,78
Horilová J.	44	Poturnayová A.	73,74
Hoťka M.	29,31	Pronayová N.	23
Huba P.	61	Račko D.	80
Hunáková Ľ.	55	Sánchez-Cortés S.	42
Huntošová V.	41	Seneci P.	14

Sisovsky V.	12
Staničová J.	35,39
Strejčková A.	39
Šebest P.	37,38
Šikurová L.	55,57,59
Šimera M.	10,78
Šipošová K.	33,63
Šnejdárková M.	73,74
Štroffeková K.	39,49,52
Sukeľová J.	65
Tomášková Z.	21,27
Uherek M.	57
Uličná O.	21,57
Uličný J.	81
Vančová O.	21
Veternik M.	10,78
Víglaský V.	16
Višňovcová N.	19
Višňovcová N. Jr.	19
Vrbovská H.	67
Výboh P.	53
Waczulíková I.	21,71
Wrobel D.	71
Zahradník I.	29,31,65
Zahradníková A.	29
Zahradníková A. Jr.	29
Závišová V.	63
Zvarík M.	55